Distribution Agreement

In presenting this thesis or dissertation as a partial fulfillment of the requirements for an advanced degree from Emory University, I hereby grant to Emory University and its agents the non-exclusive license to archive, make accessible, and display my thesis or dissertation in whole or in part in all forms of media, now or hereafter known, including display on the world wide web. I understand that I may select some access restrictions as part of the online submission of this thesis or dissertation. I retain all ownership rights to the copyright of the thesis or dissertation. I also retain the right to use in future works (such as articles or books) all or part of this thesis or dissertation.

Signature:

Anastasia Svishcheva	Date

Analysis and Simulation of Bingham fluid problems with Papanastasiou-like regularizations: Primal and Dual formulations

By

Anastasia Svishcheva
Doctor of Philosophy

Mathematics

Alessandro Veneziani, Ph.D.
Advisor

David Borthwick, Ph.D.
Committee Member

James Nagy, Ph.D.
Committee Member

Accepted:

Lisa A. Tedesco, Ph.D.
Dean of the Graduate School

Date

By

Anastasia Svishcheva
Ph.D., Emory University, 2014

Advisor: Alessandro Veneziani, Ph.D.

An abstract of
A dissertation submitted to the Faculty of the Graduate School
of Emory University in partial fulfillment
of the requirements for the degree of
Doctor of Philosophy
in Mathematics
2014

Abstract

By Anastasia Svishcheva

In this dissertation thesis I conduct analysis and simulation of Bingham fluid problems with Papanastasiou-like regularizations. I explain primal and dual formulations of the problems. I discuss the mixed (dual) formulation of Bingham-Papanastasiou problem, its well-posedness and show the numerical results. In general, common solvers for the regularized problem experience a performance degradation when the regularization parameter m gets greater. The mixed formulation enhanced numerical properties of the algorithm by introduction of an auxiliary tensor variable.

I also introduce a new regularization for the Bingham equations, so called Corrected regularization. Corrected regularization demonstrates better accuracy than other ones. I show its well-posedness, and in addition, compare its numerical results with the results obtained with the applications of other regularizations.

By

Anastasia Svishcheva
Ph.D., Emory University, 2014

Advisor: Alessandro Veneziani, Ph.D.

A dissertation submitted to the Faculty of the Graduate School
of Emory University in partial fulfillment
of the requirements for the degree of
Doctor of Philosophy
in Mathematics
2014

Acknowledgments

I would like to express my special appreciation and thanks to my advisor Professor Dr.Alessandro Veneziani, you have been a tremendous mentor for me. Your advises, help, and support are priceless. I would like to thank the dissertation committee members Dr.James Nagy and Dr. David Borthwick for making this defense possible. I warmly thank Dr.Maxim Olshanskii for his support and help. I would also like to thank all faculty, staff and graduate students of the Department for their teaching, encouragement, and understanding. I am sincerely grateful to my friends and family for being with me, and supporting in hard time.

Contents

List of Figures

List of Tables

Chapter 1

Introduction

1.1 Non-Newtonian fluids

The part of physics that studies fluids and deformations of substances is called *rheology*. Rheology involves consideration of liquids, as well as soft solids under conditions which force them to flow. A very important part of the fluid study is measuring its resistance to deformation under shear stress. To serve this purpose we use *viscosity*, the main characteristics in rheology. In other words, by viscosity we understand the "thickness" of the fluid. The "thicker" fluid, the bigger viscosity. For example, mercury has higher viscosity then water.

By the ability of fluids to change under the certain conditions, we distinguish two types of fluids - Newtonian fluids and non-Newtonian fluids.

A Newtonian fluid is a rare case. A Newtonian fluid is a fluid whose viscosity remains constant regardless of any external stress that is placed on

it. Nevertheless that Newtonian fluid may demonstrate different thickness with different temperatures, its flow stays the same and always displays the properties of the liquid, whether the external forces applied to it, or not under the fixed temperature. Water is a typical example: it is not getting compressed, and does not become more viscous, whatever stress is applied to it. If someone immerses a stick to water, there is no hole forms on the opposite surface. Although ice is thicker then water, it does not contradict with the fact that water is a Newtonian fluid, because to change the viscosity (thickness) of ice we must melt it, i.e. change its the temperature. The other examples of Newtonian fluid are: air, kerosene, ethanol [35].

But most of the fluid have a nonconstant viscosity. These fluids can become thicker or thinner when stress is applied. This type of fluids are called non-Newtonian fluids. Non-Newtonian fluids behave quite differently, and their reactions depend on the nature of external influence. Their viscosity can vary dramatically depending on their conditions. Often a non-Newtonian fluid feature viscosity depending on the shear rate.

One of the examples is quicksand. Quicksand is dangerous because it can suck in everything that gets in there. If we put on the sand some subject heavy enough, it begins to sink in it, but if someone quickly hits the quicksand, it immediately hardens.

When it is at rest, quicksand looks like a solid, but even less than 1% change in the mechanical stress on the surface results in a substantial reduction of its viscosity. To move in quicksand, a person needs to apply quite significant pressure on it. The force required to pull the leg of quicksand at a speed of 0.1 m/s is equivalent to the force that would be required to lift a medium-sized passenger car [30].

An interesting study on Non-Newtonian fluid was recently conducted by Scott R. Waitukaitis and Heinrich M. Jaeger from the University of Chicago [45]. They created a suspension of cornstarch in water so called it *oobleck*. During experiments they hit suspension with aluminum stick, and measured its position, speed, and acceleration while moving into oobleck. Based on this study was established that suspension's solidification occurs from the inner compression and pressure, spreading within oobleck from the point of the interaction. The stresses originate from an impact-generated solidification front that quickly forms a jammed region, ultimately leading to extraordinary amounts of momentum absorption. Using in their research a huge amount of substances (25 liters), the scientists have shown, that the effect of hardening, that was traditionally studied in driven suspensions with extra boundary conditions, does not depend on the presence of walls and boundaries.

Quicksand and cornstarch are two examples of *thickening fluids*, where the viscosity increases as the shear stress increases in magnitude, and the material becomes "thicker" under stress.

Thickening fluids is only one case of non-Newtonian fluids. We will name here the most significant types:

1. *Shear thickening liquids*, whose viscosity increases with the rate of shear stress.
2. *Shear thinning liquids*, whose viscosity decreases with the rate of shear stress.
3. *Bingham plastics* that behave as a solid at low stresses but flows as a viscous fluid at high stresses.

On the Figure 1.1 we can see the relationship between the shear rate and the shear stress for these three cases.

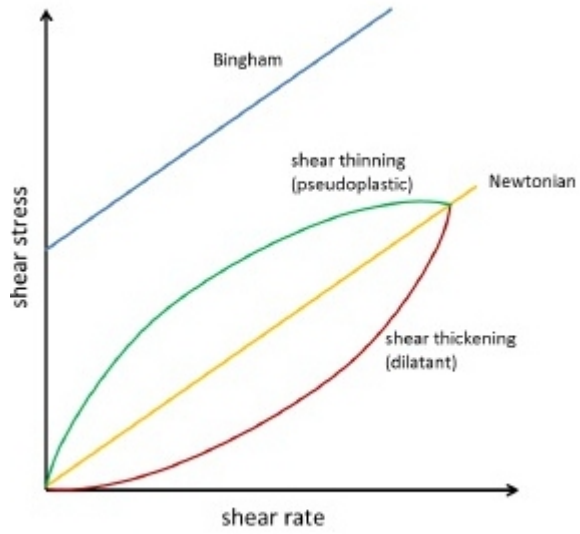

Figure 1.1: The shear stress as a function of the shear rate for Newtonian fluids (yellow), shear thickening fluids (red), shear thinning fluids (green) and visco-plastic (Bingham) fluids (blue).

Examples of shear-thinning fluids are high fruit concentrates such as orange juice concentrate or apple sauce [38], wall paint, and blood.

Visco-plastic fluids, which include Bingham fluid, show deformation only after the applied stress exceeds a certain threshold. The critical value of the stress needed to be applied to visco-plastic fluids is called the *yield stress* [32].

Let $\boldsymbol{\tau}$ denote a shear stress, $\mathbf{u}$ the velocity of the flow, and $D\mathbf{u}$ a shear rate, or the rate of deformation tensor, depending on $\mathbf{u}$. Visco-plastic fluids

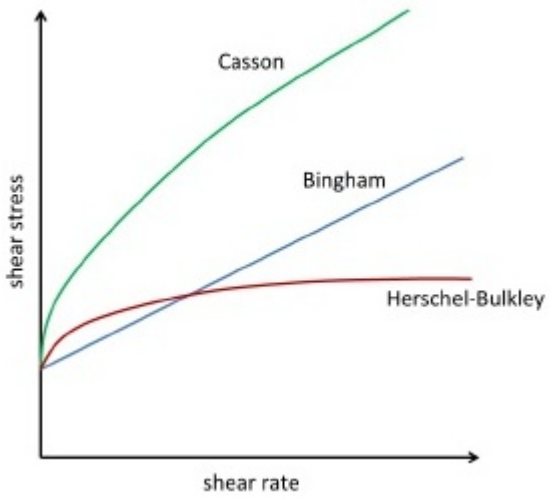

Figure 1.2: Relationship between shear stress and shear rate for Bingham (blue), Casson (green) and Herschel-Bulkley (red)fluids.

have the following subcategories, that characterize the relationship between shear stress $\boldsymbol{\tau}$ and shear rate $D\mathbf{u}$ [9, 32]:

- *Bingham fluids:*

$$\boldsymbol{\tau} = \left(2\mu + \frac{\tau_s}{|D\mathbf{u}|}\right) D\mathbf{u}, \text{ for} |\boldsymbol{\tau}| > \tau_s.$$

- *Casson fluids:*

$$\boldsymbol{\tau} = \left(\sqrt{\mu} + \sqrt{\frac{\tau_s}{|D\mathbf{u}|}}\right)^2 D\mathbf{u}, \text{ for} |\boldsymbol{\tau}| > \tau_s.$$

- *Herschel-Bulkley fluids:*

$$\boldsymbol{\tau} = \left(K|D\mathbf{u}|^{n-1} + \frac{\tau_s}{|D\mathbf{u}|}\right) D\mathbf{u}, \text{ for} |\boldsymbol{\tau}| > \tau_s.$$

In all three subcategories, $D\mathbf{u} = 0$ for $|\boldsymbol{\tau}| \leq \tau_s$. $K > 0,\ n > 0$ are given constants, μ is the so called *constant static viscosity*, and τ_s is the so called *yield stress*. The relationship between shear rate and shear stress for all three cases are shown in Figure 1.2

Examples of Casson fluids are tomato soup, honey, and concentrated fruit juices [20]; of Herschel-Bulkley fluids are minced fish paste, raisin paste [38]; for Bingham flow are ketchup, toothpaste, magma, and the flow of certain oil-bearing materials [33].

In this dissertation thesis we consider the numerical approach of the solution of the partial differential equations, describing the flow of Bingham material.

1.2 Bingham Flow

Bingham visco-plastic material is named after Eugene C. Bingham who suggested a mathematical explanation on it [8]. It behaves as a rigid body at low stresses but flows as a viscous fluid at high stress, with a total viscosity proportional to $|D\mathbf{u}|^{-1}$.

Nowadays, Bingham fluids play a very significant role in the amount of researches in various fields, such as geology, geophysics, medicine, and many others. The Bingham model is used, among others, for describing the flow of oil bearing materials, slurries, mud and magma as well as certain powder mixtures.

As examples of usage of the Bingham flow in medicine, we can mention [36], were is considered the peristaltic flow of a conducting Bingham fluid flow through a porous medium in an inclined channel, and in [39] are investigated tetra-n-butyl-ammonium bromide clathrate hydrate slurry flows in a horizontal tube, flow behavior and its rheological model. Also, Bingham model is used to simulate the flow of blood, especially under a high concentration of white blood cells or blood solutes [16].

In geology, the good example of the usage of Bingham flow is mud flow. For example in [21], Bingham fluids are used for modeling and predicting landslides.

Oil industry uses the model for analyzing start-up flows of waxy crude oils in pipelines [41, 44].

All of mentioned above is just a few examples of Bingham fluid usage in industry.

1.3 Outline of the thesis and motivation

As we discussed in previous section, Bingham flow is found in many applications. Although, the process of solving the Bingham equations, described in the next chapter, raises several mathematical challenges. The occurrence of $|D\mathbf{u}|$ at the denominator not only introduces a singularity, but also the region where this may happen is unknown.

A traditional way to avoid these difficulties is to regularize the van-

ishing term by approximating it with non-zero expression [5, 6, 34].

In addition, along with a formulation in simple variables, we consider a very useful strategy not only to avoid singularity, but also to accelerate the convergence of the algorithm, the *Mixed formulation* of the problem. The mixed formulation was first introduced by T. F. Chan, G. H. Golub, and P. Mulet [10]. Although, due to the fact that the question of its convergence is still open, we can not use mixed formulation without previous regularization. But it still serves to decrease numbers of iterations for numerical algorithm for regularized formulation.

In particular, we consider the regularization technique due to Papanastasoiu [34], comparing it to the technique of Bercovier and Engelman [5, 6]. We gradually study the convergence of two formulations, the formulation in primitive variables and the mixed formulation, for the Papanastasiou's regularization, to compare the results with the similar analysis of regularized with Bercovier-Engelman's technique Bingham equations, which was done by A.Aposporidis, E.Haber, M.Olshanski, and A.Veneziani in [4].

We also introduce a new regularization, which is obtained by modifying the Bercovier-Engelman approach by an exponential term. Later, throughout the manuscript we will refer to this technique as *Corrected regularization*. The new regularization gives better accuracy of the numerical solution.

In each chapter of the thesis we perform the analysis to Papanastasiou's and both Corrected regularizations, following the steps from [4].

In **Chapter 2** we discuss the different regularizations of the Bingham fluid flow, such as Papanastasiou's, and Corrected regularizations. For each of them we study the formulation in primitive variables. Then we introduce the mixed formulation, and establish equations for the weak formulations in each case.

In **Chapter 3** we show the well-posedness of the continuous problem in primitive and mixed formulations. We prove the existence and uniqueness of solution in mixed formulation for known before Papanastasiou's regularization, and also obtain these results for established here Corrected regularization.

In **Chapter 4** we explain discretization and continuation techniques. We present the proofs of the well-posedness of Picard linearization method, and estimate its error at each iteration with respect to the regularization parameter in each case. The Newton linearization method is presented. And finally, we discuss a finite element method of discretization.

Chapter 5 consists of the numerical results, and comparison of the performances of algorithms described.

Chapter 2

Mathematical Formulations of the Bingham problem and its regularizations

2.1 The Equations

In this section we introduce the partial differential equations describing Bingham plastic fluid flow.

Let us denote by Ω a domain of interest in 2D or 3D, and by $\mathbf{u}(\mathbf{x}, t)$ the velocity of a fluid flowing in Ω. Let $p(\mathbf{x}, t)$ be the pressure. We introduce the following notations: $D\mathbf{u} = (\nabla\mathbf{u} + \nabla\mathbf{u}^T)$ is a so called rate-of-deformation tensor. To this we associate a Frobenius norm $|D\mathbf{u}| = \sqrt{tr(D\mathbf{u} \cdot D\mathbf{u}^T)}$.

In order to model a viscoplastic flow, we introduce a constitutive law relating the tensor $D\mathbf{u}$ with the shear rate tensor $\boldsymbol{\tau}$. We set

$$\boldsymbol{\tau} \equiv 2\mu D\mathbf{u} + \tau_s \frac{D\mathbf{u}}{|D\mathbf{u}|}, \tag{2.1}$$

where τ_s is the so called *yield stress*. It represents the critical value the shear stress needs to exceed for the Birgham material to behave like an incompressible fluid.

Equation (2.1) is postulated to hold only for $|\boldsymbol{\tau}| > \tau_s$. In this case from momentum conservation and mass conservation, we get

$$\begin{cases} \rho[\frac{\partial \mathbf{u}}{\partial t} + (\mathbf{u}\cdot\nabla)\mathbf{u}] - \nabla\cdot\boldsymbol{\tau} + \nabla p = \mathbf{f} \\ \nabla\cdot\mathbf{u} = 0, \end{cases} \tag{2.2}$$

and we denote by $\Omega_f \subseteq \Omega$ the region (*fluid region*) where $|\boldsymbol{\tau}| > \tau_s$. In the region Ω_s where $|\boldsymbol{\tau}| \leq \tau_s$ the fluid behaves like a solid, and we call it the *plug region*. In Ω_s we have $D\mathbf{u} = \mathbf{0}$.

We may write the constitutive law resulting from the model as follows

$$D\mathbf{u} = \begin{cases} 0, & \text{for } |\boldsymbol{\tau}| \leq \tau_s \text{ (plug region)} \\ \left(1 - \frac{\tau_s}{|\boldsymbol{\tau}|}\right)\frac{\boldsymbol{\tau}}{2\mu}, & \text{for } |\boldsymbol{\tau}| > \tau_s \text{ (fluid region)} \end{cases} \tag{2.3}$$

Equations (2.2), (2.3) can be viewed as a generalization of the Navier-Stokes equations with shear-dependent viscosity $\hat{\mu} = 2\mu + \frac{\tau_s}{|D\mathbf{u}|}$, reducing to the classical Newton Navier-Stokes equations for $\tau_s = 0$.

The steady counterpart of (2.2), we may consider whenever the Lagrangian derivative can be dropped, reads

$$\begin{cases} -\nabla\cdot\boldsymbol{\tau} + \nabla p = \mathbf{f} \\ \nabla\cdot\mathbf{u} = 0 \end{cases}, \text{ in } \Omega. \tag{2.4}$$

Later on we will refer to (2.4) as the *steady Bingham-Stokes equations*, and to (2.2) as by the *Bingham-Navier-Stokes equations*.

2.2 Regularized Formulation

The numerical formulation of Bingham problem pinpoints two major challenges at the practical level. The first one is that plug regions are not known *a priori*, so the splitting of the domain Ω in Ω_s and Ω_f is part of unknown. The second one is that when approaching Ω_s from the point in Ω_f, $|D\mathbf{u}| \to 0$, and the equations tend to be singular, reflecting in numerical troubles. For this region, a classical approach for solving in practice the problem has been to *regularize* it, by replacing Ω_s with a fluid region featuring high viscosity. In this way no splitting is needed any longer, and the equation becomes nonsingular. The approximated plug region is recovered by inspecting high viscosity (still fluid) regions. The drawback of regularization is that it somehow arbitrary affects the accuracy of the results.

2.2.1 Bercovier-Engelman regularization

One way to regularize the strain tensor is the Bercovier-Engelman regularization [6], this corresponds to replace the viscosity $\hat{\mu}$ with

$$\hat{\mu}_\epsilon = 2\mu + \frac{\tau_s}{|D\mathbf{u}|_\epsilon},$$

where $|D\mathbf{u}|_\epsilon = \sqrt{|D\mathbf{u}|^2 + \epsilon^2}$.

Note that the plug region is eliminated here by the regularization parameter ϵ, that forces an infinitely large viscosity for the region Ω_s.

In order to reduce the perturbation of the problem, another option is to regularize only in those parts of the domain where $|D\mathbf{u}|$ is sufficiently small

$$|D\mathbf{u}|_{reg(\epsilon)} = \begin{cases} |D\mathbf{u}| & for |D\mathbf{u}| \geq \epsilon \\ \frac{|D\mathbf{u}|^2+\epsilon^2}{4\epsilon} & for |D\mathbf{u}| < \epsilon. \end{cases}$$

2.2.2 Papanastasiou's regularization

One of the regularizations considered in this work is due to Papanastasiou [34]. In this case the viscosity is replaced by

$$\hat{\mu}_m = 2\mu + \frac{\tau_s}{|D\mathbf{u}|}\left(1 - \exp(-m|D\mathbf{u}|)\right).$$

Papanastasiou predicted the rapid transition of the tensor $D\mathbf{u}$ from zero to the finite value, and reported it in [34]. The exponential parameter term thus was introduced to avoid numerical difficulties stemming from the sigmoidal form of the continuous viscoplastic equation. In particular, the exponential parameter manages to smooth this transition. It also served for solution continuation in the space of the exponential material parameter of the continuous viscoplastic equation.

Note that

$$\lim_{|D\mathbf{u}|\to 0} \frac{1 - \exp(-m|D\mathbf{u}|)}{|D\mathbf{u}|} = m, \tag{2.5}$$

and

$$\lim_{|D\mathbf{u}|\to \infty} 1 - \exp(-m|D\mathbf{u}|) = 1.$$

Thus the singularity of the original equations is substituted with the removable singularity, and that makes numerical approach possible.

The regularized formulation of the Bingham flow, using the Papanastasiou approach, reads

$$\begin{cases} \rho[\frac{\partial \mathbf{u}}{\partial t} + (\mathbf{u}\cdot\nabla)\mathbf{u}] - \nabla(2\mu D\mathbf{u} + \tau_s \frac{D\mathbf{u}}{|D\mathbf{u}|}(1-\exp(-m|D\mathbf{u}|))) + \nabla p = \mathbf{f} \\ \nabla\cdot\mathbf{u} = 0. \end{cases} \tag{2.6}$$

In case of steady Stokes type equations, reads

$$\begin{cases} -\nabla(2\mu D\mathbf{u} + \tau_s \frac{D\mathbf{u}}{|D\mathbf{u}|}(1-\exp(-m|D\mathbf{u}|))) + \nabla p = \mathbf{f} \\ \nabla\cdot\mathbf{u} = 0. \end{cases} \tag{2.7}$$

2.2.3 Corrected regularization

We also introduce here a new regularization. We call it *Corrected regularization*, since it can be regularized as a modification of the Bercovier-Engelman regularization by an exponential term. The exponential multiplier serves to minimize a parameter's impact to the value of viscosity, when $|D\mathbf{u}|$ is not close to zero.

The regularized viscosity in this case is set as

$$\hat{\mu}_{\delta,\nu,\alpha} = 2\mu + \frac{\tau_s}{|D\mathbf{u}|_c},$$

where $|D\mathbf{u}|_c = \sqrt{|D\mathbf{u}|^2 + \delta^2 \exp(-\nu|D\mathbf{u}|^\alpha)}$, $\delta > 0$, $0 < \nu < \tilde{\nu}$, $\alpha > 0$, and ν has a dimension of $|D\mathbf{u}|^{-\alpha}$.

Observe, that the approximation $\hat{\mu}_{\delta,\nu,\alpha}$ meets the advantage of being continuous and greater then zero at each point of Bercovier-Engelman approach, together with the advantage of closer approximation to the actual function of Papanastasiou's regularization, when $|D\mathbf{u}|$ is finite.

We can vary regularization parameters δ, ν, α to obtain if needed the closer approximation of μ, and thus improve the accuracy of the solution. The parameters must satisfy some conditions to obtain well posedness analysis for the regularized problem.

It is worth noting that the better approximation, the slower convergence of the numerical algorithm, as we will prove in Chapter 4 and verify in Chapter 5.

Figure 2.1 illustrates the actual graph of $|D\mathbf{u}|$ and the three regularized ones. To make results comparable, we set $\epsilon = \delta = \frac{1}{m} > 0$. For the Corrected regularization we choose $\alpha = 1/2,\ \nu = 1/\delta$. On the Figure 2.2 we demonstrate the approximation of viscosity μ for the three cases.

2.2.4 Other approaches to the numerical solution of the regularized Bingham model

In this section we mention the other key works where the original ideal Bingham model was modificated in order to avoid the discontinuity.

1. Tanner and Milthorpe [40] used a model called the bi-viscosity model, having two finite viscosity slopes (that is, combining two Newtonian

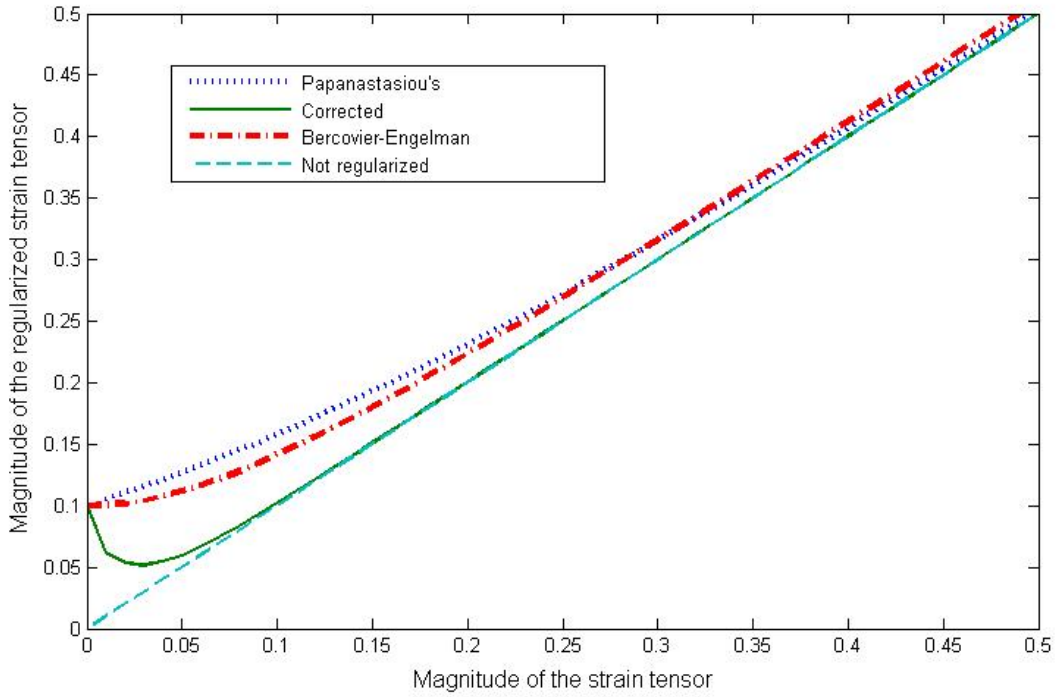

Figure 2.1: An approximation of $|D\mathbf{u}|$, $\epsilon = \delta = 1/m = 0.1$.

models):

$$\boldsymbol{\tau} = \begin{cases} 2\mu_0 D\mathbf{u} & for\ |D\mathbf{u}| < \gamma_c \\ 2\mu + \tau_s \frac{D\mathbf{u}}{|D\mathbf{u}|} & for\ |D\mathbf{u}| \geq \gamma_c, \end{cases}$$

where γ_c and μ_0 are chosen parameters. Performing multiple trials by checking the result on 1D solution for Poiseuille flow,the best values were established to be $\mu_0 = 1000\mu$, and $\gamma_c = 10^{-3}\ s^{-1}$.

2. Glowinski [12, 18] used a generalized framework of solving problems with discontinuity based on the theory of variational inequalities, introduced by Duvaut and Lions [13]. The mathematical model results to Lagrange multipliers. The minimization problem solution is based on Uzawa-type schemes. The basic idea here is to use an equivalent

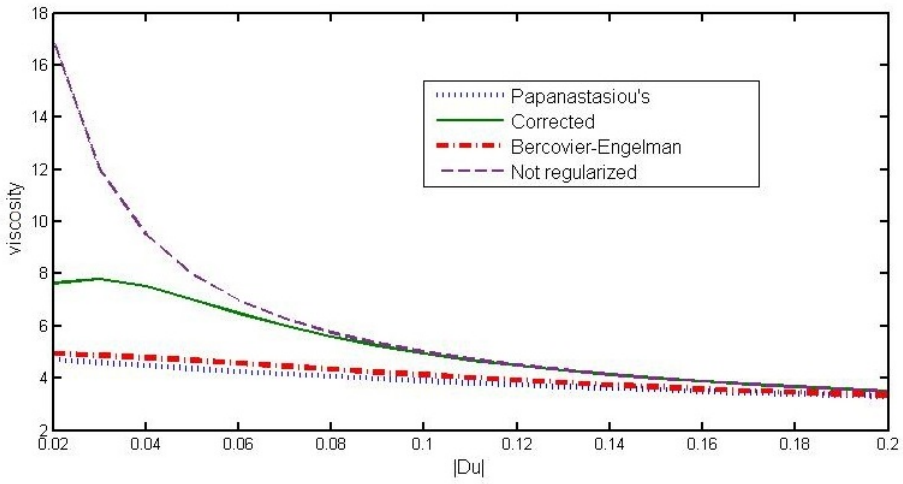

Figure 2.2: An approximation of viscosity μ, $\epsilon = \delta = 1/m = 0.1$, $\alpha = 1/2$, $\nu = 1/\delta$.

minimization problem

$$\mathcal{L}(\mathbf{u}, \gamma, \boldsymbol{\tau}) = \mu \int_\Omega |\gamma|^2 dx + \tau_s \int_\Omega |\gamma| dx + \int_\Omega (D\mathbf{u} - \gamma) : \boldsymbol{\tau} dx$$

$$+\lambda \int_\Omega |D\mathbf{u} - \gamma|^2 dx - \int_\Omega \mathbf{f} \cdot \mathbf{u} dx,$$

where $\gamma = D\mathbf{u}$, and λ is an auxiliary variable. Then the solution $\mathbf{u}$ is satisfying

$$\mathcal{L}(\mathbf{u}, \gamma, \boldsymbol{\tau}) = \min_{\boldsymbol{\sigma} \in \mathcal{L}^2_s, \mathbf{v} \in \mathbf{V}} \max_{\boldsymbol{\xi} \in \mathcal{L}^2_s} \mathcal{L}(\mathbf{v}, \boldsymbol{\sigma}, \boldsymbol{\xi}).$$

There were obtained a solution for the ideal Bingham flow. Several standard solutions for this case were consequently studied in [25,28,29, 37,41–44].

3. The approach by Beris et al. [7] essentially solved the Bercovier-Engelman regularized problem, but including the equations for a plastic solid when $|D\mathbf{u}| < \epsilon$. They solved a the benchmark problem of a sphere

falling in a Bingham plastic flow, whose boundaries are infinite. They numerically found yielded and unyielded regions, which is considered as a milestone in numerical analysis for viscoplastic fluids.

2.3 The Mixed Formulation

To avoid difficulties due to the singularity of Bingham equations in primitive variables (2.2), (2.3), in this thesis we take advantage of a different approach of formulating the problem, the so called, *mixed formulation*.

The original idea of the mixed formulation is due to T. F. Chan, G. H. Golub, and P. Mulet [10], who applied the approach to the problem of image restoration.

To explain the mixed formulation, first, we introduce an auxiliary variable tensor W, such that

$$|D\mathbf{u}|W = D\mathbf{u}.$$

Then we can rewrite the equations (2.2) in mixed formulation

$$\begin{cases} \rho[\frac{\partial \mathbf{u}}{\partial t} + (\mathbf{u}\cdot\nabla)\mathbf{u}] - \nabla\cdot(2\mu D\mathbf{u} + \tau_s W) + \nabla p = \mathbf{f} \\ \nabla\cdot\mathbf{u} = 0 \\ |D\mathbf{u}|W = D\mathbf{u}. \end{cases} \tag{2.8}$$

The idea behind mixed formulation is that the introduction of the auxiliary tensor W helps to avoid singularity. It is intended to enhance the numerical properties of considered regularized formulations, and decrease the number of iterations, required to obtain a numerical solution compared to primitive

variable formulation. Technically, now we obtain equations without singularity, that could be solved numerically. As it was shown in [4], the Picard iterations successfully solve (2.8). Although, the question of the theoretical prove of the existence of the solution in this case is still open. Thus, there is still a need of regularizing the (2.2). In [4] the mixed formulation was proposed for the Bercovier-Engelman regularization. Hereafter we present its extension to the Papanastasiou's and Corrected approaches.

Let us first consider the regularized formulation of the problem. We introduce an auxiliary symmetric tensor W, such that

$$|D\mathbf{u}|W = D\mathbf{u}(1 - \exp(-m|D\mathbf{u}|)) \tag{2.9}$$

for Papanastasiou's regularization, and is

$$|D\mathbf{u}|_c W = D\mathbf{u} \tag{2.10}$$

for Corrected regularization.

In the mixed formulations according to the different approaches (2.9) or (2.10) replace the third equation in (2.8).

Here we investigate the numerical efficiency of applying the mixed formulation to solving the problem regularized by the two approaches: Papanastasiou's and Corrected Bercovier-Engelman regularizations.

To show the existence and uniqueness of the regularized equations we carry out an analysis following steps from [4] performed for Bercovier-Engelman regularization. Throughout the proofs we assume that $0 < m < M$, $\delta > 0$, $0 \leq \nu < \tilde{\nu}$, and $\alpha > 0$. The additional conditions on $\delta,\ \nu,\ \alpha$ will be specified later.

The formulations for Stokes equations, and in case of Corrected regularization follow promptly from the previous considerations.

2.4 Weak Formulation[1]

Let

$$\hat{\mu}_r = 2\mu + \frac{\tau_s}{|D\mathbf{u}|_r},$$

denote a regularized viscosity, where $|D\mathbf{u}|_r$ is a corresponding regularized strain tensor, $r = \{m, (\delta, \nu, \alpha)\}$.

To consider the weak formulation of the primitive and mixed formulations, we introduce the following bilinear forms:

$$a(\mathbf{u}, \mathbf{v}) \equiv \int_\Omega 2\mu D\mathbf{u} : D\mathbf{v}, \text{ on } \mathbf{H}_0^1 \times \mathbf{H}_0^1,$$

$$b(\mathbf{u}, \mathbf{v}) \equiv -\int_\Omega p\nabla \cdot \mathbf{v} \text{ on } \mathcal{L}_0^2 \times \mathbf{H}_0^1,$$

$$c(\mathbf{u}, Z) \equiv \int_\Omega \tau_s D\mathbf{u} : Z \text{ on } \mathbf{H}_0^1 \times \mathcal{L}_s^2,$$

and the forms

$$a_r(\mathbf{u}, \mathbf{v}) \equiv a(\mathbf{u}, \mathbf{v}) + \int_\Omega \tau_s \frac{D\mathbf{u} : D\mathbf{v}}{|D\mathbf{u}|_r} \text{ on } \mathbf{H}_0^1 \times \mathbf{H}_0^1,$$

$$a_m(\mathbf{u}, \mathbf{v}) \equiv a(\mathbf{u}, \mathbf{v}) + \int_\Omega \tau_s \frac{D\mathbf{u}}{|D\mathbf{u}|}(1 - \exp(-m|D\mathbf{u}|)) : D\mathbf{v} \text{ on } \mathbf{H}_0^1 \times \mathbf{H}_0^1,$$

[1]For notations see Appendix.

$$a_{\delta,\nu,\alpha}(\mathbf{u},\mathbf{v}) \equiv a(\mathbf{u},\mathbf{v}) + \int_\Omega \tau_s \frac{D\mathbf{u} : D\mathbf{v}}{|D\mathbf{u}|_c} \text{ on } \mathbf{H}_0^1 \times \mathbf{H}_0^1,$$

$$g(|D\mathbf{u}|, W, Z) \equiv \int_\Omega \tau_s |D\mathbf{u}| W : Z \text{ on } \mathbf{H}_0^1 \times \mathcal{L}_s^2 \times \mathcal{L}_s^\infty,$$

$$m(\mathbf{u},\mathbf{v}) \equiv \rho \int_\Omega \Big[\frac{\partial \mathbf{u}}{\partial t} \cdot \mathbf{v} + (\mathbf{u}\cdot\nabla)\mathbf{u}\cdot\mathbf{v}\Big] \text{ on } \mathbf{H}_0^1 \times \mathbf{H}_0^1.$$

Using the forms introduced above, we write the weak formulation of the Navier-Stokes type equations in primitive variables reads: find $\mathbf{u} \in \mathbf{H}_0^1$ and $p \in L_0^2$ such that for any $\mathbf{v} \in \mathbf{H}_0^1$ and $q \in L_0^2$

$$m(\mathbf{u},\mathbf{v}) + a_r(\mathbf{u},\mathbf{v}) - b(p,\mathbf{v}) + b(q,\mathbf{u}) = (\mathbf{f},\mathbf{v}). \tag{2.11}$$

And in the mixed formulation, we have: find $\mathbf{u} \in \mathbf{H}_0^1$, $p \in L_0^2$ and $W \in \mathcal{L}_s^2$ such that for any $\mathbf{v} \in \mathbf{H}_0^1$, $q \in L_0^2$ and $Z \in \mathcal{L}_s^\infty$

$$m(\mathbf{u},\mathbf{v}) + a_r(\mathbf{u},\mathbf{v}) - b(p,\mathbf{v}) + c(\mathbf{v},W) + b(q,\mathbf{u}) + c(\mathbf{u},Z) \tag{2.12}$$

$$-g(|D\mathbf{u}|_r), W, Z) = (\mathbf{f},\mathbf{v}).$$

The weak formulation of the regularized primitive steady Stokes type equations reads: find $\mathbf{u} \in \mathbf{H}_0^1$ and $p \in L_0^2$ such that for any $\mathbf{v} \in \mathbf{H}_0^1$ and $q \in L_0^2$ we have

$$\int_\Omega 2\mu D\mathbf{u} : D\mathbf{v} + \int_\Omega \tau_s \frac{D\mathbf{u} : D\mathbf{v}}{|D\mathbf{u}|_r} - \int_\Omega p\nabla\cdot\mathbf{v} - q\nabla\cdot\mathbf{u} = (\mathbf{f},\mathbf{v})$$

or

$$a_r(\mathbf{u},\mathbf{v}) - b(p,\mathbf{v}) + b(q,\mathbf{u}) = (\mathbf{f},\mathbf{v}). \tag{2.13}$$

For the mixed formulation the weak formulation of the Stokes type equations reads as follows: find $\mathbf{u} \in \mathbf{H}_0^1$, $p \in L_0^2$ and $W \in \mathcal{L}_s^2$ such that for any $\mathbf{v} \in \mathbf{H}_0^1$,

$q \in L_0^2$ and $Z \in \mathcal{L}_s^\infty$

$$\begin{aligned} a_r(\mathbf{u},\mathbf{v}) - b(p,\mathbf{v}) + c(\mathbf{v},W) + b(q,\mathbf{u}) + c(\mathbf{u},Z) \\ -g(|D\mathbf{u}|_r),W,Z) = (\mathbf{f},\mathbf{v}). \end{aligned} \tag{2.14}$$

Substituting in (2.11), (2.12), (2.13) and (2.14) a_r with a_m or $a_{\delta,\nu,\alpha}$, and $|D\mathbf{u}|_r$ with $|D\mathbf{u}|/(1-\exp(-m|D\mathbf{u}|)$ or $|D\mathbf{u}|_c$, we similarly can write the weak formulations for Papanastasiou's and Corrected regularization correspondingly.

Chapter 3

Well-Posedness analysis of the Bingham-Papanastasiou problem

3.1 Preliminaries

Here we remind some important inequalities [13], that we will use later.

From the vector identities $2\mathbf{div}D = \Delta + \nabla\nabla\cdot$ and $\nabla\nabla\cdot = \Delta + \nabla\times\nabla\times$ applying integration by parts one gets the following Korn type inequalities [23]

$$||D\mathbf{u}|| \leq ||\nabla\mathbf{u}|| \leq \sqrt{2}||D\mathbf{u}||, \tag{3.1}$$

for all $\mathbf{u} \in \mathbf{H}_0^1$.

Also, we will need the Friedrich's inequality, also known as Poincaré

inequality

$$||\mathbf{u}|| \leq C_F ||\nabla \mathbf{u}||, \tag{3.2}$$

for all $\mathbf{u} \in \mathbf{H}_0^1$, $C_F > 0$ is a constant depending only on the domain Ω.

In this chapter Ω is assumed to be polygonal or $\partial\Omega \in \mathcal{C}^{1,1}$, and $\mathbf{f} \in \mathbf{L}^2$. We also assume for simplicity homogeneous Dirichlet boundary conditions, i.e. $\mathbf{u} = 0$ on $\partial\Omega$.

The analysis is done for the regularized steady Stokes type case, but the generalization to mixed Dirichlet and Neumann boundary problems is also possible.

3.2 Theoretical tools

Let us remind the following fundamental results [15]:

Theorem 3.1. (Brouwer's Fixed Point Theorem)

Assume

$$\mathbf{g}(\mathbf{x}) : B(0,1) \to B(0,1)$$

is continuous, where $B(0,1)$ denotes the closed unit ball in $\mathbb{R}^d$, $d < \infty$. Then $\mathbf{g}(\mathbf{x})$ has a fixed point, i.e. there is a point $\mathbf{x} \in B(0,1)$ such that

$$\mathbf{g}(\mathbf{x}) = \mathbf{x}.$$

We recall here the monotonicity method described in the Section 9.1.

in [15]. Let $u : \Omega \to \mathbb{R}$, and consider the following PDE

$$\begin{cases} -\nabla \cdot \mathbf{a}(D\mathbf{u}) = \mathbf{f} & \text{in } \Omega \\ u = 0 & \text{on } \partial\Omega, \end{cases} \tag{3.3}$$

where the function $f \in L^2(\Omega)$ and the smooth vector field $\mathbf{a} : \mathbb{R}^d \to \mathbb{R}^d$ are given and $u \in H_0^1(\Omega)$ is the unknown.

Definition 3.2. *A vector field $\mathbf{a} : \mathbb{R}^d \to \mathbb{R}^d$ is called monotone if*

$$(\mathbf{a}(\mathbf{x}) - \mathbf{a}(\mathbf{y})) \cdot (\mathbf{x} - \mathbf{y}) \geq 0 \tag{3.4}$$

for all $\mathbf{x}, \mathbf{y} \in \mathbb{R}^d$.

Assume

$$|\mathbf{a}(\mathbf{x})| \leq C(1 + |\mathbf{x}|) \tag{3.5}$$

and

$$\mathbf{a}(\mathbf{x}) \cdot \mathbf{y} \geq \alpha|\mathbf{x}|^2 - \beta \tag{3.6}$$

for any $\mathbf{x}, \mathbf{y} \in \mathbb{R}^d$, and some $C, \alpha > 0$, $\beta \geq 0$.

Then, we recall the following

Theorem 3.3. (Browder-Minty) *[15] Assume $\mathbf{a}(\cdot, \cdot)$ to be monotone, and to satisfy* (3.5) *and* (3.6)*. Then there exists a weak solution of the nonlinear problem* (3.3)*.*

Definition 3.4. *A vector field $\mathbf{a} : \mathbb{R}^d \to \mathbb{R}^d$ is called strictly monotone if*

$$(\mathbf{a}(\mathbf{x}) - \mathbf{a}(\mathbf{y})) \cdot (\mathbf{x} - \mathbf{y}) \geq \theta|\mathbf{x} - \mathbf{y}|^2 \tag{3.7}$$

for all $\mathbf{x}, \mathbf{y} \in \mathbb{R}^d$, and some $\theta > 0$.

With the additional assumption of strict monotonicity, we will have uniqueness of the solution.

Theorem 3.5. *[15] Assume* $\mathbf{a}(\cdot)$ *is strictly monotone, then the solution of* (3.3) *is unique.*

3.3 Well-Posedness of the Primitive Formulation

In [4] was shown the well posedness for Bercovier-Engelman regularized Bingham problem. We conduct the proofs presented here for Papanastasiou's, and Corrected regularizations following the approach from [4].

Assume that $|D\mathbf{u}|_r$ is bounded from below

$$|D\mathbf{u}|_r \geq r_0 \geq 0. \tag{3.8}$$

Assume also that

$$|D\mathbf{u}|_r \geq |D\mathbf{u}|.$$

Let $\mathbf{V} \subset \mathbf{H}_0^1$ be a divergence free subspace. Then the problem (2.13) reduces to

$$a_m(\mathbf{u}, \mathbf{v}) = (\mathbf{f}, \mathbf{v}). \tag{3.9}$$

Proposition 3.6. *Let the form* a_r *be continuous*

$$a_r(\mathbf{u}, \mathbf{v}) \leq c(2\mu + \frac{\tau_s}{r_0})||\mathbf{u}||_1||\mathbf{v}||_1; \tag{3.10}$$

coercive

$$a_r(\mathbf{u}, \mathbf{u}) \geq c||\mathbf{u}||_1^2; \tag{3.11}$$

and the corresponding to it vector field be monotone.

Then the problem (2.13) *has a unique solution* $\{\mathbf{u}, p\} \in \mathbf{H}_0^1 \times L_0^2$ *satisfying the estimate*

$$||\nabla \mathbf{u}|| \leq \frac{1}{\mu}||\mathbf{f}||_{-1}, \ ||p|| \leq c(||\mathbf{f}||_{-1} + \tau_s \min\{1, \frac{1}{r_0}||\mathbf{f}||_{-1}\}). \tag{3.12}$$

Proof. By monotonicity , coercivity , continuity of a_r, and since $\mathbf{V} \subset \mathbf{H}_0^1$, we can apply Browder-Minty method of strictly monotone operators (Theorem 3.3) to prove the existence and uniqueness of the solution for (2.13).

To prove the equivalence of (2.13) and (3.9), and also existence and uniqueness of the pressure as Lagrange multiplier corresponding to the divergence free constraint, we can use the classical arguments from [17].

Let $\mathbf{u} = \mathbf{v}$, $q = p$, in (2.13). For $(\mathbf{f}, \mathbf{v}) \leq ||\mathbf{f}||_{-1}||\nabla \mathbf{v}||$, we have

$$2\mu||D\mathbf{u}||^2 \leq a_r(\mathbf{u}, \mathbf{u}) = (\mathbf{f}, \mathbf{u}) \leq ||\mathbf{f}||_{-1}||\mathbf{u}||.$$

Using the last inequality together with $||D\mathbf{u}|| \geq ||\nabla \mathbf{u}||/\sqrt{2}$ (3.1), we prove the first estimate in (3.19)

$$\mu||\nabla \mathbf{u}||^2 \leq 2\mu||D\mathbf{u}||^2 \leq ||\mathbf{f}||_{-1}||\nabla \mathbf{u}||.$$

To show the second estimate set $q = 0$ and divide (2.13) by $||\mathbf{v}||$, for $||\mathbf{v}|| \neq 0$, then, using $(\mathbf{f}, \mathbf{v}) \leq ||\mathbf{f}||_{-1}||\nabla \mathbf{v}||$, and the fact that $||D\mathbf{u}|| \leq ||\nabla \mathbf{u}||$ (3.1) we get

$$\frac{(\nabla \cdot \mathbf{v}, p)}{||\nabla \mathbf{v}||} = \frac{2\mu(D\mathbf{u}, D\mathbf{v}) + \tau_s(|D\mathbf{u}|_r^{-1} D\mathbf{u}, D\mathbf{v}) - (\mathbf{f}, \mathbf{v})}{||\nabla \mathbf{v}||}$$

$$\leq \frac{2\mu||\nabla \mathbf{u}||||\nabla \mathbf{v}|| + \tau_s(1, D\mathbf{v}) - ||\mathbf{f}||_{-1}||\nabla \mathbf{v}||}{||\nabla \mathbf{v}||} \leq 2\mu||\nabla \mathbf{u}|| + \tau_s\sqrt{|\Omega|} + ||\mathbf{f}||_{-1}.$$

Then we use the first estimate from (3.19) with Nečas inequality [23]

$$||p|| \leq c \sup_{\mathbf{v}\in\mathbf{H}_0^1} \frac{(\nabla \cdot \mathbf{v}, p)}{|\nabla \mathbf{v}|}, \tag{3.13}$$

applied to the last estimate. We have

$$||p|| \leq c(2\mu||\nabla \mathbf{u}|| + \tau_s\sqrt{|\Omega|} + ||\mathbf{f}||_{-1}).$$

On the other hand, it is easy to see that

$$||p|| \leq c(2\mu + \frac{\tau_s}{r_0})||\nabla \mathbf{u}|| + ||\mathbf{f}||_{-1}.$$

Then,

$$||p|| \leq 2c\mu||\nabla \mathbf{u}|| + c_1||\mathbf{f}||_{-1} + c\min\{\tau_s\sqrt{\Omega}, \frac{\tau_s}{r_0}||\nabla \mathbf{u}||\}. \tag{3.14}$$

Note that $2\mu||\nabla \mathbf{u}|| \leq \frac{1}{\mu}||\mathbf{f}||_{-1}$ and $\frac{\tau_s}{r_0}||\nabla \mathbf{u}|| \leq \frac{\tau_s}{\mu}||f||_{-1}$. Plugging these estimates to (3.14), we obtain the upper bound for p.

□

Let now show that the Proposition 3.6 is valid for the regularizations we consider.

3.3.1 Papanastasiou's regularization

Lemma 3.7. *The form $a_m(\cdot,\cdot)$ introduced in section 2.4 is coercive and continuous for any $0 < m < M$, for M finite.*

Proof. Using the Korn and Friedrich's inequalities, since $m > 0$ we have for any $\mathbf{u} \in H_0^1(\Omega)$.

$$a_m(\mathbf{u},\mathbf{u}) = \int_\Omega 2\mu D\mathbf{u} : D\mathbf{u} + \int_\Omega \tau_s \frac{D\mathbf{u}}{|D\mathbf{u}|}(1-\exp(-m|D\mathbf{u}|)) : D\mathbf{u} \geq$$
$$\geq \int_\Omega 2\mu |D\mathbf{u}|^2 = 2\mu|\Omega||D\mathbf{u}|^2 \geq c||\mathbf{u}||_1^2. \tag{3.15}$$

In addition, notice that

$$a_m(\mathbf{u},\mathbf{v}) = \int_\Omega 2\mu D\mathbf{u} : D\mathbf{v} + \int_\Omega \tau_s \frac{D\mathbf{u}}{|D\mathbf{u}|}(1-\exp(-m|D\mathbf{u}|)) : D\mathbf{v}$$
$$\leq \int_\Omega 2\mu |D\mathbf{u} : D\mathbf{v}| + \int_\Omega \tau_s \frac{|D\mathbf{u} : D\mathbf{v}|}{|D\mathbf{u}|}(1-\exp(-m|D\mathbf{u}|))$$
$$\leq |\Omega|(2\mu+\tau_s m)|D\mathbf{u}||D\mathbf{v}| \leq c(2\mu+\tau_s m)||\mathbf{u}||_1||\mathbf{v}||_1. \tag{3.16}$$

Here we have used the fact that $\frac{1-\exp(-m|x|)}{|x|}$ has the only maximum in $|x| = 0$ where it has a removable singularity, and by (2.5) takes the value m. The form is therefore continuous with continuity constant $2\mu + \tau_s m$. Note that for $m \to \infty$ (not regularized case) the continuity constant tends to infinity. The results therefore hold for $m \leq M$, $\tau_M = 2\mu + \tau_s M$.

□

To satisfy the conditions of Proposition 3.6, we need to show the monotonicity of the corresponding vector field.

Lemma 3.8. *Let* $\tilde{\mathbf{a}}_m(\mathbf{w}) = \mu\mathbf{w} + \tau_s \frac{\mathbf{w}}{|\mathbf{w}|}(1-\exp(-m|\mathbf{w}|))$ *be a vector field, and define a scalar product as*

$$(\mathbf{w},\mathbf{v}) = \int_\Omega D\mathbf{w} : D\mathbf{v}.$$

Then, the vector field $\tilde{\mathbf{a}}_m(\cdot)$ *is monotone.*

Proof. In (3.4) set $\mathbf{x} = \mathbf{u}$, and $\mathbf{y} = \mathbf{u} - \mathbf{v}$. Showing that the vector field $\tilde{\mathbf{a}}_m$ is monotone is equivalent to showing that the form a_m satisfies the following

$$a_m(\mathbf{u}, \mathbf{v}) - a_m(\mathbf{u} - \mathbf{v}, \mathbf{v}) \geq c||\mathbf{v}||_1^2. \tag{3.17}$$

Consider

$$\begin{gathered} a_m(\mathbf{u}, \mathbf{v}) - a_m(\mathbf{u} - \mathbf{v}, \mathbf{v}) = \\ \int_\Omega 2\mu D\mathbf{u} : D\mathbf{v} + \int_\Omega \tau_s \frac{D\mathbf{u}}{|D\mathbf{u}|}(1 - \exp(-m|D\mathbf{u}|)) : D\mathbf{v} \\ - \int_\Omega 2\mu D(\mathbf{u} - \mathbf{v}) : D\mathbf{v} - \int_\Omega \tau_s \frac{D(\mathbf{u} - \mathbf{v})}{|D(\mathbf{u} - \mathbf{v})|}(1 - \exp(-m|D(\mathbf{u} - \mathbf{v})|)) : D\mathbf{v}. \end{gathered} \tag{3.18}$$

Then we combine the common terms in (3.18)

$$\int_\Omega 2\mu|D\mathbf{v}|^2 + \int_\Omega \tau_s \Big[\frac{D\mathbf{u}}{|D\mathbf{u}|}(1-\exp(-m|D\mathbf{u}|)) - \frac{D(\mathbf{u}-\mathbf{v})}{|D(\mathbf{u}-\mathbf{v})|}(1-\exp(-m|D(\mathbf{u}-\mathbf{v})|))\Big] : D\mathbf{v}$$

$$= \int_\Omega 2\mu|D\mathbf{v}|^2 + \int_\Omega \tau_s \Big[\frac{D\mathbf{u}}{|D\mathbf{u}|}(1-\exp(-m|D\mathbf{u}|)) - \frac{D(\mathbf{u})}{|D(\mathbf{u}-\mathbf{v})|}(1-\exp(-m|D(\mathbf{u}-\mathbf{v})|))\Big] : D\mathbf{v}$$

$$+ \int_\Omega \tau_s \frac{|D\mathbf{v}|^2}{|D(\mathbf{u}-\mathbf{v})|}(1 - \exp(-m|D(\mathbf{u}-\mathbf{v})|)).$$

Note that $\frac{1-\exp(-mx)}{x}$ is a decreasing function for $x > 0$.

We prove that

$$\int_\Omega \tau_s \Big[\frac{D\mathbf{u}}{|D\mathbf{u}|}(1 - \exp(-m|D\mathbf{u}|))$$

$$-\frac{D\mathbf{u}}{|D(\mathbf{u}-\mathbf{v})|}(1-\exp(-m|D(\mathbf{u}-\mathbf{v})|))\Big] : D\mathbf{v} \geq 0.$$

We distinguish four possible cases.

Case 1. $|D\mathbf{u}| < |D(\mathbf{u}-\mathbf{v})|,\ D\mathbf{u} : D\mathbf{v} > 0$

In this case we have

$$\int_\Omega \tau_s\Big[\frac{D\mathbf{u}}{|D\mathbf{u}|}(1-\exp(-m|D\mathbf{u}|)) - \frac{D(\mathbf{u})}{|D(\mathbf{u}-\mathbf{v})|}(1-\exp(-m|D(\mathbf{u}-\mathbf{v})|))\Big] : D\mathbf{v}$$
$$\geq \int_\Omega \tau_s\Big[\frac{D\mathbf{u}}{|D\mathbf{u}|}(1-\exp(-m|D\mathbf{u}|)) - \frac{D\mathbf{u}}{|D\mathbf{u}|}(1-\exp(-m|D\mathbf{u}|))\Big] : D\mathbf{v} = 0.$$

Case 2. $|D\mathbf{u}| > |D(\mathbf{u}-\mathbf{v})|,\ D\mathbf{u} : D\mathbf{v} > 0.$

In this case

$$\int_\Omega \tau_s\Big[\frac{D\mathbf{u}}{|D\mathbf{u}|}(1-\exp(-m|D\mathbf{u}|)) - \frac{D(\mathbf{u})}{|D(\mathbf{u}-\mathbf{v})|}(1-\exp(-m|D(\mathbf{u}-\mathbf{v})|))\Big] : D\mathbf{v}$$
$$\geq \int_\Omega \tau_s\Big[\frac{D(\mathbf{u})}{|D(\mathbf{u}-\mathbf{v})|}(1-\exp(-m|D(\mathbf{u}-\mathbf{v})|))$$
$$-\frac{D(\mathbf{u})}{|D(\mathbf{u}-\mathbf{v})|}(1-\exp(-m|D(\mathbf{u}-\mathbf{v})|))\Big] : D\mathbf{v} = 0.$$

Case 3. $|D\mathbf{u}| > |D(\mathbf{u}-\mathbf{v})|,\ D\mathbf{u} : D\mathbf{v} < 0.$

Now we have

$$\int_\Omega \tau_s\Big[\frac{D\mathbf{u}}{|D\mathbf{u}|}(1-\exp(-m|D\mathbf{u}|)) - \frac{D(\mathbf{u})}{|D(\mathbf{u}-\mathbf{v})|}(1-\exp(-m|D(\mathbf{u}-\mathbf{v})|))\Big] : D\mathbf{v}$$

$$\geq \int_\Omega \tau_s \Big[\frac{D\mathbf{u}}{|D\mathbf{u}|}(1-\exp(-m|D\mathbf{u}|)) - \frac{D\mathbf{u}}{|D\mathbf{u}|}(1-\exp(-m|D\mathbf{u}|)) \Big] : D\mathbf{v} = 0.$$

Case 4. $|D\mathbf{u}| < |D(\mathbf{u}-\mathbf{v})|,\ D\mathbf{u} : D\mathbf{v} < 0.$

Suitable steps as for the previous cases will give

$$\int_\Omega \tau_s \Big[\frac{D\mathbf{u}}{|D\mathbf{u}|}(1-\exp(-m|D\mathbf{u}|)) - \frac{D(\mathbf{u})}{|D(\mathbf{u}-\mathbf{v})|}(1-\exp(-m|D(\mathbf{u}-\mathbf{v})|)) \Big] : D\mathbf{v}$$
$$\geq \int_\Omega \tau_s \Big[\frac{D(\mathbf{u})}{|D(\mathbf{u}-\mathbf{v})|}(1-\exp(-m|D(\mathbf{u}-\mathbf{v})|))$$
$$-\frac{D(\mathbf{u})}{|D(\mathbf{u}-\mathbf{v})|}(1-\mathbf{e}(-m|D(\mathbf{u}-\mathbf{v})|)) \Big] : D\mathbf{v} = 0.$$

Since $\int_\Omega \tau_s \frac{|D\mathbf{v}|^2}{|D(\mathbf{u}-\mathbf{v})|}(1-\exp(-m|D(\mathbf{u}-\mathbf{v})|)) \geq 0$, we conclude that for any $\mathbf{u}, \mathbf{v} \in \mathbf{H}_0^1$ there exists $c > 0$ such that

$$a_m(\mathbf{u},\mathbf{v}) - a_m(\mathbf{u}-\mathbf{v},\mathbf{v}) \geq \int_\Omega 2\mu |D\mathbf{v}|^2 \geq 0,$$

and (3.17) holds.

□

Therefore, Papanastasiou's regularization satisfies all conditions of Proposition 3.6, and can be reformulated the following way

Proposition 3.9. *For $0 < m < M$, the problem (2.13) with $|D\mathbf{u}|_r = |D\mathbf{u}|/(1-\exp(-m|D\mathbf{u}|)$ has a unique solution $\{\mathbf{u}, p\} \in \mathbf{H}_0^1 \times L_0^2$ satisfying the estimate*

$$||\nabla \mathbf{u}|| \leq \frac{1}{\mu}||\mathbf{f}||_{-1},\ ||p|| \leq c(||\mathbf{f}||_{-1} + \tau_s \min\{1, m||\mathbf{f}||_{-1}\}). \tag{3.19}$$

Notice that the results of the Proposition 3.9 hold only for $0 < m < M$. If $m \to \infty$, the continuity constant $2\mu + \tau_s m \to \infty$, so the conditions of Theorem 3.3 are not satisfied, and the results do not hold. In this case the correction term $1 - \exp(-m|D\mathbf{u}|) = 1$, and we arrive to the classical Bingham problem, for that the question is still open.

3.3.2 Corrected regularization

To perform the proofs for the case of Corrected regularization, we need to know the lower estimate of $|D\mathbf{u}|_c$. By construction, $|D\mathbf{u}|_c$ is bounded from below, therefore we find the bound as a function of δ, ν, α.

Lemma 3.10. *Let*

$$\phi(x) = \sqrt{x^2 + \delta^2 \exp(-2\nu x^\alpha)},\ x > 0,$$

then for any $0 < \delta < 1$, $0 < \nu < \bar{\nu}$, *and* $\alpha > 0$

$$\phi(x) = \sqrt{x^2 + \delta^2 \exp(-2\nu x^\alpha)} \geq \min\{\frac{\delta}{e}, \frac{1}{\nu^{1/\alpha}}\}.$$

Proof. Let first $0 \leq x \leq \frac{1}{\nu^{1/\alpha}}$. Since $\delta^2 \exp(-2\nu x^\alpha)$ is decreasing, we have the following estimate

$$\sqrt{x^2 + \delta^2 \exp(-2\nu x^\alpha)} \geq \delta \exp(-\nu x^\alpha) \geq \frac{\delta}{e}.$$

Assume now that $x > \frac{1}{\nu^{1/\alpha}}$. In this case the estimate will be

$$\sqrt{x^2 + \delta^2 \exp(-2\nu x^\alpha)} \geq x \geq \frac{1}{\nu^{1/\alpha}}.$$

Combining these results, we prove Lemma. □

Then, using the result of Lemma 3.10, we can exactly repeat the steps from [4], performed there to establish the well-posedness for the problem regularized by Bercovier-Engelman approach. And in case of Corrected regularization, we obtain the following statements.

Lemma 3.11. *The form $a_{\delta,\nu,\alpha}(\cdot,\cdot)$ introduced in section 2.4 is coercive and continuous for any $\delta > 0$, $0 < \nu < \bar{\nu}$ finite, and $\alpha > 0$ i.e.*

$$a_{\delta,\nu,\alpha}(\mathbf{u},\mathbf{u}) =\geq c||\mathbf{u}||_1^2, \tag{3.20}$$

$$a_{\delta,\nu,\alpha}(\mathbf{u},\mathbf{v}) \leq c(2\mu + \tau_s \max\{\frac{e}{\delta}, \nu^{1/\alpha}\})||\mathbf{u}||_1||\mathbf{v}||_1. \tag{3.21}$$

Proof. Applying the Korn and Friedrich's inequalities on $a_{\delta,\nu,\alpha}(\mathbf{u},\mathbf{u})$, we have for any $\mathbf{u} \in H_0^1(\Omega)$.

$$a_{\delta,\nu,\alpha}(\mathbf{u},\mathbf{u}) = \int_\Omega 2\mu D\mathbf{u} : D\mathbf{u} + \int_\Omega \tau_s \frac{D\mathbf{u} : D\mathbf{u}}{|D\mathbf{u}|_c} \geq$$

$$\geq \int_\Omega 2\mu |D\mathbf{u}|^2 = 2\mu|\Omega||D\mathbf{u}|^2 \geq c||\mathbf{u}||_1^2. \tag{3.22}$$

Also, notice that

$$a_{\delta,\nu,\alpha}(\mathbf{u},\mathbf{v}) = \int_\Omega 2\mu D\mathbf{u} : D\mathbf{v} + \int_\Omega \tau_s \frac{D\mathbf{u} : D\mathbf{v}}{|D\mathbf{u}|_c}$$

$$\leq \int_\Omega 2\mu |D\mathbf{u} : D\mathbf{v}| + \int_\Omega \tau_s \frac{|D\mathbf{u} : D\mathbf{v}|}{|D\mathbf{u}|_c}$$

$$\leq |\Omega|(2\mu + \tau_s m)|D\mathbf{u}||D\mathbf{v}| \leq c(2\mu + \tau_s \max\{\frac{e}{\delta}, \nu^{1/\alpha}\})||\mathbf{u}||_1||\mathbf{v}||_1. \tag{3.23}$$

□

Remark 3.12. *The continuity constant of the form is $2\mu + \tau_s \max\{\frac{e}{\delta}, \nu^{1/\alpha}\}$. Therefore, the conditions $\delta > 0$, $0 < \nu < \bar{\nu}$ with $\bar{\nu}$ finite are crucial, and if they break the result does not hold.*

Lemma 3.13. *Let* $\tilde{\mathbf{a}}_{\delta,\nu,\alpha}(\mathbf{w}) = \mu\mathbf{w} + \tau_s \frac{\mathbf{w}}{|\mathbf{w}|_c}$ *be a vector field, and define a scalar product as*

$$(\mathbf{w}, \mathbf{v}) = \int_\Omega D\mathbf{w} : D\mathbf{v}.$$

Then, the vector field $\tilde{\mathbf{a}}_{\delta,\nu,\alpha}(\cdot)$ *is monotone, that is*

$$a_{\delta,\nu,\alpha}(\mathbf{u}, \mathbf{u}-\mathbf{v}) - a_{\delta,\nu,\alpha}(\mathbf{v}, \mathbf{u}-\mathbf{v}) \geq c||\mathbf{u}-\mathbf{v}||_1^2. \tag{3.24}$$

Proof. Consider $a_{\delta,\nu,\alpha}(\mathbf{u}, \mathbf{u}-\mathbf{v}) - a_{\delta,\nu,\alpha}(\mathbf{v}, \mathbf{u}-\mathbf{v}) = \int_\Omega 2\mu D\mathbf{u} : D(\mathbf{u}-\mathbf{v}) +$
$\int_\Omega \tau_s \frac{D\mathbf{u}}{|D\mathbf{u}|_c} \,:\, D(\mathbf{u}-\mathbf{v}) - \int_\Omega 2\mu D\mathbf{v} \,:\, D(\mathbf{u}-\mathbf{v}) + \int_\Omega \tau_s \frac{D\mathbf{v}}{|D\mathbf{v}|_c} \,:\, D(\mathbf{u}-\mathbf{v})$
$= \int_\Omega 2\mu |D(\mathbf{u}-\mathbf{v})|^2 + \int_\Omega \tau_s \left(\frac{D\mathbf{u}-D\mathbf{v}}{|D\mathbf{u}|_c} - \frac{|D\mathbf{u}|_c - |D\mathbf{v}|_c}{|D\mathbf{u}|_c |D\mathbf{v}|_c} D\mathbf{v} \right) \,:\, D(\mathbf{u}-\mathbf{v})$
$\geq \int_\Omega 2\mu |D(\mathbf{u}-\mathbf{v})|^2 + \int_\Omega \frac{\tau_s}{|D\mathbf{u}|_c} \left(|D\mathbf{u}-D\mathbf{v}|^2 - \frac{|D\mathbf{u}-D\mathbf{v}|}{|D\mathbf{v}|_c} D\mathbf{v} : D(\mathbf{u}-\mathbf{v}) \right)$
$\geq \int_\Omega 2\mu |D(\mathbf{u}-\mathbf{v})|^2 + \int_\Omega \frac{\tau_s |D\mathbf{u}-D\mathbf{v}|^2}{|D\mathbf{u}|_c} \left(1 - \frac{D\mathbf{v}}{|D\mathbf{v}|_c} \right) \geq \int_\Omega 2\mu |D(\mathbf{u}-\mathbf{v})|^2.$

Applying Korn's inequality (3.1) to the last line, we prove (3.24). □

Consider now the weak formulation of the regularized with the Corrected regularization primitive steady Stokes type equations: find $\mathbf{u} \in \mathbf{H}_0^1$ and $p \in L_0^2$ such that for any $\mathbf{v} \in \mathbf{H}_0^1$ and $q \in L_0^2$ we have

$$a_{\delta,\nu,\alpha}(\mathbf{u}, \mathbf{v}) - b(p, \mathbf{v}) + b(q, \mathbf{u})) = (\mathbf{f}, \mathbf{v}). \tag{3.25}$$

Thus, Corrected regularization also satisfies all conditions of Proposition 3.6, and reads:

Proposition 3.14. *For* $\delta > 0$, $\alpha > 0$, *and* $0 < \nu < \tilde{\nu}$ *the problem* (3.25) *with* $|D\mathbf{u}|_r = |D\mathbf{u}|_c$ *has a unique solution* $\{\mathbf{u}, p\} \in \mathbf{H}_0^1 \times L_0^2$ *satisfying the*

estimate

$$||\nabla \mathbf{u}|| \leq \frac{1}{\mu}||\mathbf{f}||_{-1},\ ||p|| \leq c(||\mathbf{f}||_{-1} + \tau_s \min\{1, \max\{\frac{e}{\delta}, \nu^{1/\alpha}\}||\mathbf{f}||_{-1}\}). \quad (3.26)$$

Observe that the results of the Proposition 3.14, similarly to previous case (Propositions 3.9), hold only for $\delta > 0$, $0 < \nu < \bar{\nu}$, and $\alpha > 0$.

3.4 Well-Posedness of The Mixed Formulation

In this section we consider the well-posedness of Bingham problem in the mixed formulation.

Theorem 3.15. *Let $W \in \mathcal{L}^\infty_s$. The problem* (2.14) *has a unique solution $\{\mathbf{u}, p, W\} \in \mathbf{H}^1_0 \times L^2_0 \times L^2_s$ such that*

$$||\mathbf{u}||^2_1 + \tau_s r_0 ||W||^2 \leq ||\mathbf{f}||_{-1}, \quad ||p|| \leq c(||\mathbf{f}||_{-1} + \tau_s \min\{1, \frac{1}{r_0}||\mathbf{f}||_{-1}\}) \quad (3.27)$$

Proof. First we show the equivalence between (2.13) and (2.14).

Let $\{\mathbf{u}, p\} \in \mathbf{H}^1_0 \times L^2_0$ be a solution of (2.13). Recall $W = \frac{D\mathbf{u}}{|D\mathbf{u}|_r}$.

Since $W \in \mathcal{L}^\infty_s$, the equalities $W = \frac{D\mathbf{u}}{|D\mathbf{u}|_r}$ together with $D\mathbf{u} = \frac{|D\mathbf{u}|_r}{W}$ both hold in $\mathcal{L}^2_s$.

Therefore, in case of mixed formulation

$$a(\mathbf{u}, \mathbf{v}) + c(\mathbf{v}, W) \equiv a_r(\mathbf{u}, \mathbf{v}). \quad (3.28)$$

This means that $\{\mathbf{u}, p, W\}$ satisfies (2.14) for all $\{\mathbf{v}, q, Z\} \in \mathbf{H}_0^1 \times L_0^2 \times \mathcal{L}_s^\infty$. Then, by Proposition 3.6, the solution of (2.14) exists.

Assume now that we have a solution $\{\mathbf{u}, p, W\}$ of the equation (2.14). Let $\mathbf{v} = 0, q = 0$, $Z \in \mathcal{L}_s^\infty$. Then

$$\int_\Omega \tau_s D\mathbf{u} : Z - \tau_s |D\mathbf{u}|_r W : Z = 0,$$

and

$$W = \frac{D\mathbf{u}}{|D\mathbf{u}|_r}, \tag{3.29}$$

holds almost everywhere in $\mathcal{L}_s^1 \equiv (\mathcal{L}_s^\infty)'$.

Now, set $Z = 0$, and plug (3.29) into (2.14). We have that $\mathbf{u}, p$ satisfy (2.13). By Proposition 3.6, the solution of (2.14)unique.

To obtain estimates (3.27), we set $\mathbf{v} = \mathbf{u}, q = p, Z = W$, and apply to (2.14), then the proof is similar to the proof of (3.19).

□

3.4.1 Papanastasiou's regilarization

The mixed formulation in this case reads: find $\mathbf{u} \in \mathbf{H}_0^1$, $p \in L_0^2$ and $W \in \mathcal{L}_s^2$ such that for any $\mathbf{v} \in \mathbf{H}_0^1$, $q \in L_0^2$ and $Z \in \mathcal{L}_s^\infty$,

$$a_m(\mathbf{u}, \mathbf{v}) - b(p, \mathbf{v}) + c(\mathbf{v}, W) + b(q, \mathbf{u})) \tag{3.30}$$

$$+c(\mathbf{u}, Z) - g(|D\mathbf{u}|/(1 - exp(-m|D\mathbf{u}|)), W, Z) = (\mathbf{f}, \mathbf{v}).$$

Theorem 3.16. *For $0 < m < M$, Papanastasiou's regularization satisfies Theorem 3.15 with*

$$||\mathbf{u}||_1^2 + \frac{\tau_s}{m}||W||^2 \leq ||\mathbf{f}||_{-1}, \quad ||p|| \leq c(||\mathbf{f}||_{-1} + \tau_s \min\{1, m||\mathbf{f}||_{-1}\}) \tag{3.31}$$

Moreover $W \in L_s^\infty$ and

$$||W||_{L^\infty} \leq 1.$$

Proof. First, we need to make sure that W is measurable.

Let $W = \phi(|D\mathbf{u}|)D\mathbf{u}$, where $\phi = \frac{1-\exp(-m|D\mathbf{u}|)}{|D\mathbf{u}|}$. Note, that $D\mathbf{u}$ is measurable, since $D\mathbf{u} \in \mathcal{L}_s^2$. Define $\phi_n = \frac{k}{n}$, for $k \in \mathbb{N}$, if $\frac{k}{n} \leq \phi < \frac{k+1}{n}$. The way we construct the sequences is shown on Figure 3.1.

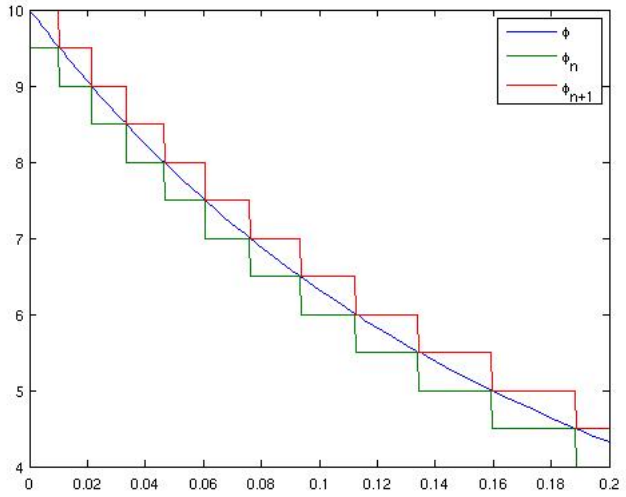

Figure 3.1: The construction of the sequences.

Note, that this approach of building sequences is possible as long as the function ϕ is bounded from both sides ($0 < \phi < m$). Then $|\phi - \phi_n| < \frac{1}{n}$

and ϕ_n converges uniformly to ϕ. Hence, ϕ is a measurable function, and W is measurable as a product of measurable functions.

Now, by construction $|W| = 1 - \exp(-m|D\mathbf{u}|) < 1$. Then $W \in \mathcal{L}_s^\infty$. □

Observe that the Theorem 3.16 is valid only in case $0 < m < M$, and is not valid if $m \to \infty$. The extension of the results of the Theorem 3.16 and Proposition 3.9 to the case $m \to \infty$, i.e. to the case of non-regularized formulation, is still an open issue.

3.4.2 Corrected regularization

For the mixed formulation in this case: find $\mathbf{u} \in \mathbf{H}_0^1$, $p \in L_0^2$ and $W \in \mathcal{L}_s^2$ such that for any $\mathbf{v} \in \mathbf{H}_0^1$, $q \in L_0^2$ and $Z \in \mathcal{L}_s^\infty$,

$$a_{\delta,\nu,\alpha}(\mathbf{u},\mathbf{v}) - b(p,\mathbf{v}) + c(\mathbf{v},W) + b(q,\mathbf{u})) + c(\mathbf{u},Z) - g(|D\mathbf{u}|_c,W,Z) = (\mathbf{f},\mathbf{v}), \tag{3.32}$$

we prove the following theorem.

Theorem 3.17. *For $\delta > 0$, $0 < \nu < \bar{\nu}$, and $\alpha > 0$, Corrected regularization satisfies Theorem 3.15 with*

$$\begin{gathered} ||\mathbf{u}||_1^2 + \tau_s \max\{\tfrac{e}{\delta}, \nu^{1/\alpha}\}||W||^2 \le ||\mathbf{f}||_{-1}, \\ ||p|| \le c\left(||\mathbf{f}||_{-1} + \tau_s \min\left\{1, \max\{\tfrac{e}{\delta}, \nu^{1/\alpha}\}||\mathbf{f}||_{-1}\right\}\right) \end{gathered} \tag{3.33}$$

Moreover $W \in L_s^\infty$ and

$$||W||_{L^\infty} \le 1.$$

Proof.

As long as $D\mathbf{u} \in \mathcal{L}_s^\infty$, it is measurable, and $|D\mathbf{u}|_c > 0$, we conclude that W is measurable as a product of measurable functions.

Now, by construction $|W| < 1$. Then $W \in \mathcal{L}_s^\infty$, and we can apply Theorem 3.15. $\square$

Chapter 4

Numerical Approximation

4.1 The Picard Linearization Method

Bingham-Papanastasiou problem is a non-linear system of partial differential equations that can be solved analytically only in special cases. In general, it requires a numerical approximation procedure to perform a quantitative analysis. As for any non-linear system of partial differential equations, two steps are crucial

1. Linearization of the non-linear terms,
2. Discretization of the differential problem.

The two steps can be performed in any order, but in general they do not have the same results. Here we first linearize, and then discretize, to emphasize the role of the mixed formulation in the regularization of the problem. This

formulation actually improves the regularity properties of the problem to be regularized, and this reflects into better numerical performances. With this, we mean that the mixed formulation requires less numerical iterations to converge vs. the primal one.

In particular, we consider the linearization of the formulation in primitive variables the following way. For an initial choice $\mathbf{u}^0$ the iterations will be: find

$$\begin{cases} \rho[\frac{\partial \mathbf{u}^k}{\partial t} + (\mathbf{u}^{k-1} \cdot \nabla)\mathbf{u}^k] - \nabla(2\mu D\mathbf{u}^k & \\ +\tau_s \frac{|\mathbf{u}^k|}{|D\mathbf{u}^{k-1}|_r}) + \nabla p^k & = \mathbf{f} \\ \nabla \mathbf{u}^k & = 0 \end{cases} \tag{4.1}$$

$k = 1, 2, ...$ up to some k, for which the convergence criterion is satisfied. As a convergence criterion, if not stated otherwise, we use $\frac{||r_k||_\infty}{||r_0||_\infty} \leq tol$, where $||r_0||_\infty$ is the initial residual, $||r_k||_\infty$ is the residual after k-th iteration, and tol is a chosen tolerance.

For the mixed formulation the initial choice is $\mathbf{u}^{(0)}$, and iterations are

$$\begin{cases} \rho[\frac{\partial \mathbf{u}^{(k)}}{\partial t} + (\mathbf{u}^{(k-1)} \cdot \nabla)\mathbf{u}^{(k)}] - \nabla(2\mu D\mathbf{u}^{(k)} + \tau_s W^{(k)}) + \nabla p^{(k)} = \mathbf{f} \\ \nabla \mathbf{u}^{(k)} = 0 \\ |D\mathbf{u}^{(k-1)}|_r W^{(k)} = D\mathbf{u}^{(k)}. \end{cases} \tag{4.2}$$

4.1.1 Well-Posedness of the Picard Iteration

Let $\beta \in \mathbf{H}_0^1$ be a given vector field.

The first auxiliary problem will read the following way: find $\mathbf{u}$, p such

that

$$\begin{cases} -\nabla \cdot \left((2\mu D\mathbf{u} + \tau_s \frac{1}{|D\beta|_r})D\mathbf{u}\right) + \nabla p = \mathbf{f} \\ \nabla \mathbf{u} = 0 \end{cases} \text{ in } \Omega \tag{4.3}$$

$$\mathbf{u} = 0 \text{ on } \partial\Omega.$$

Set

$$a_\beta(\mathbf{u}, \mathbf{v}) = \int_\Omega \left(2\mu + \frac{1}{|D\beta|_r}\right) D\mathbf{u} : D\mathbf{v}$$

on $\mathbf{V} \times \mathbf{V}$. Then the weak formulation is for all $(\mathbf{v}, q) \in \mathbf{H}_0^1 \times L_0^2$ find $(\mathbf{u}, p) \in \mathbf{H}_0^1 \times L_0^2$ such that

$$a_\beta(\mathbf{u}, \mathbf{v}) + b(p, \mathbf{v}) - b(q, \mathbf{u}) = (\mathbf{f}, \mathbf{v}). \tag{4.4}$$

Proposition 4.1. *Given $\mathbf{f} \in \mathbf{L}^2$ and $\beta \in \mathbf{H}_0^1$ there exists a unique solution $(\mathbf{u}, p)$ to*

$$a_\beta(\mathbf{u}, \mathbf{v}) + b(p, \mathbf{v}) - b(q, \mathbf{u}) = (\mathbf{f}, \mathbf{v}) \tag{4.5}$$

Proof. Coercivity of a_β is straightforward from Korn and Friedrich's inequalities (3.1), (3.2):

$$a_\beta(\mathbf{u}, \mathbf{u}) = \int_\Omega \left(2\mu + \frac{1}{|D\beta|_r}\right) D\mathbf{u} : D\mathbf{u}$$

$$\geq 2\mu |Du|^2 \geq c\mu ||\nabla \mathbf{u}||^2 \geq c||\mathbf{u}||_1^2.$$

We can equivalently define the divergence free subspace $\mathbf{V}$ as

$$\mathbf{V} = \{\mathbf{v} \in \mathbf{H}_0^1 : b(q, \mathbf{v}) = 0 \ \forall q \in L_0^2\},$$

and then by Corollary 5.1 from [17] we also have continuity of a_β. □

We continue here the analysis for Stokes equations, started in Chapters 2,3. The second auxiliary problem then reads: find $(\mathbf{u}, p, W) \in \mathbf{H}_0^1 \times L_0^2 \times \mathcal{L}_s^2$ such that

$$\begin{cases} -\nabla(2\mu D\mathbf{u} + \tau_s W) + \nabla p = \mathbf{f} \\ \nabla \cdot \mathbf{u} = 0 \quad \text{in } \Omega. \\ |D\beta|_r W = D\mathbf{u} \end{cases} \tag{4.6}$$

Let us introduce a bilinear form

$$g_r(W, Z) = \int_\Omega \tau_s |D\beta|_r W : Z.$$

Then we can formulate a weak form of the second auxiliary problem (4.6): find $(\mathbf{u}, p, W) \in \mathbf{H}_0^1 \times L_0^2 \times \mathcal{L}_s^2$ such that for any $(\mathbf{v}, q, Z) \in \mathbf{H}_0^1 \times L_0^2 \times \mathcal{L}_s^\infty$

$$a(\mathbf{u}, \mathbf{v}) + b(p, \mathbf{v}) - b(q, \mathbf{u}) + c(\mathbf{v}, W) - c(\mathbf{u}, Z) + g_r(W, Z) = (\mathbf{f}, \mathbf{v}). \tag{4.7}$$

Proposition 4.2. *There exists a unique solution* $(\mathbf{u}, p, W) \in \mathbf{H}_0^1 \times L_0^2 \times \mathcal{L}_s^2$ *of* (4.7)

Proof. Let $W = \frac{D\mathbf{u}}{|D\beta|_r} \in \mathcal{L}_s^\infty$. Let $(\mathbf{u}, p)$ be a solution of (4.4). Then $(\mathbf{u}, p, W)$ solves (4.7).

Assume now that $(\mathbf{u}, p, W)$ is a solution of (4.7). Set $\mathbf{v} = 0, q = 0,$

and let $Z \in \mathcal{L}_s^\infty$. We will get that

$$W = \frac{D\mathbf{u}}{|D\beta|_r} \text{ in } (\mathcal{L}_s^\infty)' \equiv \mathcal{L}_s^1.$$

Plugging it into (4.7), and setting $Z = 0$, we obtain that $(\mathbf{u}, p)$ is a solution of (4.4).

Therefore, equations (4.4) and (4.7) are equivalent. Applying Proposition 4.1, we have Proposition 4.2 proved. □

4.1.2 Error Estimates for the Picard Iterative Scheme

Here we conduct the analysis of error estimates for formulation in primitive variables, and for the mixed formulation. The importance of the section result is that we estimate the rate of convergence, and the impact of the regularization parameter in it for both approaches, and for two considered regularizations.

Papanastasiou's regularization

Denote by $(\mathbf{u}, p, W)$ the solution of (2.14). Then $(\mathbf{u}, p)$ also solve (2.13).

Let $\mathbf{e}^{(k)} \equiv \mathbf{u}^{(k)} - \mathbf{u}$, $e^{(k)} = p^{(k)} - p$ and $E^{(k)} = W^{(k)} - W$. We first consider the iterations for the problem in primitive variables (4.1) with $|D\mathbf{u}|_r = |D\mathbf{u}|/(1-\exp(-m|D\mathbf{u}|))$. Equations (2.13) and (4.1) yield the error equation

$$a(\mathbf{e}^{(k)}, \mathbf{v}) + \int_\Omega \tau_s \Big[\frac{D\mathbf{u}^{(k)}}{|D\mathbf{u}^{(k-1)}|} \big(1 - \exp(-m|D\mathbf{u}^{(k-1)}|)\big) \tag{4.8}$$

$$-\frac{D\mathbf{u}}{|D\mathbf{u}|}\big(1-\mathbf{e}(-m|D\mathbf{u}|)\big)\Big] : D\mathbf{v} + b(\mathbf{v}, e^{(k)}) - b(\mathbf{e}^{(k)}, q) = 0$$

for all $\mathbf{v} \in \mathbf{V}$ and $q \in L_0^2$.

Proposition 4.3. *The velocity error of the iterations* (4.1) *satisfies*

$$||\mathbf{e}^{(k)}||_1 \leq c(m + \frac{1}{e})||\mathbf{e}^{(k-1)}||_1 + O(||\mathbf{e}^{(k-1)}||_1^2) \tag{4.9}$$

Proof. Let $\mathbf{v} = \mathbf{e}^{(k)}, q = e^{(k)}$, and plug it to (4.8):

$$a(\mathbf{e}^{(k)}, \mathbf{e}^{(k)}) + \int_\Omega \tau_s \Big[\frac{D\mathbf{u}^{(k)}}{|D\mathbf{u}^{(k-1)}|}\big(1-\exp(-m|D\mathbf{u}^{(k-1)}|)\big)\Big] : D\mathbf{e}^{(k)}$$

$$- \int_\Omega \tau_s \Big[\frac{D\mathbf{u}}{|D\mathbf{u}|}\big(1-\exp(-m|D\mathbf{u}|)\big)\Big] : D\mathbf{e}^{(k)}$$

$$= a(\mathbf{e}^{(k)}, \mathbf{e}^{(k)}) + \int_\Omega \tau_s \Big[\frac{D\mathbf{e}^{(k)}}{|D\mathbf{u}^{(k-1)}|}\big(1-\exp(-m|D\mathbf{u}^{(k-1)}|)\big)\Big] : D\mathbf{e}^{(k)}$$

$$+ \int_\Omega \tau_s \Big[\frac{D\mathbf{u}}{|D\mathbf{u}^{(k-1)}|}\big(1-\exp(-m|D\mathbf{u}^{(k-1)}|)\big)\Big] : D\mathbf{e}^{(k)}$$

$$- \int_\Omega \tau_s \Big[\frac{D\mathbf{u}}{|D\mathbf{u}|}\big(1-\exp(-m|D\mathbf{u}|)\big)\Big] : D\mathbf{e}^{(k)}$$

$$= a(\mathbf{e}^{(k)}, \mathbf{e}^{(k)}) + \int_\Omega \tau_s \Big[\frac{D\mathbf{e}^{(k)}}{|D\mathbf{u}^{(k-1)}|}\big(1-\exp(-m|D\mathbf{u}^{(k-1)}|)\big)\Big] : D\mathbf{e}^{(k)}$$

$$+ \int_\Omega \tau_s \Big[\frac{1}{|D\mathbf{u}^{(k-1)}|}\big(1-\exp(-m|D\mathbf{u}^{(k-1)}|)\big)$$

$$-\frac{1}{|D\mathbf{u}|}\big(1-\exp(-m|D\mathbf{u}|)\big)\Big] D\mathbf{u} : D\mathbf{e}^{(k)}$$

By applying Taylor expansion with Frechet differential, we obtain

$$\frac{1}{|D\mathbf{u}^{(k-1)}|}\big(1-\exp(-m|D\mathbf{u}^{(k-1)}|)\big)-\frac{1}{|D\mathbf{u}|}\big(1-\exp(-m|D\mathbf{u}|)\big)$$

$$=\Big[-\big(1-\exp(-m|D\mathbf{u}|)\big)\frac{1}{|D\mathbf{u}|^3}-\frac{m}{|D\mathbf{u}|}\exp(-m|D\mathbf{u}|)\Big]D\mathbf{u}:D\mathbf{e}^{(k-1)}+O\bigg(|D\mathbf{e}^{(k-1)}|^2\bigg).$$

Therefore, we have

$$a(\mathbf{e}^{(k)},\mathbf{e}^{(k)})+\int_\Omega \tau_s\Big[\frac{D\mathbf{e}^{(k)}}{|D\mathbf{u}^{(k-1)}|}\big(1-\exp(-m|D\mathbf{u}^{(k-1)}|)\big)\Big]:D\mathbf{e}^{(k)}$$

$$+\int_\Omega \tau_s\Big[-\big(1-\exp(-m|D\mathbf{u}|)\big)\frac{1}{|D\mathbf{u}|^3}$$

$$-\frac{m}{|D\mathbf{u}|}\exp(-m|D\mathbf{u}|)\Big]D\mathbf{u}:D\mathbf{e}^{(k-1)}D\mathbf{u}:D\mathbf{e}^{(k)}+\text{ h.o.t. }=0.$$

Let $x>0$, consider the function

$$\big(1-e^{-mx}\big)\tfrac{1}{x}+mxe^{-mx}.$$

$\max\frac{1-e^{-mx}}{x}=m$, $\max mxe^{-mx}=\frac{1}{e}$.

Then

$$\big(1-e^{-mx}\big)\tfrac{1}{x}+mxe^{-mx}\le m+\tfrac{1}{e}.$$

Plugging it to the last inequality, we get

$$|a(\mathbf{e}^{(k)},\mathbf{e}^{(k)})|\le c(m+\tfrac{1}{e})|D\mathbf{e}^{(k-1)}||D\mathbf{e}^{(k)}|+\text{ h.o.t.}$$

Then

$$\mu||\mathbf{e}^{(k)}||_1^2 \leq c(m+\tfrac{1}{e})||\mathbf{e}^{(k-1)}||_1 + O(||\mathbf{e}^{(k-1)}||^2)||\mathbf{e}^{(k)}||_1. \qquad \square$$

Compare with Bercovier-Engelman regularization [4]

$$||\mathbf{e}^{(k)}||_1 \leq \frac{c}{\epsilon}||\mathbf{e}^{(k-1)}||_1 + O(||\mathbf{e}^{(k-1)}||_1^2) \tag{4.10}$$

Note that the estimation from the last proposition also shows that the velocity error linearly depends on the value of the parameter m. Thus, if m has a large magnitude, the convergence of the numerical algorithm may slow down.

For the mixed formulation we can show the corresponding results:

Proposition 4.4. *The error of the iterative scheme* (4.2) *satisfies*

$$||e^{(k)}||_1 + \frac{1}{\sqrt{m}}||E^{(k)}|| \leq C\tau_s\sqrt{m}||e^{(k-1)}||_1 + O\bigg(|D\mathbf{e}^{k-1}|^2\bigg). \tag{4.11}$$

Proof.

After a memberwise subtraction of (4.2) and (2.14) and standard manipulations with $\mathbf{v} = \mathbf{e}^{(k)}$, $q = e^{(k)}$, and $Z = E^{(k)}$, we get

$$a(\mathbf{e}^{(k)}, \mathbf{e}^{(k)}) + g(\frac{|D\mathbf{u}^{(k-1)}|}{1-\exp(-m|D\mathbf{u}^{(k-1)}|)} - \frac{|D\mathbf{u}|}{1-\exp(-m|D\mathbf{u}|)}, W, E^{(k)}) \tag{4.12}$$
$$+g(\frac{|D\mathbf{u}^{(k-1)}|}{1-\exp(-m|D\mathbf{u}^{(k-1)}|)}, E^{(k)}, E^{(k)}) = 0.$$

Based on Taylor expansion with Frechet differential, the following holds

$$\frac{|D\mathbf{u}^{(k-1)}|}{1-\exp(-m|D\mathbf{u}^{(k-1)}|)} - \frac{|D\mathbf{u}|}{1-\exp(-m|D\mathbf{u}|)} = \tag{4.13}$$

$$-\frac{D\mathbf{u}}{|D\mathbf{u}|} : D\mathbf{e}^{(k-1)} \frac{1-\exp(-m|D\mathbf{u}|) - m|D\mathbf{u}|\exp(-m|D\mathbf{u}|)}{(1-\exp(-m|D\mathbf{u}|))^2} + O\Big(|D\mathbf{e}^{k-1}|^2\Big).$$

Consider

$$\begin{aligned}
&g\Big(\frac{|D\mathbf{u}^{(k-1)}|}{1-\exp(-m|D\mathbf{u}^{(k-1)}|)} - \frac{|D\mathbf{u}|}{1-\exp(-m|D\mathbf{u}|)}, W, E^{(k)}\Big) \\
&= \int_\Omega \tau_s \Bigg[\frac{|D\mathbf{u}^{(k-1)}|}{1-\exp(-m|D\mathbf{u}^{(k-1)}|)} \\
&- \frac{|D\mathbf{u}|}{1-\exp(-m|D\mathbf{u}|)}\Bigg] \frac{(1-\exp(-m|D\mathbf{u}|))D\mathbf{u} : E^{(k)}}{|D\mathbf{u}|} \\
&= \int_\Omega \tau_s \Bigg[- \frac{D\mathbf{u}}{|D\mathbf{u}|} : De^{(k-1)} \frac{1-\exp(-m|D\mathbf{u}|) - m|D\mathbf{u}|\exp(-m|D\mathbf{u}|)}{(1-\exp(-m|D\mathbf{u}|))^2} \\
&+ O\Big(\frac{|D\mathbf{e}^{k-1}|}{m^2}\Big)\Bigg] \frac{(1-\exp(-m|D\mathbf{u}|))D\mathbf{u} : E^{(k)}}{|D\mathbf{u}|} \\
&\leq \int_\Omega \tau_s |De^{(k-1)}||E^{(k)}| \Bigg[1 + \frac{m|D\mathbf{u}|\exp(-m|D\mathbf{u}|)}{1-\exp(-m|D\mathbf{u}|)} + h.o.t.\Bigg]
\end{aligned}$$

Notice that $\max \frac{m|D\mathbf{u}|\exp(-m|D\mathbf{u}|)}{1-\exp(-m|D\mathbf{u}|)} \leq 1$. Therefore, recalling that

$$g\big(\frac{|D\mathbf{u}^{(k-1)}|}{1-\exp(-m|D\mathbf{u}^{(k-1)}|)}, E^{(k)}, E^{(k)}\big) \geq \frac{1}{m}||E^{(k)}||^2,$$

from (4.12) we obtain the inequality

$$\mu||\nabla \mathbf{e}^{(k)}||_1^2 + \frac{1}{m}||E^{(k)}||^2 \leq 2\tau_s||e^{(k-1)}||_1||E^{(k)}|| \leq \frac{\tau_s^2}{2m}||e^{(k-1)}||_1^2 + \frac{1}{2m}||E^{(k)}||^2.$$

Thus

$$||e^{(k)}||_1^2 + \frac{1}{m}||E^{(k)}||^2 \leq 2C\tau_s^2 m||e^{(k-1)}||_1^2 + O\Big(|D\mathbf{e}^{k-1}|^2\Big).$$

□

Compare with Bercovier-Engelman regularization

$$||e^{(k)}||_1 + \sqrt{\epsilon}||E^{(k)}|| \leq \frac{C}{\sqrt{\epsilon}}||e^{(k-1)}||_1 \tag{4.14}$$

It is important to note that the dependence of the error on m in (4.11) is milder then in (4.9), i.e the dependence is not linear, as for primitive variables formulation, but is order $\frac{1}{2}$ (although, we have to note that the higher terms in the error estimation for the mixed formulation (4.11) did not disappear, as they do in Bercovier-Engelman case [4]). Besides, the velocity and pressure iterations from (4.1) and (4.2) are the same, since the auxiliary systems are equivalent. Thus, the velocity error $\mathbf{e}^{(k-1)}$ satisfies not only (4.9), but also should satisfy the improved bound (4.11). In discrete case, though, it may not be true, since the equivalence does not necessary hold any longer.

In general, we may say, that we arrived to the similar conclusions about the mixed formulation for Papanastasiou's regularization, as it was done in [4] for Bercovier-Engelman regularization.

Corrected regularization

Assume that $(\mathbf{u}, p, W)$ is the solution of (3.32). Then $(\mathbf{u}, p)$ also satisfies (3.25).

Set $\mathbf{e}^{(k)} \equiv \mathbf{u}^{(k)} - \mathbf{u}$, $e^{(k)} = p^{(k)} - p$ and $E^{(k)} = W^{(k)} - W$, and consider the iterations of the problem in primitive variables (4.1) with $|D\mathbf{u}|_r = |D\mathbf{u}|_c$.

The error equation corresponding to (3.25) and (4.1) will be the following:

$$a(\mathbf{e}^{(k)},\mathbf{v})+\int_\Omega \tau_s\Big[\frac{D\mathbf{u}^{(k)}}{|D\mathbf{u}^{(k-1)}|_c}-\frac{D\mathbf{u}}{|D\mathbf{u}|_c}\Big] : D\mathbf{v}+b(\mathbf{v},e^{(k)})-b(\mathbf{e}^{(k)},q)=0. \quad (4.15)$$

for all $\mathbf{v}\in\mathbf{V}$ and $q\in L^2_0$.

Proposition 4.5. *The velocity error of the iterations* (4.1) *satisfies*

$$||\mathbf{e}^{(k)}||_1 \le c\max\{\frac{e}{\delta},\nu^{1/\alpha}\}||\mathbf{e}^{(k-1)}||_1+O(||\mathbf{e}^{(k-1)}||_1^2), \quad (4.16)$$

with additional conditions

$$\alpha\nu\le\frac{2}{\delta^2},\ \textit{and}\ \alpha\le 2. \quad (4.17)$$

Proof. Let $\mathbf{v}=\mathbf{e}^{(k)}, q=e^{(k)}$. Plug it to (4.15) gives:

$$a(\mathbf{e}^{(k)},\mathbf{e}^{(k)})+\int_\Omega \tau_s\Big[\frac{D\mathbf{u}^{(k)}}{|D\mathbf{u}^{(k-1)}|_c}\Big] : D\mathbf{e}^{(k)} - \int_\Omega \tau_s\Big[\frac{D\mathbf{u}}{|D\mathbf{u}|_c}\Big] : D\mathbf{e}^{(k)}$$

$$= a(\mathbf{e}^{(k)},\mathbf{e}^{(k)})+\int_\Omega \tau_s\Big[\frac{D\mathbf{e}^{(k)}}{|D\mathbf{u}^{(k-1)}|_c}\Big] : D\mathbf{e}^{(k)} + \int_\Omega \tau_s\Big[\frac{D\mathbf{u}}{|D\mathbf{u}^{(k-1)}|_c}\Big] : D\mathbf{e}^{(k)}$$

$$-\int_\Omega \tau_s\Big[\frac{D\mathbf{u}}{|D\mathbf{u}|_c}\Big] : D\mathbf{e}^{(k)} = a(\mathbf{e}^{(k)},\mathbf{e}^{(k)})+\int_\Omega \tau_s\Big[\frac{D\mathbf{e}^{(k)}}{|D\mathbf{u}^{(k-1)}|_c}\Big] : D\mathbf{e}^{(k)}$$

$$+\int_\Omega \tau_s\Big[\frac{1}{|D\mathbf{u}^{(k-1)}|_c}-\frac{1}{|D\mathbf{u}|_c}\Big]D\mathbf{u} : D\mathbf{e}^{(k)}$$

The Taylor expansion with Frechet differential gives us the following equality:

$$\frac{1}{|D\mathbf{u}^{(k-1)}|_c}-\frac{1}{|D\mathbf{u}|_c}$$
$$=\frac{D\mathbf{u} : D\mathbf{e}^{(k-1)}}{|D\mathbf{u}|_c^3}\Big[1-\frac{\alpha\nu\delta^2}{2}|D\mathbf{u}|^{\alpha-2}\exp(-\nu|D\mathbf{u}|^\alpha)\Big]+O\Big(|D\mathbf{e}^{(k-1)}|^2\Big).$$

Thus, after plugging it to the previous expression, we have

$$a(\mathbf{e}^{(k)},\mathbf{e}^{(k)})+\int_\Omega \tau_s\Big[\frac{D\mathbf{e}^{(k)}}{|D\mathbf{u}^{(k-1)}|_c}\Big]:D\mathbf{e}^{(k)}$$
$$+\int_\Omega \frac{\tau_s}{|D\mathbf{u}|_c^3}\Big[1-\frac{\alpha\nu\delta^2}{2}|D\mathbf{u}|^{\alpha-2}\exp(-\nu|D\mathbf{u}|^\alpha)\Big](D\mathbf{u}:D\mathbf{e}^{(k-1)})(D\mathbf{u}:D\mathbf{e}^{(k)})$$
$$+O\bigg(|D\mathbf{e}^{(k-1)}|^2\bigg)|D\mathbf{e}^{(k)}|$$

Assume that $x>0$, then consider the function

$$\phi=\frac{2x^2-\alpha\nu\delta^2x^\alpha\exp(-\nu x^\alpha)}{2\sqrt{(x^2+\delta^2\exp(-\nu x^\alpha))^3}}.$$

We can estimate the function ϕ with the following bound:

$$|\phi|\le\frac{1}{\sqrt{x^2+\delta^2\exp(-\nu x^\alpha)}}\le\max\{\frac{e}{\delta},\nu^{1/\alpha}\}. \tag{4.18}$$

Indeed, consider the difference

$$\frac{1}{\sqrt{x^2+\delta^2\exp(-\nu x^\alpha)}}-\phi.$$

After multiplication the previous expression by the denominator $2\sqrt{(x^2+\delta^2\exp(-\nu x^\alpha))^3}>0$, we will have

$$2x^2+2\delta^2\exp(-\nu x^\alpha)-2x^2+\alpha\nu\delta^2x^\alpha\exp(-\nu x^\alpha)$$

$$=\delta^2\exp(-\nu x^\alpha)(2+\alpha x^\alpha)>0,\text{ as } x\ge0.$$

Note also that by assumption (4.17) function ϕ is non-negative. And that finishes the proof of (4.18).

Using the estimate (4.18) the expression with Frechet derivative, we have

$$|a(\mathbf{e}^{(k)}, \mathbf{e}^{(k)})| \leq c \max\{\frac{e}{\delta}, \nu^{1/\alpha}\}|D\mathbf{e}^{(k-1)}||D\mathbf{e}^{(k)}| + \text{h.o.t.}$$

Then

$$\mu||\mathbf{e}^{(k)}||_1^2 \leq c \max\{\frac{e}{\delta}, \nu^{1/\alpha}\}||\mathbf{e}^{(k-1)}||_1||\mathbf{e}^{(k)}||_1 + O(||\mathbf{e}^{(k-1)}||^2)||\mathbf{e}^{(k)}||_1$$

. □

Note that by setting $\nu = 0$, $\delta = \epsilon > 0$ we arrive to the conditions for the Bercovier-Engelman regularization with

$$\max\{\frac{e}{\delta}, \nu^{1/\alpha}\} = \max\{\frac{e}{\epsilon}, 0\} = \frac{e}{\epsilon}.$$

By setting $\nu = \frac{1}{\delta}$, $\alpha = \frac{1}{2}$, we have

$$\max\{\frac{e}{\delta}, \nu^{1/\alpha}\} = \max\{\frac{e}{\delta}, \frac{1}{\delta^2}\} = \frac{1}{\delta^2},$$

since the smallness assumption on δ. We obtained the conditions for the case of Corrected regularization, that we use later in Chapter 5 for comparison its performance with Bercovier-Engelman and Papanastasiou's regularizations.

The estimate for the number of iterations depends on the choice of δ, ν, α. With the conditions (4.17), the slowest convergence together with the best approximation of $|D\mathbf{u}|$ is obtained if $\nu = \frac{2}{\alpha\delta^2}$, and the inequality (4.16) will take the form

$$||\mathbf{e}^{(k)}||_1 \leq c \max\{\frac{e}{\delta}, \left(\frac{2}{\alpha\delta}\right)^{1/\alpha}\}||\mathbf{e}^{(k-1)}||_1 + O(||\mathbf{e}^{(k-1)}||_1^2). \tag{4.19}$$

If now we chose $\alpha = 2$, the convergence will be comparable to Bercovier-Engelman with slightly better the approximation of $|D\mathbf{u}|$. Decreasing of the power will lead to slower convergence with the more precise, due to better approximation of the problem, solution $\mathbf{u}$.

Now we continue the error analysis for the mixed formulation.

Proposition 4.6. *The error of the iterative scheme* (4.2) *with* $|D\mathbf{u}|_r = |D\mathbf{u}|_c$ *satisfies*

$$||e^{(k)}||_1 \leq C\tau_s \max\{\sqrt{\frac{e}{\delta}}, \nu^{1/(2\alpha)}\}||e^{(k-1)}||_1 + O\Big(|De^{(k-1)}|^2\Big). \tag{4.20}$$

Proof. Substract memberwise (4.2) and (3.32), and set $\mathbf{v} = \mathbf{e}^{(k)}$, $q = e^{(k)}$, and $Z = E^{(k)}$. This yields in

$$a(\mathbf{e}^{(k)}, \mathbf{e}^{(k)}) + g_{\delta,\nu,\alpha}(|D\mathbf{u}^{(k-1)}|_c - |D\mathbf{u}|, W, E^{(k)}) + g_{\delta,\nu,\alpha}(|D\mathbf{u}^{(k-1)}|_c, E^{(k)}, E^{(k)}) = 0. \tag{4.21}$$

A Taylor expansion with Frechet differential gives

$$|D\mathbf{u}^{(k-1)}|_c - |D\mathbf{u}|_c = \tag{4.22}$$
$$-\frac{D\mathbf{u} : De^{(k-1)}}{|D\mathbf{u}|_c}\Big[1 - \frac{\alpha\nu\delta^2}{2}|D\mathbf{u}|^{\alpha-2}\exp(-\nu|D\mathbf{u}|^\alpha)\Big] + O\Big(|De^{(k-1)}|^2\Big).$$

Then

$$g_{\delta,\nu,\alpha}(|D\mathbf{u}^{(k-1)}|_c - |D\mathbf{u}|, W, E^{(k)})$$

$$= \int_\Omega \tau_s\Big[-\frac{D\mathbf{u} : De^{(k-1)}}{|D\mathbf{u}|_c}\Big[1 - \frac{\alpha\nu\delta^2}{2}|D\mathbf{u}|^{\alpha-2}\exp(-\nu|D\mathbf{u}|^\alpha)\Big]$$

$$+O\Big(|De^{(k-1)}|^2\Big)\Big]\frac{D\mathbf{u}:E^{(k)}}{|D\mathbf{u}|_c} \leq ||e^{(k-1)}||_1||E^{(k)}|| + h.o.t$$

Recall that by Lemma 3.10

$$g_{\delta,\nu,\alpha}\big(|D\mathbf{u}^{(k-1)}|_c, E^{(k)}, E^{(k)}\big) \geq \min\{\frac{\delta}{e}, \nu^{-1/\alpha}\}||E^{(k)}||^2.$$

Then from (4.21) we obtain the inequality

$$\mu||\nabla \mathbf{e}^{(k)}||_1^2 + \min\{\frac{\delta}{e}, \nu^{-1/\alpha}\}||E^{(k)}||^2 \leq 2\tau_s||e^{(k-1)}||_1||E^{(k)}||.$$

Then, making suitable perturbations and simplifications, we arrive to the conclusion:

$$||e^{(k)}||_1 \leq C \max\{\sqrt{\frac{e}{\delta}}, \nu^{1/(2\alpha)}\}||e^{(k-1)}||_1 + O\Big(|De^{(k-1)}|^2\Big).$$

□

The error estimate suggest that for mixed formulation the convergence is faster then in case of formulation in primitive variables. Again, substituting $\nu = \frac{1}{\delta}$, $\alpha = \frac{1}{2}$, we have

$$\max\{\sqrt{\frac{e}{\delta}}, \nu^{1/(2\alpha)}\} = \frac{1}{\delta},$$

which supports the results for Corrected regularization.

Setting $\nu = 0$, $\delta = \epsilon > 0$ we have the Bercovier-Engelman regularization with

$$\max\{\sqrt{\frac{e}{\delta}}, \nu^{1/(2\alpha)}\} = \max\{\sqrt{\frac{e}{\epsilon}}, 0\} = \sqrt{\frac{e}{\epsilon}}.$$

The choice of δ, ν, α also affects the number of iterations together with the preciseness of the answer.

4.2 The Newton method

In this section we introduce the Newton algorithms to solving Bingham fluid equations in four cases:

1. Papanastasiou's regularization in primitive variables formulation:

$$\begin{cases} -\nabla\cdot\Big(2\mu+\frac{\tau_s}{|D\mathbf{u}^{(k-1)}|}(1-\exp(-m|D\mathbf{u}^{(k-1)}|))\big(1-\frac{D\mathbf{u}^{(k-1)}:D\mathbf{u}^{(k-1)}}{|D\mathbf{u}^{(k-1)}|^2}\big) \\ \qquad +m\tau_s\frac{D\mathbf{u}^{(k-1)}:D\mathbf{u}^{(k-1)}}{|D\mathbf{u}^{(k-1)}|^2}\exp(-m|D\mathbf{u}^{(k-1)}|)\Big)D\mathbf{u}^{(k)}+\nabla p^{(k)} \\ \qquad =\mathbf{f}-\tau_s\nabla\cdot\frac{D\mathbf{u}^{(k-1)}}{|D\mathbf{u}^{(k-1)}|}(1-\exp(-m|D\mathbf{u}^{(k-1)}|)) \\ \qquad \nabla\cdot\mathbf{u}^{(k)}=0. \end{cases} \tag{4.23}$$

2. Papanastasiou's regularization in the mixed formulation:

$$\begin{cases} -\nabla\cdot\big(2\mu D\mathbf{u}^{(k)}+\tau_s W^{(k)}=\mathbf{f} \\ \nabla\cdot\mathbf{u}^{(k)}=0 \\ |D\mathbf{u}^{(k-1)}|(1-\exp(-m|D\mathbf{u}^{(k-1)}|))D\mathbf{u}^{(k)}- \\ |D\mathbf{u}^{(k-1)}|^2(W^{(k)}-W^{(k-1)})=\big(1-\exp(-m|D\mathbf{u}^{(k-1)}|)+ \\ m\exp(-m|D\mathbf{u}^{(k-1)}|)|D\mathbf{u}^{(k-1)}|\big)D\mathbf{u}^{(k-1)}:D\mathbf{u}^{(k)}W^{(k-1)}. \end{cases} \tag{4.24}$$

3. Corrected regularization ($\nu=1/\delta,\ \alpha=1/2$) in primitive variable formulation:

$$\begin{cases} -\nabla\cdot\Big(2\mu+\frac{\tau_s}{|D\mathbf{u}^{(k-1)}|_C}-\tau_s\frac{D\mathbf{u}^{(k-1)}:D\mathbf{u}^{(k-1)}}{|D\mathbf{u}^{(k-1)}|_c^3}\big(1- \\ \frac{\delta\exp(-2\sqrt{|D\mathbf{u}^{(k-1)}|})}{|D\mathbf{u}^{(k-1)}|_c^3}\big)\Big)D\mathbf{u}^{(k)}+\nabla p^{(k)}=\mathbf{f}-\tau_s\nabla\cdot\frac{D\mathbf{u}^{(k-1)}|D\mathbf{u}^{(k-1)}|_c^2}{|D\mathbf{u}^{(k-1)}|_c^3} \\ \nabla\cdot\mathbf{u}^{(k)}=0. \end{cases} \tag{4.25}$$

4. Corrected regularization ($\nu=1/\delta,\ \alpha=1/2$) in the mixed formulation:

$$\begin{cases} -\nabla\cdot\big(2\mu D\mathbf{u}^{(k)}+\tau_s W^{(k)}=\mathbf{f} \\ \nabla\cdot\mathbf{u}^{(k)}=0 \\ |D\mathbf{u}^{(k-1)}|_c\sqrt{|D\mathbf{u}^{(k-1)}|^3}D\mathbf{u}^{(k)}-|D\mathbf{u}^{(k-1)}|^2(W^{(k)}-W^{(k-1)})= \\ \big(\sqrt{|D\mathbf{u}^{(k-1)}|^3}-\frac{\delta}{2}\exp(-2\sqrt{|D\mathbf{u}^{(k-1)}|}/\delta)\big)D\mathbf{u}^{(k-1)}:D\mathbf{u}^{(k)}W^{(k-1)}. \end{cases} \tag{4.26}$$

Each formulation was obtained by using standard Newton algorithm with applying a Frechet derivative on the functions.

Later, in Chapter 5, we will discuss the applicability of the Newton method to the solution of the Bingham equations for two regularizations: Papanastasiou's and Corrected.

4.3 Discretization

In this thesis we use Galerkin finite element discretization method. We conduct here the proves and statements for Papanastasiou's and Corrected regularizations.

Let $\mathbf{H}_h \subset \mathbf{H}_0^1$, $Q_h \subset L_0^2$, and $\mathcal{W}_h \subset \mathcal{L}_s^2$ be the finite dimensional subspaces for the velocity, pressure, and auxiliary variable W. We assume that the pair of spaces $\mathbf{H}_h$ and Q_h is LBB stable [17]. By $\mathbf{u}_h, \rho_h$ and W_h we denote finite element approximations to $\mathbf{u}, p$ and W respectively.

In case of Papanastasiou's regularization the finite element method for (2.14) reads: Find $\mathbf{u}_h \in \mathbf{H}_h$, $p_h \in Q_h$, and $W_h \in \mathcal{W}_h$ such that

$$\begin{aligned} a(\mathbf{u}_h, \mathbf{v}_h) - b(p_h, \mathbf{v}_h) + c(\mathbf{v}_h, W_h) + b(q_h, \mathbf{u}_h) \\ +c(\mathbf{u}_h, Z_h) - g_m(\mathbf{u}_h, W_h, Z_h) = (\mathbf{f}, \mathbf{v}_h), \end{aligned} \tag{4.27}$$

for any $\mathbf{v}_h \in \mathbf{H}_h$, $q_h \in Q_h$, and $Z_h \in \mathcal{W}_h$.

And similarly, for the Corrected regularization, for the equation (2.14) the finite element method reads: Find $\mathbf{u}_h \in \mathbf{H}_h$, $p_h \in Q_h$, and $W_h \in \mathcal{W}_h$ such

that

$$a(\mathbf{u}_h, \mathbf{v}_h) - b(p_h, \mathbf{v}_h) + c(\mathbf{v}_h, W_h) + b(q_h, \mathbf{u}_)) + c(\mathbf{u}_h, Z_h) - g_\delta(\mathbf{u}_h, W_h, Z_h) = (\mathbf{f}, \mathbf{v}_h), \tag{4.28}$$

for any $\mathbf{v}_h \in \mathbf{H}_h$, $q_h \in Q_h$, and $Z_h \in \mathcal{W}_h$.

4.3.1 Well-Posedness of the Discrete Mixed Problem

Recall the Schlaefer's extention of the Brouwer Theorem [15].

Theorem 4.7. *Let X denote a real Banach space. Suppose*

$$F : X \to X$$

is a continuous and compact mapping. Assume further that the set

$$\{u \in X |\ u = \lambda F[u] \text{ for some } \lambda \text{ with } 0 \leq \lambda \leq 1\}$$

is bounded. Then F has a fixed point.

Papanastasiou's regularization

To show well-posedness of the discrete solution in case of Papanastasiou's regularization, we prove the following theorem.

Theorem 4.8. *The problem* (4.27) *has a solution $\{\mathbf{u}, p, W\}$ from $\mathbf{H}_h \times Q_h \times \mathcal{W}_h$ such that*

$$\mu ||\nabla \mathbf{u}_h||^2 + \frac{\tau_s}{m} ||W_h||^2 \leq \frac{1}{\mu} ||\mathbf{f}||^2_{-1}, \quad ||p_h|| \leq c(1 + \tau_s m)||f||_{-1} \tag{4.29}$$

for a constant $c > 0$. With an additional assumption that

$$||\mathbf{f}||_{-1} \leq 2\big(\sqrt{\mu} + \frac{1}{\sqrt{m}}\big) \tag{4.30}$$

the solution is unique.

Proof. Let us define the divergence free subspace of $\mathbf{H}_h$ as

$$\mathbf{V}_h = \{\mathbf{v}_h \in \mathbf{H}_h : \ b(q_h, \mathbf{v}_h) = 0 \text{ for all } q_h \in Q_h\}.$$

Let λ be such that $0 \leq \lambda \leq 1$. We consider the problem: find $\mathbf{u}_h^\lambda \in \mathbf{V}_h$, $W_h^\lambda \in \mathbf{W}_h$ such that

$$\begin{aligned} a(\mathbf{u}_h^\lambda, \mathbf{v}_h) + \lambda c(\mathbf{v}_h, W_h^\lambda) &= \lambda(\mathbf{f}, \mathbf{v}_h) \\ g_m(\mathbf{u}_h^\lambda, W_h^\lambda, Z_h) - \lambda c(\mathbf{u}_h^\lambda, Z_h) &= 0 \end{aligned} \tag{4.31}$$

for any $\mathbf{v}_h \in \mathbf{H}_h$ and $Z_h \in \mathcal{W}_h$. Note that if $\lambda = 1$, then the problem (4.31) is equivalent to (4.27).

We aim to apply Theorem 4.7. To satisfy its conditions, first we find the bound for $\{\mathbf{u}_h^\lambda, W_h^\lambda\}$. Set $\mathbf{v}_h = \mathbf{u}_h^\lambda$, $Z_h = W_h^\lambda$, and plug into (4.31). Summing up two equations gives

$$a(\mathbf{u}_h^\lambda, \mathbf{u}_h^\lambda) + g_m(\mathbf{u}_h^\lambda, W_h^\lambda, W_h^\lambda) = \lambda(\mathbf{f}, \mathbf{u}_h^\lambda).$$

Recalling that by Korn inequality (3.1) $a(\mathbf{u}_h^\lambda, \mathbf{v}_h) \geq \mu||\nabla \mathbf{u}_n^\lambda||$, and that $(\mathbf{f}, \mathbf{u}_h^\lambda) \leq ||\mathbf{f}||_{-1}||\nabla \mathbf{u}_h^\lambda||^2$, from the last equality we have

$$\mu||\nabla \mathbf{u}_h^\lambda||^2 + \frac{\tau_s}{m}||W_h^\lambda||^2 \leq ||\mathbf{f}||_{-1}||\nabla \mathbf{u}_h^\lambda||.$$

Note that also

$$\mu||\nabla \mathbf{u}_h^\lambda||^2 \leq a(\mathbf{u}_h^\lambda, \mathbf{u}_h^\lambda) \leq ||\mathbf{f}||_{-1}||\nabla \mathbf{u}_h^\lambda||,$$

which gives us $\mu||\nabla \mathbf{u}_h^\lambda|| \leq ||\mathbf{f}||_{-1}$. Therefore, combining all estimates above, we obtain the boundedness condition

$$\mu||\nabla \mathbf{u}_h^\lambda||^2 + \frac{\tau_s}{m}||W_h^\lambda||^2 \leq \frac{1}{\mu}||\mathbf{f}||_{-1}||^2.$$

Thus, the set of solutions of the system (4.31) is uniformly bounded with respect to λ.

Now, it is left to show that the mapping $\{\mathbf{u}_h^{old}, W_h^{old}\} \to \{\mathbf{u}_h^{new}, W_h^{new}\}$ defined by

$$\begin{aligned} a(\mathbf{u}_h^{new}, \mathbf{v}_h) &= (\mathbf{f}, \mathbf{v}_h) - c(\mathbf{v}_h, W_h^{old}) \quad \text{for all } \mathbf{v}_h \in \mathbf{V}_h, \\ g_m(\mathbf{u}_h^{old}, W_h^{new}, Z_h) &= c(\mathbf{u}_h^{old}, Z_h) \quad \text{for all } \mathbf{Z}_h \in \mathcal{W}_h \end{aligned} \tag{4.32}$$

is continuous and bounded.

Set in (4.32) $\mathbf{v}_h = \mathbf{u}_h^{new}$, $Z_h = W_h^{new}$. By Cauchy and Friedrich's inequalities (3.2), we have the following estimates:

$$\begin{aligned} ||\nabla \mathbf{u}_n^{new}|| &\leq c(\tau_s||W_n^{old}|| + ||\mathbf{f}||_{-1}||), \\ \tfrac{1}{m}||W_n^{new}|| &\leq ||\nabla \mathbf{u}_n^{old}||. \end{aligned}$$

The continuity of (4.32) with respect to each argument is following straightforward from the continuity of the forms in the equations. Therefore, since all spaces are finite dimensional , by showing the boundedness and continuity of the mapping (4.32), we have proved its compactness. Thus, all conditions of the Theorem 4.7 are satisfied, and the solution of (4.31) exists for $\lambda = 1$.

To show the uniqueness, assume that we have two sets of solution $\{\mathbf{u}_1, W_1\}$ and $\{\mathbf{u}_2, W_2\}$. Let $\mathbf{e}_h = \mathbf{u}_1 - \mathbf{u}_2$, and $E_h = W_1 - W_2$. Let also $\mathbf{v}_h = \mathbf{e}_h$, $Z_h = E_h$, and plug them to (4.31) for $\{\mathbf{u}_1, W_1\}$, and then for

$\{\mathbf{u}_2, W_2\}$. After subtraction the expression obtained for $\{\mathbf{u}_2, W_2\}$ from the expression for $\{\mathbf{u}_1, W_1\}$, we have

$$\begin{aligned} 2\mu||D\mathbf{e}_h||^2 + g_m(\mathbf{u}_1, W_1, E_h) - g_m(\mathbf{u}_2, W_2, E_h) = 2\mu||D\mathbf{e}_h||^2 \\ +g_m(\mathbf{u}_1, E_h, E_h) + [g_m(\mathbf{u}_1, W_2, E_h) - g_m(\mathbf{u}_2, W_2, E_h)] = 0. \end{aligned} \tag{4.33}$$

After obvious estimations, the following inequality holds

$$2\mu||D\mathbf{e}_h||^2 + \frac{1}{m}||E_h||^2 - ||W_2||_{L^\infty}||D\mathbf{e}_h||||E_h|| \leq 0.$$

Thus, with the condition (4.30), we obtain the uniqueness of the solution.

To show the estimate for p_h, in (4.27) we set $q_h = 0$, $\mathbf{v}_h = \mathbf{u}_h$, and $Z_h = W_h$, then divide both sides of the resulting equality by $||\mathbf{v}|| \neq 0$. Applying the Korn (3.1) and Nečas (3.13) inequalities, we infer

$$c||p_h|| + \frac{(\mathbf{f}, \mathbf{u}_h)}{||\nabla \mathbf{u}_h||} \leq \frac{2\mu||\nabla \mathbf{u}_h|| + \tau_s||\mathbf{f}||_{-1}||\nabla \mathbf{u}_h||}{||\nabla \mathbf{u}_h||}.$$

And the estimate (4.29) follows from the last expression. Then, using the standard classical arguments from [17], we obtain the existence and uniqueness of the solution of (4.27) for pressure p_h, as a Lagrange multiplier.

□

Corrected regularization

Following the same steps as for the proof of the Theorem 4.8, we prove the following theorem for Corrected regularization case.

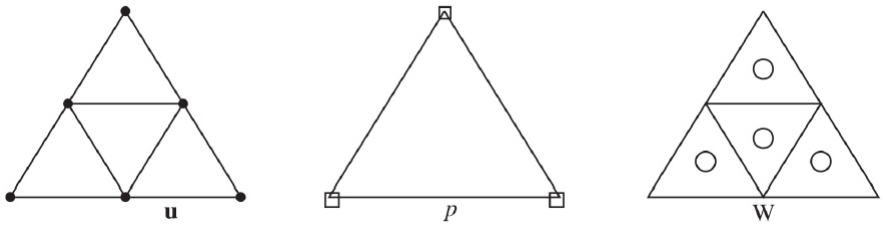

Figure 4.1: Degrees of freedom for the P1isoP2-P1-P0isoP2. • are the degrees of freedom for the velocity components, □ for the pressure and ∘ for the tensor W. Images by Maxim A. Olshanskii, Department of Mechanics and Mathematics, Moscow State University.

Theorem 4.9. *The problem* (4.28) *has a solution* $\{\mathbf{u}, p, W\}$ *from* $\mathbf{H}_h \times Q_h \times \mathcal{W}_h$ *such that*

$$\begin{gathered} \mu||\nabla \mathbf{u}_h||^2 + \tau_s \min\{\frac{\delta}{e}, \nu^{-1/\alpha}\}||W_h||^2 \leq \frac{1}{\mu}||\mathbf{f}||_{-1}^2, \\ ||p_h|| \leq c(1 + \tau_s \max\{\tfrac{e}{\delta}, \nu^{1/\alpha}\})||f||_{-1} \end{gathered} \tag{4.34}$$

for a constant $c > 0$. *With an additional assumption that*

$$||f||_{-1} \leq 2\big(\sqrt{\mu} + \min\{\frac{\delta}{e}, \nu^{-1/\alpha}\}\big) \tag{4.35}$$

the solution is unique.

The mapping $\{\mathbf{u}_h^{old}, W_h^{old}\} \to \{\mathbf{u}_h^{new}, W_h^{new}\}$ in this case is defined by

$$\begin{aligned} a(\mathbf{u}_h^{new}, \mathbf{v}_h) &= (\mathbf{f}, \mathbf{v}_h) - c(\mathbf{v}_h, W_h^{old}) \quad \text{for all } \mathbf{v}_h \in \mathbf{V}_h, \\ g_{\delta,\nu,\alpha}(\mathbf{u}_h^{old}, W_h^{new}, Z_h) &= c(\mathbf{u}_h^{old}, Z_h) \quad \text{for all } \mathbf{Z}_h \in \mathcal{W}_h. \end{aligned} \tag{4.36}$$

Mind that the equivalence between the formulation in primitive and mixed variables does not hold in general on the discrete level. Although it

is possible to choice such selection of finite elements, that the formulations are equivalent. In particular it is P1isoP2 for velocity, P1 for pressure, and P0isoP2 for W. In this case $\mathbf{V}_h$ is a set of continuous piecewise linear functions with respect to the triangulation built by connecting the middle points of the edges of the original triangulation, and $\mathcal{W}_h$ is a set of piecewise constant functions with respect to the same refined triangulation. Figure 4.1 illustrates the degrees of freedom of $\mathbf{u}$, p and W in this case.

Time dependent case

Even though that this dissertation thesis is focused on studying the numerical solution in steady state case, it worth to mention a usage of a finite difference discretization for time dependent Navier-Stokes equations.Following the algorithm described in [5], we use a fully implicit scheme. Let $\{\mathbf{u}_h^k, p_h^k, W_h^k\}$ satisfy (4.27). Let $t \in [0, T]$ and set

$$m(\mathbf{u}, \mathbf{v}) = m_1(\mathbf{u}, \mathbf{v}) + m_2(\mathbf{u}, \mathbf{v}), \text{ where}$$

$$m_1(\mathbf{u}, \mathbf{v}) \equiv \rho \int_\Omega \frac{\partial \mathbf{u}}{\partial t} \cdot \mathbf{v}, \text{ and } m_2(\mathbf{u}, \mathbf{v}) \equiv \int_\Omega (\mathbf{u} \cdot \nabla)\mathbf{u} \cdot \mathbf{v}.$$

Assume that $\{\mathbf{u}_h^k, p_h^k, W_h^k\}$ is the solution of (2.12) at time $k \cdot dt$. Then we solve the following equation for $\{\mathbf{u}_h^{k+1}, p_h^{k+1}, W_h^{k+1}\}$ at time $(k+1)dt$. The equation (2.12) in case of Papanastasiou's approach then reads: find $\mathbf{u}_h^{k+1} \in \mathbf{H}_h$, $p_h^{k+1} \in Q_h$, and $W_h^{k+1} \in \mathcal{W}_h$ such that

$$\begin{aligned} m_1\left(\tfrac{\mathbf{u}_h^{k+1} - \mathbf{u}_h^k}{\Delta t}, \mathbf{v}_h\right) + m_2(\mathbf{u}_h^{k+1}, \mathbf{v}_h) + a(\mathbf{u}_h^{k+1}, \mathbf{v}_h) + b(p_h^{k+1}, \mathbf{v}_h) + c(\mathbf{v}_h, W_h^k) \\ - b(q_h, \mathbf{u}_h^k)) - c(\mathbf{u}_h^k, Z_h) - g_m(\mathbf{u}_h^k, W_h^{k+1}, Z_h) = (\mathbf{f}, \mathbf{v}_h), \end{aligned} \tag{4.37}$$

for any $\mathbf{v}_h \in \mathbf{H}_h$, $q_h \in Q_h$, and $Z_h \in \mathcal{W}_h$.

And for Corrected regularization we correspondingly have: find $\mathbf{u}_h^{k+1} \in \mathbf{H}_h$, $p_h^{k+1} \in Q_h$, and $W_h^{k+1} \in \mathcal{W}_h$ such that

$$m_1\left(\frac{\mathbf{u}_h^{k+1}-\mathbf{u}_h^k}{\Delta t}, \mathbf{v}_h\right) + m_2(\mathbf{u}_h^{k+1}, \mathbf{v}_h) + a(\mathbf{u}_h^{k+1}, \mathbf{v}_h) + b(p_h^{k+1}, \mathbf{v}_h) + c(\mathbf{v}_h, W_h^k) \\ -b(q_h, \mathbf{u}_h^k)) - c(\mathbf{u}_h^k, Z_h) - g_{\delta,\nu,\alpha}(\mathbf{u}_h^k, W_h^{k+1}, Z_h) = (\mathbf{f}, \mathbf{v}_h), \tag{4.38}$$

for any $\mathbf{v}_h \in \mathbf{H}_h$, $q_h \in Q_h$, and $Z_h \in \mathcal{W}_h$. Here we assume that the initial guess $\{\mathbf{u}_h^k, p_h^k, W_h^k\}$ is the solution of (4.28).

4.3.2 Algebraic properties

Let $N_{\mathbf{u}}$, N_p and N_W be the numbers of degrees of freedom of each component of velocity in $\mathbf{H}_h$, of the pressure in Q_h, and of the symmetric tensor in $\mathcal{W}_h$, respectively. Define by $\{\psi_i\}$ for $i = 1, ..., N_{\mathbf{u}}$ the basis functions for each velocity component, by $\{q_i\}$ the basis functions of each pressure component, and by $\{z_i\}$ the basis functions of each entry of the symmetric tensors. For a 2D problems we set matrix A $(2N_{\mathbf{u}} \times 2N_{\mathbf{u}})$ as

$$A = \begin{bmatrix} A^{11} & A^{12} \\ A^{21} & A^{22} \end{bmatrix}, \begin{cases} A_{ij}^{11} = \int_\Omega \mu\big(\frac{\partial\psi_j}{\partial x_1}\frac{\partial\psi_i}{\partial x_1} + \frac{1}{2}\frac{\partial\psi_j}{\partial x_2}\frac{\{}{\partial}\psi_i\partial x_2\big), \\ A_{ij}^{12} = A_{ji}^{21} = \int_\Omega \mu\frac{\partial\psi_j}{\partial x_1}\frac{\partial\psi_i}{\partial x_2}, \\ A_{ij}^{22} = \int_\Omega \mu\big(\frac{\partial\psi_j}{\partial x_2}\frac{\partial\psi_i}{\partial x_2} + \frac{1}{2}\frac{\partial\psi_j}{\partial x_1}\frac{\partial\psi_i}{\partial x_1}\big). \end{cases} \tag{4.39}$$

Matrix B has dimensions $2N_{\mathbf{u}} \times N_p$, and defined the following way

$$B = \begin{bmatrix} B^1 & B^2 \end{bmatrix}, \quad B_{ij}^1 = -\int_\Omega q_i \frac{\partial\psi_j}{\partial x_1}, \; B_{ij}^2 = -\int_\Omega q_i \frac{\partial\psi_j}{\partial x_2}. \tag{4.40}$$

The finite elements for $\mathbf{u}$ and p are assumed to be inf-sup compatible, in order to have matrix B full-rank [4].

Set matrix C $(2N_{\mathbf{u}} \times 3N^W)$ such that

$$C = \begin{bmatrix} C^{1,1} & C^{1,2} & C^{12,1} \\ C^{2,1} & C^{2,2} & C^{12,2} \end{bmatrix},$$

$$\begin{cases} C_{ij}^{1,1} = \int_\Omega \tau_s z_j \frac{\partial \psi_i}{\partial x_1}, & C_{ij}^{2,1} = 0, & C_{i,j}^{12,1}, = \int_\Omega \tau_s z_j \frac{1}{2} \frac{\partial \psi_i}{\partial x_2}, \\ C_{ij}^{1,2} = 0, & C_{ij}^{2,2} = \int_\Omega \tau_s z^j \frac{\partial \psi_i}{\partial x_2}, & C^{12,1} = \int_\Omega \tau_s z_j \frac{\partial \psi_i}{\partial x_1}. \end{cases} \quad (4.41)$$

The block diagonal matrix N $(3N_W \times 3N_W)$ is denoted by

$$N = \begin{bmatrix} N^1 & 0 & 0 \\ 0 & N^2 & 0 \\ 0 & 0 & N^3 \end{bmatrix}, \quad (4.42)$$

where in case of Papanastasiou's regularization $N = N(m)$, and

$$N_{ij}^l(m) = \int_\Omega \tau_s \frac{|D\mathbf{u}_h^{(k)}|}{1 - \exp(-m|D\mathbf{u}_h^{(k)}|)} z_i z_j, \ l = 1, 2, 3,$$

and for Corrected regularization $N = N(\delta)$ with components

$$N_{ij}^l(\delta) = \int_\Omega \tau_s |D\mathbf{u}_h^{(k)}|_c z_i z_j, \ l = 1, 2, 3.$$

In case of 3D problem the settings of the matrices are done similarly to 2D case, and we will have $A \in \mathbb{R}^{3N_{\mathbf{u}} \times 3N_{\mathbf{u}}}$, $B \in \mathbb{R}^{N_p \times 3N_{\mathbf{u}}}$, and W will have 6 different components. Note that while each element of $N(\delta)$ is non-singular by the construction of $|D\mathbf{u}_h^{(k)}|_c > 0$, the definition of the elements of $N(m)$ needs extra assumptions on their value at $|D\mathbf{u}_h^{(k)}| = 0$ to avoid singularity. To resolve this problem, it is natural to define

$$\left. \frac{|D\mathbf{u}_h^{(k)}|}{1 - \exp(-m|D\mathbf{u}_h^{(k)}|)} \right|_{|D\mathbf{u}_h^{(k)}|=0} = \frac{1}{m}.$$

Therefore, to perform one iteration of Picard method for discrete mixed formulation we need to solve the linear system

$$\mathcal{A}\begin{bmatrix} \mathbf{u} \\ p \\ W \end{bmatrix} = \begin{bmatrix} \mathbf{f} \\ 0 \\ \mathbf{0} \end{bmatrix}, \tag{4.43}$$

where

$$\mathcal{A} = \begin{bmatrix} A & B^T & C^T \\ B & 0 & 0 \\ C & 0 & -N \end{bmatrix}. \tag{4.44}$$

Papanastasiou's regularization

Proposition 4.10. *For $0 < m < M$ the linear system* (4.43) *is non-singular for any choice of finite element subspace $\mathcal{W}$.*

Proof. Clearly, we can reorder the rows and the columns of $\mathcal{A}$ without changing rank($\mathcal{A}$):

$$\tilde{\mathcal{A}} = \begin{bmatrix} -N & C & 0 \\ C^T & A & B^T \\ 0 & B & 0 \end{bmatrix} = \begin{bmatrix} \mathcal{D} & \mathcal{B} \\ \mathcal{B}^T & 0 \end{bmatrix}, \tag{4.45}$$

where

$$\mathcal{D} = \begin{bmatrix} -N & C \\ C^T & A \end{bmatrix}, \text{ and } \mathcal{B} = \begin{bmatrix} 0 & B \end{bmatrix}.$$

First let us show that [$\mathcal{D}$ is non-singular. Consider the decomposition of $\mathcal{D}$:

$$\mathcal{D} = \begin{bmatrix} I & 0 \\ -C^T N^{-1} & I \end{bmatrix} \begin{bmatrix} -N & 0 \\ 0 & \Sigma_W \end{bmatrix} \begin{bmatrix} I & -N^{-1}C \\ 0 & I \end{bmatrix}. \tag{4.46}$$

Here $\Sigma_W = A + C^T N^{-1} C$ is the Schur complement matrix. Obviously, since $0 < m < M$, the matrix N is non-singular, and A is symmetric and positive definite. Therefore $\det(\mathcal{D}) = (-1)^{3N_W} \det(N) \det(\Sigma_W) \neq 0$.

Then the following decomposition of $\mathcal{A}$ holds:

$$\tilde{\mathcal{A}} = \begin{bmatrix} I & 0 \\ \mathcal{B}\mathcal{D}^{-1} & I \end{bmatrix} \begin{bmatrix} \mathcal{D} & 0 \\ 0 & -\mathcal{B}\mathcal{D}\mathcal{B}^T \end{bmatrix} \begin{bmatrix} I & \mathcal{D}^{-1}B^T \\ 0 & I \end{bmatrix}.$$

The Schur complement of the last decomposition $-\mathcal{B}\mathcal{D}\mathcal{B}^T = BAB^T$ is a symmetric positive definite matrix, and together with non-singularity of $\mathcal{D}$, it gives us the proof of the theorem. □

Note that the result is valid only for $0 < m < M$. If we tend m to infinity, the non-singularity is not guaranteed.

Corrected regularization

Proposition 4.11. *For $\delta > 0$, $0 < \nu < \bar{\nu}$, and $\alpha > 0$ the linear system* (4.43) *is non-singular for any choice of finite element subspace $\mathcal{W}$.*

The proof of this proposition is analogous to the proof of the Proposition 4.10. For $\delta = 0$, or $\nu \to \infty$ likewise for $m \to \infty$, the question of

the selection of finite dimensional spaces forcing the well-posedness of the discrete problem is still open.

Chapter 5

Numerical Results

In this chapter we present the results of numerical computations based on algorithms discussed above. We first introduce an analytical solution for the region $\Omega = [0,1]^2$. Then we use it to compare the results obtained numerically for Bingham equations regularized with three regularizations: Bercovier-Engelman, Papanastasiou's, and Corrected with a particular choice $\nu = 1/\delta,\ \alpha = 1/2$. This choice of parameters was made to obtain a balance between the number of iterations of the algorithm and the accuracy of the solution. Although, depending on the goal of a particular research, some other choice can be more beneficial. We also investigate the pace of converges comparing two approaches: formulation in primitive variables and the fixed formulation.

We consider the Corrected regularizations for other choices for $\delta,\ \nu,\ \alpha$ in order to support the theoretical predictions of its convergence speed and the accuracy of the solution.

Then we run Newton method with the mixed formulation for the problem on the same region $\Omega = [0,1]^2$. We study the stability of the numerical

algorithm in this case.

Lid Driven cavity is one of the most known problems in rheology. We test the regularized Bingham problem on it, applying Papanastasiou and Corrected to compare their solutions to the result obtained with Bercovier-Engelman regularization.

And finally, we solve the inertia flow problem using mixed formulation applied on Bingham-Papanastasiou problem. We find plug and fluid regions for various Bingham numbers, and conclude on the dependence between the value of Bingham number and the size of plug region.

5.1 An Analytical Test Case

We compare the results of the numerical solution with the analytical case [4], where described the flow between two parallel plates, and in two dimensions its solution is given by

$$u_1 = \begin{cases} \frac{1}{8}[(1-2\tau_s)^2 - (1-2\tau_s-2y)^2, & \text{if } 0 \le y < \frac{1}{2} - \tau_s, \\ \frac{1}{8}[(1-2\tau_s)^2, & \text{if } \frac{1}{2} - \tau_s \le y \le \frac{1}{2} + \tau_s, \\ \frac{1}{8}[(1-2\tau_s)^2 - (2y-2\tau_s-1)^2, & \text{if } \frac{1}{2} + \tau_s \le y < 1 \end{cases} \tag{5.1}$$

$u_2 \equiv 0$, $p = -x$. The rigid region $\{y \in \Omega | \frac{1}{2} - \tau_s \le y \le \frac{1}{2} + \tau_s\}$ is the kernel moving at a constant velocity. The chosen domain $\Omega = [0,1]^2$, $\tau_s = 0.3$.

$$\mathbf{u} = [u_1, u_2].$$

5.2 Picard's Method

In this section we compare the results of applying Picard's Method to solve the equations (2.7) by Papanastasiou's approach and with Bercovier-Engelman regularization, studied in [4].

For the implementation we use the Incompressible Flow Iterative Solution Software (IFISS) [14] package in MatLab. The package is written in MatLab, and is focused on solving a specific four steady-state equations: Poisson, the Stokes, Navier-Stokes equations, and the convention-diffusion equation. Starting with the zero vector as the initial guess, we perform Picard iterations until the initial residual r_0 drops by six orders of magnitude, i.e. $\frac{||r_k||_\infty}{||r_0||_\infty} \leq 10^{-6}$. Unless stated otherwise, we choose $\mu = 1$, $f = 0$, $\tau_s = 0.3$, and $\Omega = [0,1] \times [0,1]$. MATLAB's backslash operator serves as the linear solver at each nonlinear iteration step.

We consider the comparison of the results after performing calculations for three regularizations:

1. Bercovier-Engelman regularization;
2. Papanastasiou's regularization;
3. Corrected regularization with $\nu = 1/\delta,\ \alpha = 1/2$.

We run algorithms for different choice of the mesh size $h = \frac{1}{8},\ \frac{1}{16},\ \frac{1}{32},\ \frac{1}{64},\ \frac{1}{128}$, and with different choices of regularization parameters. To make algorithms comparable, we set everywhere $\epsilon = \delta = \frac{1}{m}$. These settings are established, to make it easier to compare the regularized viscosities, since ϵ, δ, and $\frac{1}{m}$ are the

values of $\hat{\mu}_\epsilon$, $\hat{\mu}_m$, and $\hat{\mu}_\delta$ respectively at zero. We compare the numerically obtained solutions with the exact solution (5.1).

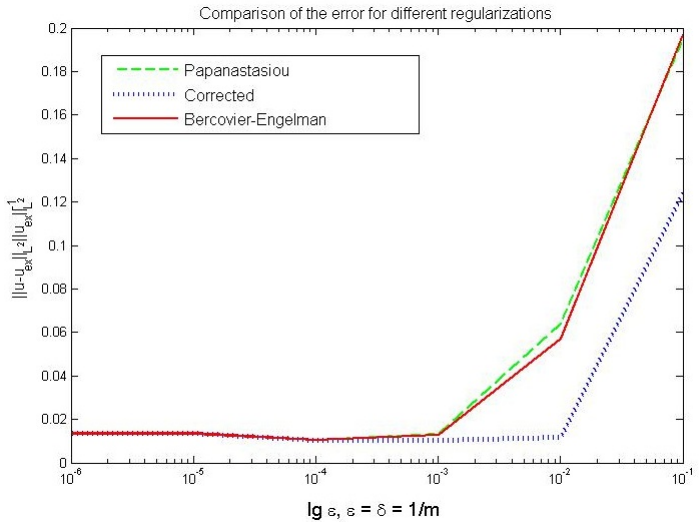

Figure 5.1: Error $\frac{||\mathbf{u}_{exect}-\mathbf{u}_{numerical}||_{L^2}}{||\mathbf{u}_{exact}||_{L^2}}$, depending on ϵ; $h = \frac{1}{32}$.

First we discuss the dependence of the "normalized" errors $\frac{||\mathbf{u}_{exect}-\mathbf{u}_{numerical}||_{L^2}}{||\mathbf{u}_{exact}||_{L^2}}$ and $\frac{||p_{exect}-p_{numerical}||_{L^2}}{||p_{exact}||_{L^2}}$ of the regularization parameter value. This normalization was taken in account to emphasize the value of difference in error for three regularizations.

If not stated otherwise, we use the following notations:

- $\mathbf{u}_{exact}, p_{exact}$ is the exact solution (5.1);
- $\mathbf{u}_1, p_1$ is the numerical solution with Papanastasiou regularization;
- $\mathbf{u}_2, p_2$ is the numerical solution with Bercovier-Engelman regularization;

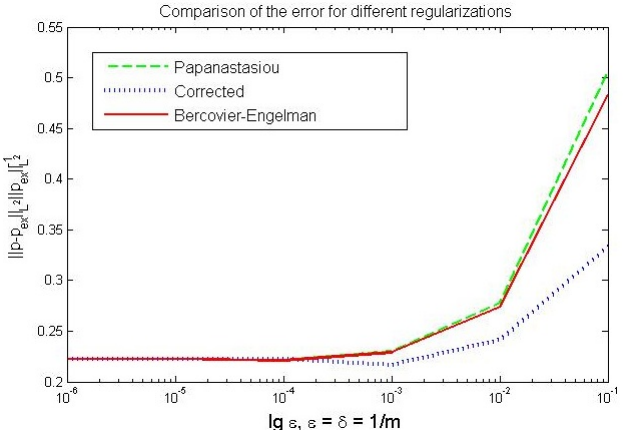

Figure 5.2: Error $\frac{||p_{exect}-p_{numerical}||_{L^2}}{||p_{exact}||_{L^2}}$, depending on ϵ; $h = \frac{1}{32}$.

- $\mathbf{u}_3, p_3$ is the numerical solution with Corrected regularization with $\nu = 1/\delta,\ \alpha = 1/2$.

Figures 5.2, and 5.1 illustrate these relations in case $h = \frac{1}{32}$. Observe that while Bercovier-Engelman and Papanastasiou's regularizations show pretty much the same results, Corrected regularization gets more accurate solution with bigger choice of $\delta = \epsilon$, and in general have produced better results with respect to the value of the error. Although, the smaller δ, the less difference between the algorithms' performances, and after some point all three approaches demonstrated the same preciseness.

Figures 5.4 and 5.3 support these conclusions for $h = \frac{1}{16}$.

Next we discuss the dependence of the error of the mesh size with fixed $\epsilon = 10^{-2}$. As it is possible to see on Figure 5.5, Papanastasiou's and Bercovier-Engelman regularizations still demonstrate the similar performance. Note that (see Figure 5.5) that the error is decreasing while h

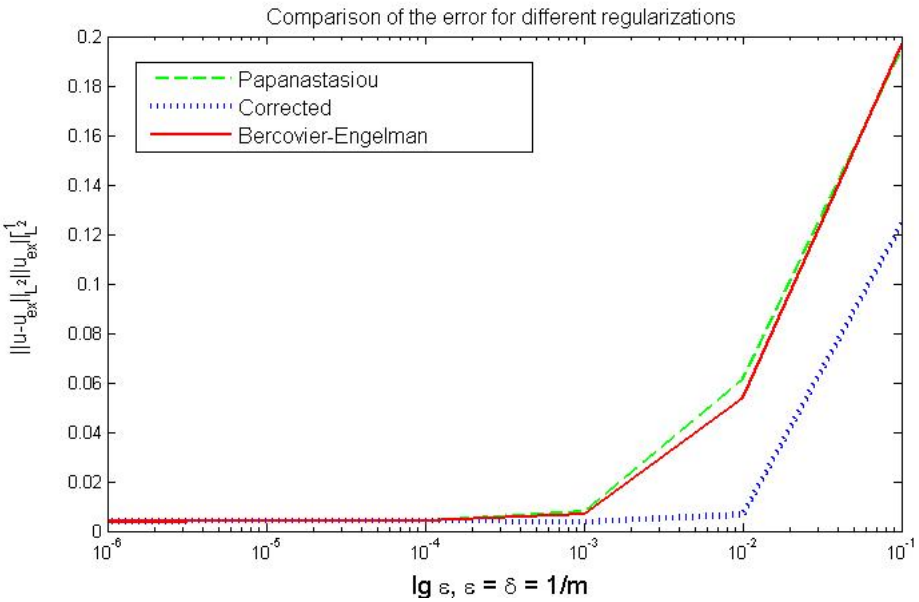

Figure 5.3: Error $\frac{||\mathbf{u}_{exect}-\mathbf{u}_{numerical}||_{L^2}}{||\mathbf{u}_{exact}||_{L^2}}$, depending on ϵ; $h = \frac{1}{16}$.

drops from 1/8 to 1/32, and then, for smaller h it is slightly increasing. This result is due to the dependency of the error of the Matlab precision.

The Corrected regularization again obtains smaller error with different mesh size. We can see it on Figures 5.3, 5.4, 5.5.

This fact could be quite beneficial for numerical computations, since decreasing of h leads to longer time needed for each iteration.

On the pictures 5.7, 5.6, and 5.8 demonstrated the magnitude of the strain tensor for the difference between the numerical solutions and the exact solution (5.1), and the difference between the pressure fields for Papanastasiou's, Bercovier-Emgelman, and Corrected regularizations respectively.

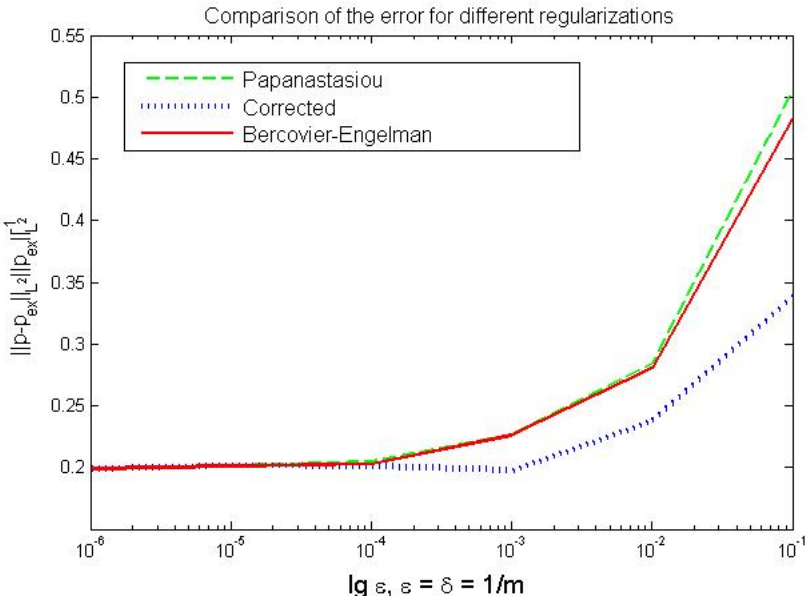

Figure 5.4: Error $\frac{||p_{exect} - p_{numerical}||_{L^2}}{||p_{exact}||_{L^2}}$, depending on ϵ; $h = \frac{1}{16}$.

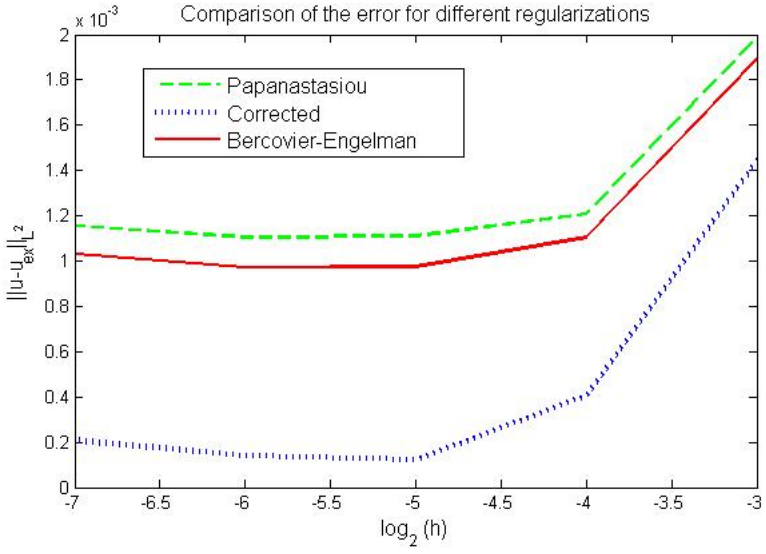

Figure 5.5: Error $||u_{exect} - u_{numerical}||_{L^2}$, depending on h; $\epsilon = 10^{-2}$.

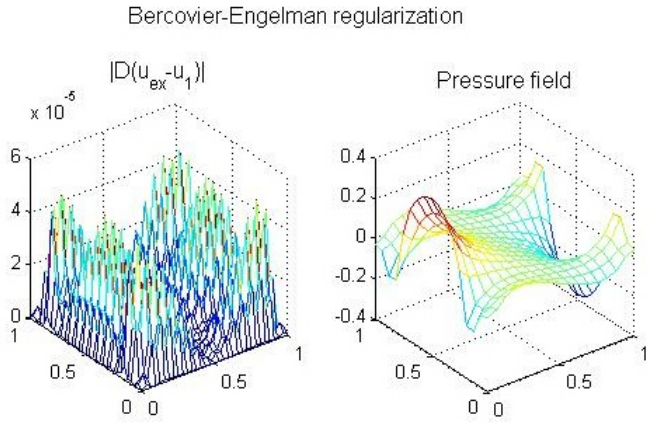

Figure 5.6: $|D(u_{ex} - u_1)|$. Pressure field for $p_{ex} - p_1$. $\epsilon = 10^{-6}$, $h = \frac{1}{32}$.

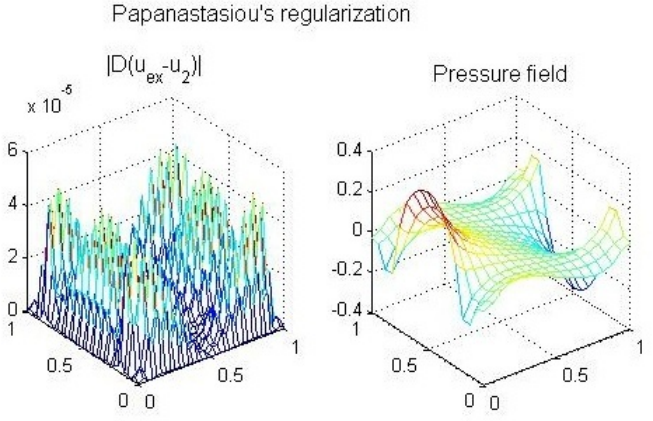

Figure 5.7: $|D(u_{ex} - u_2)|$. Pressure field for $p_{ex} - p_2$. $m = 10^6$, $h = \frac{1}{32}$.

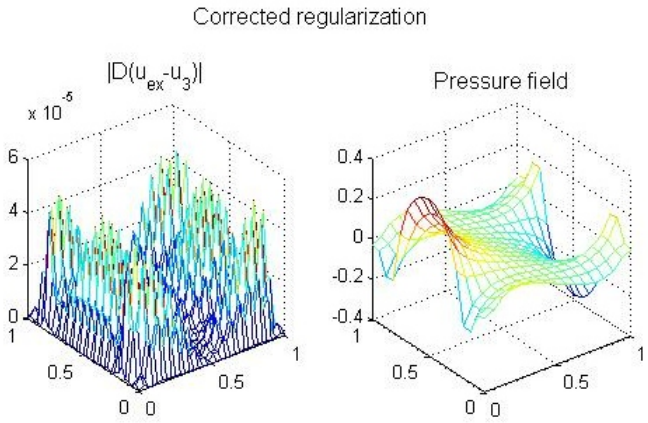

Figure 5.8: $|D(u_{ex} - u_3)|$. Pressure field for $p_{ex} - p_3$. $\delta = 10^{-6}$, $h = \frac{1}{32}$.

5.2.1 Comparison of the iteration numbers

In Chapter 4 we obtained theoretical estimates (4.11), (4.20), (4.9) and (4.16), that predict the pace of convergence in two cases: for formulation in primitive variables and the mixed formulations. Let us compare theoretical conclusions with the results of numerical simulations.

Table 5.1: **The number of iterations for the fixed mesh size $h = \frac{1}{8}$, $res = 10^{-5}$ for the primitive variables formulation (primal) and the mixed one (dual).**

	Bercovier-Egelman		**Papanastasiou**		**Corrected**	
ϵ	Dual	Primal	Dual	Primal	Dual	Primal
10^{-1}	3	3	3	3	5	5
10^{-2}	6	7	6	6	10	10
10^{-3}	9	10	8	10	10	10
10^{-4}	10	22	10	16	10	31
10^{-5}	10	57	10	71	10	31

It worth to compare the error for the case $\epsilon = 10^{-4}$, where we obtained the same number of iterations for each regularization with the mixed formulation.

1. Bercovier-Engelman - $||\mathbf{u}_{ex} - \mathbf{u}_1||_{L^2} = 2.995892\text{e-}03$;
2. Papanastasiou's - $||\mathbf{u}_{ex} - \mathbf{u}_2||_{L^2} = 2.995892\text{e-}03$;
3. Corrected - $||\mathbf{u}_{ex} - \mathbf{u}_3||_{L^2} = 1.442836\text{e-}03$.

As we can see, Corrected regularization provides more accurate result even if it takes algorithm the same number of iterations to converge.

Table 5.1 reports numbers of iterations it took algorithm to converge with numerical error less then 10^{-5} for six different formulations, and mesh size $h = \frac{1}{8}$. As we can note, the prediction of faster convergence of Bercovier-Engelman and Papanastasiou's approaches, made in Chapter 4 after comparing the error estimates, is fully approved by the results. It is also demonstrated by the data on Tables 5.2, 5.3, 5.4, for $h = \frac{1}{16}, \frac{1}{32}, \frac{1}{64}$ respectively.

Table 5.2: **The number of iterations for the fixed mesh size $h = \frac{1}{16}$, $res = 10^{-5}$ for the primitive variables formulation (primal) and the mixed one (dual).**

	Bercovier-Egelman		**Papanastasiou**		**Corrected**	
ϵ	Dual	Primal	Dual	Primal	Dual	Primal
10^{-1}	3	3	3	3	4	4
10^{-2}	5	5	5	5	8	10
10^{-3}	8	9	8	8	10	11
10^{-4}	9	11	9	10	12	20
10^{-5}	12	14	12	14	12	21

Consideration the results of Corrected regularization, performed for the same meshes, and also introduced by Tables 5.1, 5.2, 5.3, 5.4, shows the same picture. By (4.9) and (4.11), the mixed formulation suppose to give faster convergence then the formulation in primitive variables, and this found an experimental approval. Moreover, the better convergence with the mixed formulation is even more significant then in two other cases.

The theoretical conclusion on slower convergence of the Corrected regularization, according the experiments conducted, is found to be correct. That is the cost of the closer, then in other approaches, approximation of $|D\mathbf{u}|$, and of the more accurate result of the solution.

Table 5.3: **The number of iterations for the fixed mesh size $h = \frac{1}{32}$, $res = 10^{-5}$ for the primitive variables formulation (primal) and the mixed one (dual).**

	Bercovier-Egelman		**Papanastasiou**		**Corrected**	
ϵ	Dual	Primal	Dual	Primal	Dual	Primal
10^{-1}	6	6	6	6	11	11
10^{-2}	8	8	8	8	9	10
10^{-3}	10	10	8	10	11	14
10^{-4}	10	10	9	10	11	17
10^{-5}	11	14	11	14	11	17

For three different regularizations we found the best choice of $\epsilon = \delta$ to obtain the faster convergence. It is reported:

- Bercovier-Engelman regularization.

$$N_{it} = 3,\ ||\mathbf{u}_{exact} - \mathbf{u}_{numerical}||_{L^2} = 3.5 \cdot 10^{-3},\ \epsilon = 0.1.$$

- Papanastasiou's regularization.

$$N_{it} = 3,\ ||\mathbf{u}_{exact} - \mathbf{u}_{numerical}||_{L^2} = 3.5 \cdot 10^{-3},\ \delta = 0.001.$$

- Corrected regularization.

$$N_{it} = 5,\ ||\mathbf{u}_{exact} - \mathbf{u}_{numerical}||_{L^2} = 2 \cdot 10^{-3},\ \delta = 0.1.$$

We also found the best value for ϵ in order to minimize the error.

- Bercovier-Engelman regularization.

$$N_{it} = 11,\ ||\mathbf{u}_{exact} - \mathbf{u}_{numerical}||_{L^2} = 8 \cdot 10^{-5},\ \epsilon = 10^{-4}.$$

Table 5.4: **The number of iterations for the fixed mesh size $h = \frac{1}{64}$, $res = 10^{-5}$ for the primitive variables formulation (primal) and the mixed one (dual).**

	Bercovier-Egelman		**Papanastasiou**		**Corrected**	
ϵ	Dual	Primal	Dual	Primal	Dual	Primal
10^{-1}	4	4	4	4	7	7
10^{-2}	8	9	8	8	13	13
10^{-3}	11	11	11	12	16	16
10^{-4}	14	15	14	15	16	17
10^{-5}	14	15	14	15	17	17

- Papanastasiou's regularization.

$$N_{it} = 12,\ ||\mathbf{u}_{exact} - \mathbf{u}_{numerical}||_{L^2} = 7 \cdot 10^{-5},\ \delta = 10^{-6}.$$

- Corrected regularization ($\nu = 1/\delta,\ \alpha = 1/2$).

$$N_{it} = 11,\ ||\mathbf{u}_{exact} - \mathbf{u}_{numerical}||_{L^2} = 7 \cdot 10^{-5},\ \delta = 0.001.$$

Thus, we can conclude, that Papanastasiou's and Bercovier-Engelman regularizations behave somehow alike, and each of which has their advantages and disadvantages. The Corrected regularization, overall the analysis, provides more precise result for bigger parameter δ, and despite the theory, does not slow down the algorithm.

5.2.2 Corrected regularization. General case

In this section we compare the performance of Corrected regularization depending on the choice of the regularization parameters δ, ν, α. We consider the following cases:

1. $\nu = \delta, \alpha = 1/4$;
2. $\nu = \delta^2, \alpha = 1/4$;
3. $\nu = \delta, \alpha = 1/2$;
4. $\nu = \delta^2, \alpha = 1/2$;
5. $\nu = \delta, \alpha = 1$;
6. $\nu = \delta^2, \alpha = 1$;

Note that all cases satisfy conditions (4.17), necessary for existences of the solution. Thus, for each case the estimate (4.16) from the Proposition 4.5 will have the following form:

1.
$$||\mathbf{e}^{(k)}||_1 \leq \frac{c}{\delta^4}||\mathbf{e}^{(k-1)}||_1 + O(||\mathbf{e}^{(k-1)}||_1^2); \tag{5.2}$$

2.
$$||\mathbf{e}^{(k)}||_1 \leq \frac{c}{\delta^8}||\mathbf{e}^{(k-1)}||_1 + O(||\mathbf{e}^{(k-1)}||_1^2); \tag{5.3}$$

3.
$$||\mathbf{e}^{(k)}||_1 \leq \frac{c}{\delta^2}||\mathbf{e}^{(k-1)}||_1 + O(||\mathbf{e}^{(k-1)}||_1^2); \tag{5.4}$$

4.
$$||\mathbf{e}^{(k)}||_1 \leq \frac{c}{\delta^4}||\mathbf{e}^{(k-1)}||_1 + O(||\mathbf{e}^{(k-1)}||_1^2); \tag{5.5}$$

5.
$$||\mathbf{e}^{(k)}||_1 \leq \frac{c}{\delta}||\mathbf{e}^{(k-1)}||_1 + O(||\mathbf{e}^{(k-1)}||_1^2); \tag{5.6}$$

6.
$$||\mathbf{e}^{(k)}||_1 \leq \frac{c}{\delta^2}||\mathbf{e}^{(k-1)}||_1 + O(||\mathbf{e}^{(k-1)}||_1^2). \tag{5.7}$$

Figure 5.9 shows the regularization of $|D\mathbf{u}|$ for each six cases. We can see that the closest approximation is regularization 2, and according the result (5.3) it supposed to provide the slowest convergence. The regularization 4 looks the same as 2 at Figure 5.9, but in fact it is slightly further from $|D\mathbf{u}|$, and its convergence theoretically is the same order then the convergence of approximation 1, see estimates (5.5), (5.2). The regularizations 3

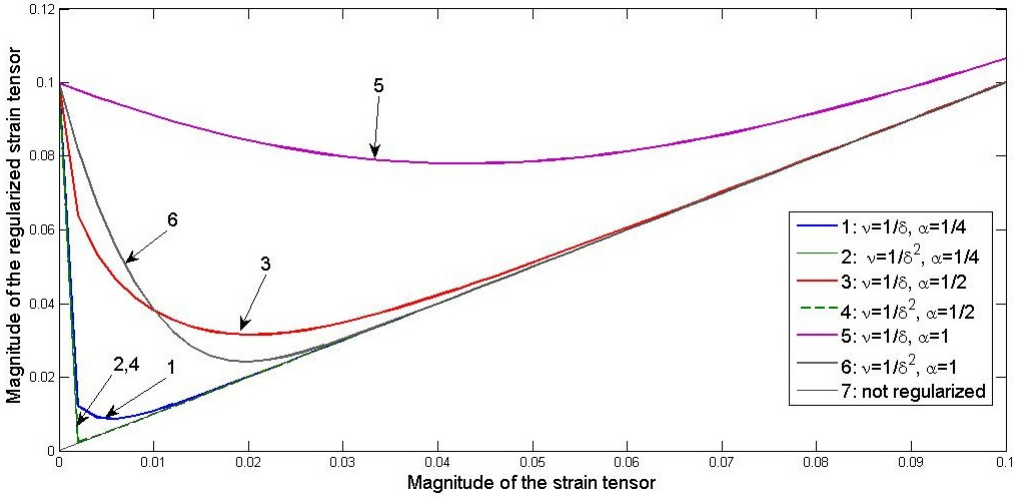

Figure 5.9: An approximation of $|D\mathbf{u}|$, Corrected regularization, $\delta = 0.1$.

and 6 are showing similar approximations with the same rate of convergence

(5.4), (5.7). Observe that the regularization 3 is exactly the case of Corrected regularization we used to compare with Bercovier-Engelman and Papanastasiou's one. Finally, for the regularization 5 we have the worst approximation with the fastest convergence of the algorithm. In fact, its theoretical estimate is the same order as for Bercovier-Engelman regularization. The Figure 5.10

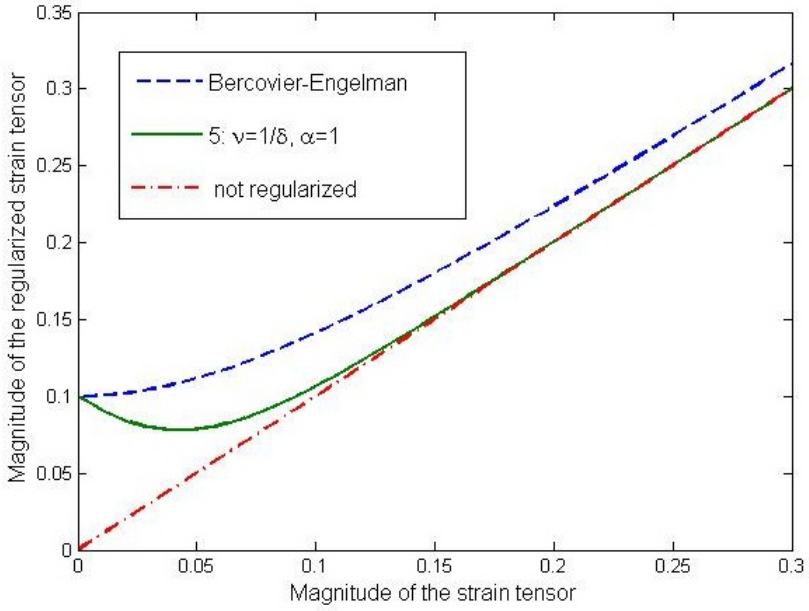

Figure 5.10: An approximation of $|D\mathbf{u}|$, Corrected regularization and Bercovier-Engelman regularization, $\delta = \epsilon = 0.1$.

pictures the Bercovier-Engelman regularized $|D\mathbf{u}|_\epsilon$ next to the approximation of $|D\mathbf{u}|$ by regularization 5, and not regularized case. We can see that, nevertheless, the convergence of the algorithms predicted to be of the same rate, see (4.10), (5.6), but the approximation with regularization 5 is closer.

Table 5.5: **The number of iterations (N_i) and the error $er = ||\mathbf{u}_{ex} - \mathbf{u}_i||_{\mathcal{L}^2}$, $i = 1, .., 6$, for the fixed mesh size $h = \frac{1}{32}$, $res = 10^{-6}$.**

case	**1**		**2**		**3**		**4**		**5**		**6**	
δ	N_i	er	N_i	er	N_i	er	N_i	er	N_i	er	N_i	er
10^{-1}	9	7.5e-4	11	7.1e-5	8	2.2e-3	23	2.5e-4	5	3.7e-3	9	2.1e-3
10^{-2}	9	7.1e-5	11	7.1e-5	11	1.2e-4	11	7.1e-5	9	6.5e-4	16	8.3e-5
10^{-3}	11	7.1e-5	11	7.8e-5	11	7.1e-5	11	7.1e-5	11	1.0e-4	11	7.1e-5
10^{-4}	11	7.8e-5	11	7.9e-5	11	7.8e-5	11	7.8e-5	11	7.8e-5	11	7.8e-5
10^{-5}	11	7.9e-5	12	7.3e-5	11	7.9e-5	11	8.0e-5	11	7.9e-5	11	7.9e-5
10^{-6}	12	7.3e-5	8	1.2e-4	12	7.4e-5	12	7.4e-5	12	7.4e-5	12	7.3e-5

On the Table 5.5 we summarized the data for a particular mesh size $h = \frac{1}{32}$. Here we compare the numbers of iterations that takes each algorithm to converge, and the accuracy of the results. As we can see, the different choice of regularization parameters is making a difference in the speed of convergence, and/or in accuracy of the answer, only for small values of δ. Mind also that compared with Bercovier-Engelman and Papanastasiou's regularizations, Corrected regularization provides more accurate result. Ob-

Table 5.6: **The number of iterations (N_i) and the error $er = ||\mathbf{u}_{ex} - \mathbf{u}||_{\mathcal{L}^2}$, in case of Bercovier-Engelman regularization for the fixed mesh size $h = \frac{1}{32}$, $res = 10^{-6}$.**

ϵ	10^{-1}	10^{-2}	10^{-3}	10^{-4}	10^{-5}	10^{-6}
N_i	4	8	11	11	11	12
er	3.551e-3	9.770e-4	1.299e-4	7.92e-5	7.94e-5	7.35e-5

serve also the result for $\delta = 10^{-6}$, regularization 2. This regularisation gives the closest approximation for the Bingham equations, thus, its convergence has to be the slowest (5.3), and the error the smallest. However the result we discuss is not supporting this observations, and this fact is due to the interplay between the space discretization error and iterative errors.

Clearly, the theoretical predictions about relations between the accuracy of the solution and the rate of convergence, are fully supported by the numerical results. The slowest and the most accurate approach is the regularization 2, and the fastest one with the least close to the actual answer solutions is regularization 5. On Table 5.6 we recall the same result for Bercovier-Engelman regularization. It's easy to see that the regularization 5 provides very close results as in accuracy, so in the numbers of iterations needed for convergence, to the Bercovier-Engelman. This fact also supports

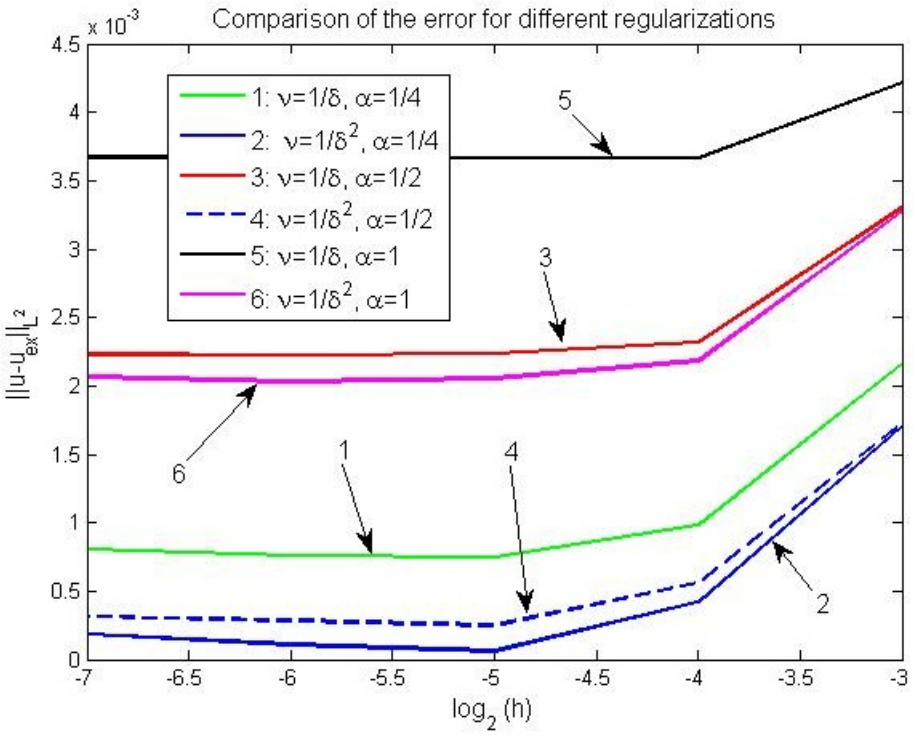

Figure 5.11: Comparison of the velocity error for Corrected regularization, $\delta = 0.1$.

the theory.

In addition we show the dependence between the choice of regularization parameter δ and the norm $||\mathbf{u}_{ex} - \mathbf{u}_i||_{\mathcal{L}^2}$, as long as the dependence between the mesh size and the norm $||\mathbf{u}_{ex} - \mathbf{u}_i||_{\mathcal{L}^2}$, $i = 1, .., 6$, for all six considered cases of Corrected regularization. The Figure 5.12 shows the error dependence of δ for fixed $h = \frac{1}{16}$, and the Figure 5.11 pictures the change of error with different choice of the mesh size with the fixed $\delta = 0.1$.

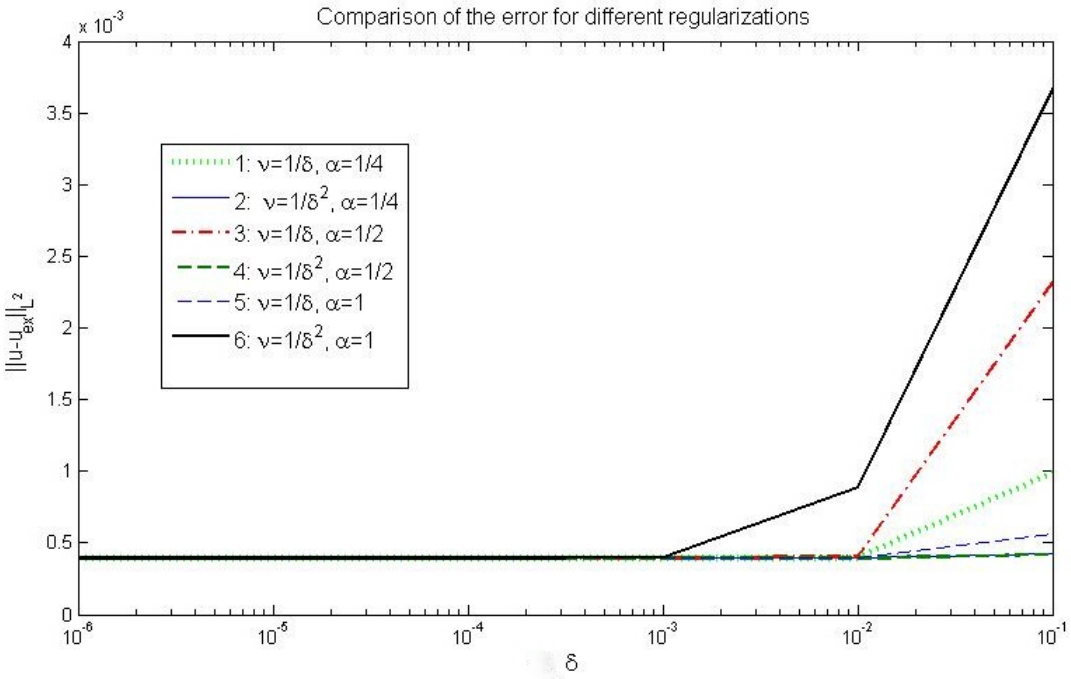

Figure 5.12: Comparison of the velocity error for Corrected regularization, $h = 1/32$.

Therefore, we conclude that the Corrected regularization can be very applicable in the scenario when the accuracy of the results is preferable. On the other hand, the better chosen regularization approximates the initial Bingham equations, the slower convergence we observe.

5.3 Newton Method

Newton method is usually a good alternative to the Picard iterations. Moreover, it has quadratic convergence. However, the application of Newton method on solving the Bingham equations raises certain computational issues. The domain of convergence of the method shrinks as $m \to \infty$ for Papanastasiou's regularization, and as $\epsilon \to 0$ for Bercovier-Engelman [11,19,24]. Thus the Newton method is not robust with respect to the regularization parameter.

We run experiments to estimate how applicable could be the combination of Newton Method algorithm and the mixed formulation for numerical solution of Bingham problem. Here we keep solving the same problem as for the Picard iterations.

In Tables 5.7, 5.8 and 5.9 we summarize the results for Bercovier-Engelman, Papanastasiou's and Corrected ($\nu = 1/\delta,\ \alpha = 1/2$) regularizations respectively. We set the maximum possible number of iterations equal to 100, residual norm for termination is 10^{-6}, and for each choice of $\epsilon = \delta = \frac{1}{m}$ and h, calculate the number of Jacobian matrices whose condition number is greater then 10^{14}, denoted by n_c^{14}, and the number of Jacobian matrices whose condition number is greater then 10^{12} (n_c^{12}). Notation n_i states for the number of iterations it took algorithm to converge. In case when algorithm fails to converge, we obtain $n_i = 100$.

As it is easy to see, the algorithm is not only not convergent for some ϵ, h choice, but also shows instability almost at each iteration. Condition number of the Jacobian is huge ($10^{12} < cond(J) < 10^{14}$) for most cases.

Table 5.7: **Newton method. Number of iterations and Number of Ill-conditioned matrices. Bercovier-Egelman regularization.**

$h \rightarrow$	$\frac{1}{8}$			$\frac{1}{16}$			$\frac{1}{32}$			$\frac{1}{64}$			$\frac{1}{128}$		
$\downarrow \epsilon$	n_i	n_c^{12}	n_c^{14}	n_i	n_c^{12}	n_c^{14}	n_i	n_c^{12}	n_c^{14}	n_i	n_c^{12}	n_c^{14}	n_i	n_c^{12}	n_c^{14}
10^{-1}	6	6	0	6	6	0	6	6	0	5	5	4	4	4	3
10^{-2}	9	9	0	14	14	0	13	13	0	12	12	7	9	9	6
10^{-3}	12	12	0	14	14	0	23	23	0	18	18	8	12	12	7
10^{-4}	100	100	0	19	19	0	26	26	0	20	20	8	13	13	7
10^{-5}	100	100	0	22	22	1	27	27	0	23	23	10	11	11	7
10^{-6}	100	100	1	22	22	1	27	27	1	24	24	12	16	16	9

Table 5.8: **Newton method. Papanastasiou's regularization.**

$h \rightarrow$	$\frac{1}{8}$			$\frac{1}{16}$			$\frac{1}{32}$			$\frac{1}{64}$			$\frac{1}{128}$		
$\downarrow \epsilon$	n_i	n_c^{14}	n_c^{12}	n_i	n_c^{14}	n_c^{12}	n_i	n_c^{14}	n_c^{12}	n_i	n_c^{14}	n_c^{12}	n_i	n_c^{14}	n_c^{12}
10^{-1}	100	100	0	27	27	0	5	5	0	5	5	4	4	4	3
10^{-2}	9	9	0	15	15	0	13	13	0	11	11	7	9	9	6
10^{-3}	12	12	0	13	13	0	24	24	0	19	19	8	12	12	6
10^{-4}	100	100	0	19	19	0	26	26	0	20	20	8	13	13	7
10^{-5}	100	100	0	21	21	1	27	27	0	23	23	10	11	11	7
10^{-6}	100	100	1	22	22	1	27	27	1	24	24	12	16	16	9

Therefore, even if the Newton method converges, its results could not be reliable. However, comparison of the answers to the exact solution $\mathbf{u}_{ex}$ (5.1) demonstrate that despite the highly ill-conditioned Jacobian, Newton algorithm applied to the Bingham equations still can provide the close to correct solution, see Figures 5.13, 5.14. Note, that again Corrected regularization shows the smaller error with slightly bigger number of iterations. Nevertheless, for practical usage we need a priori reliability on the results obtained, and the better choice would be Picard method.

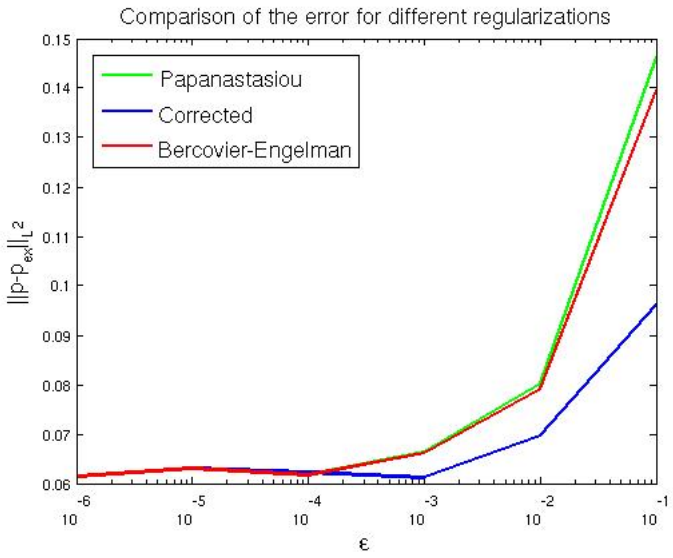

Figure 5.13: The dependence between $\epsilon = \frac{1}{m}$ and $||p\_p_{ex}||_{L^2}$, res=10^{-6}, $h = \frac{1}{32}$.

Another way to get over instability of Newton method is to use Newton continuation, described in [4]. In this method first, set ϵ to be the biggest possible choice of the regularization parameter. Then Newton iterations are stopped ones the L^2 norm of the nonlinear residual is less then ϵ, and regularization parameter decreases. Continuing this process, we calculate the best, in terms of stability, choice for ϵ for each case. Although, if we arise

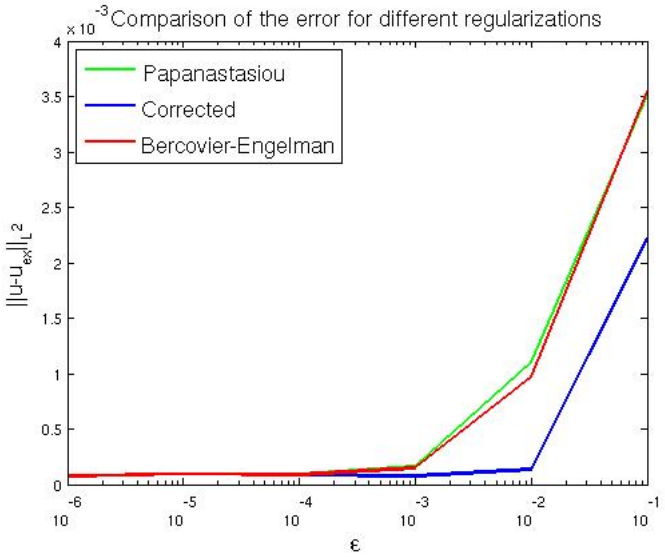

Figure 5.14: The dependence between $\epsilon = \frac{1}{m}$ and norms $||\mathbf{u} - \mathbf{u}_{ex}||_{L^2}$, res=$10^{-6}$, $h = \frac{1}{32}$.

a question of finding plug-regions, there appears the other difficulty. In particular, we would need to decrease the value of ϵ, which is not guarantied in Newton continuation method. Therefore, we again arrive to the conclusion of Picard iterations preference for Bingham problem.

Table 5.9: **Newton method. Corrected regularization.**

$h \rightarrow$	$\frac{1}{8}$			$\frac{1}{16}$			$\frac{1}{32}$			$\frac{1}{64}$			$\frac{1}{128}$		
$\downarrow \epsilon$	n_i	n_c^{14}	n_c^{12}	n_i	n_c^{14}	n_c^{12}	n_i	n_c^{14}	n_c^{12}	n_i	n_c^{14}	n_c^{12}	n_i	n_c^{14}	n_c^{12}
10^{-1}	8	8	0	13	13	0	12	12	0	11	11	7	9	9	5
10^{-2}	100	100	0	18	18	0	24	24	0	17	17	8	13	13	7
10^{-3}	100	100	0	100	100	0	24	24	0	21	21	9	13	13	7
10^{-4}	100	100	0	19	19	0	26	26	0	21	21	8	13	13	7
10^{-5}	100	100	0	22	22	1	28	28	0	100	100	10	11	11	7
10^{-5}	100	100	1	22	22	1	27	27	1	100	100	12	11	11	9

5.4 Lid Driven Cavity

The lid-driven cavity is a benchmark problem for viscous incompressible fluid flow [32]. Its geometry is presented on Figure 5.15.

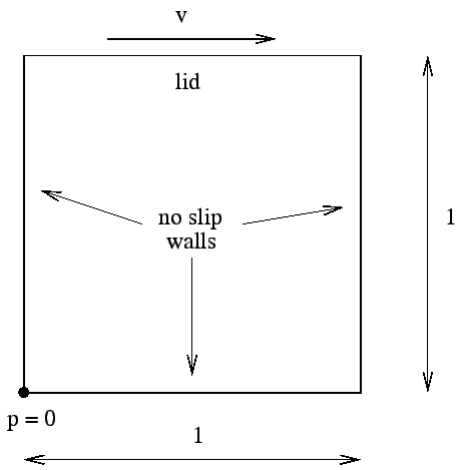

Figure 5.15: Geometry of the Lid-Driven Cavity

The standard case is the following: fluid contained in a square domain with Dirichlet boundary conditions on all sides, with three stationary sides and one moving side (with velocity tangent to the side).

We perform here the simulation in the unit square domain $\Omega = [0,1] \times [0,1]$. We solve (2.2) and (2.3) $\rho = 0$ imposing Dirichlet boundary conditions by $\mathbf{u}|_{y=1} = (0,1)^T$, and $\mathbf{u} = \mathbf{0}$. We set $\tau_s = 0.3$, and solve the equations using Bercovier-Engelman, and compare it to the solutions obtained with both Papanastasiou's and Corrected ($\nu = 1/\delta,\ \alpha = 1/2$) regularizations.

In Table 5.10 are presented the number of steps it takes algorithms to arrive to the residual norm less then 10^{-6}. We ran Picard iterations for the mixed formulation of each problem.

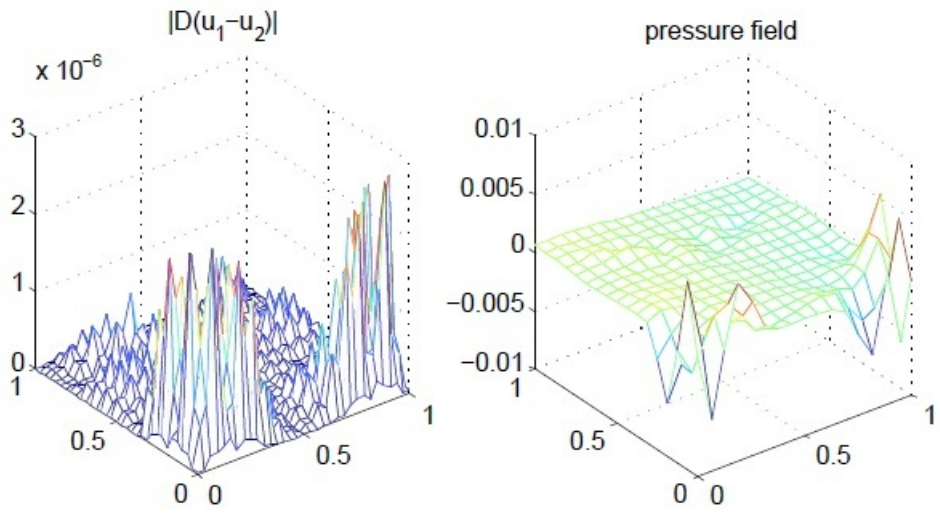

Figure 5.16: Tensor norm $|D(\mathbf{u}_1 - \mathbf{u}_2)|$. Pressure field for $p_1 - p_2$. $\epsilon = 10^{-3}$, $m = 10^3$, $h = \frac{1}{32}$.

Clearly, all three methods of regularization are solving the problem with almost equal number of iterations. It supports the theoretical results (4.11). Solver based on Papanastasiou's regularization is as fast as the one based on Bercovier-Engelman regularization. Although, the Corrected regularization shows the same velocity as other two algorithms despite theoretical predictions. Thus, using Corrected regularization for Lid-Driven Cavity, we can benefit with more precise results and not loosing in the speed of the convergence. The suggestion about the smaller error with Corrected regularization is made by the fact the the initial approximation to the viscosity μ (see Chapter 2) in this case is closer then with Bercovier-Engelman and Papanastasiou's regularizations; and also based on the results of the Section 5.2.

Figure 5.16 shows $|D(\mathbf{u}_1 - \mathbf{u}_2)|$, and the pressure field difference $p_1 - p_2$.

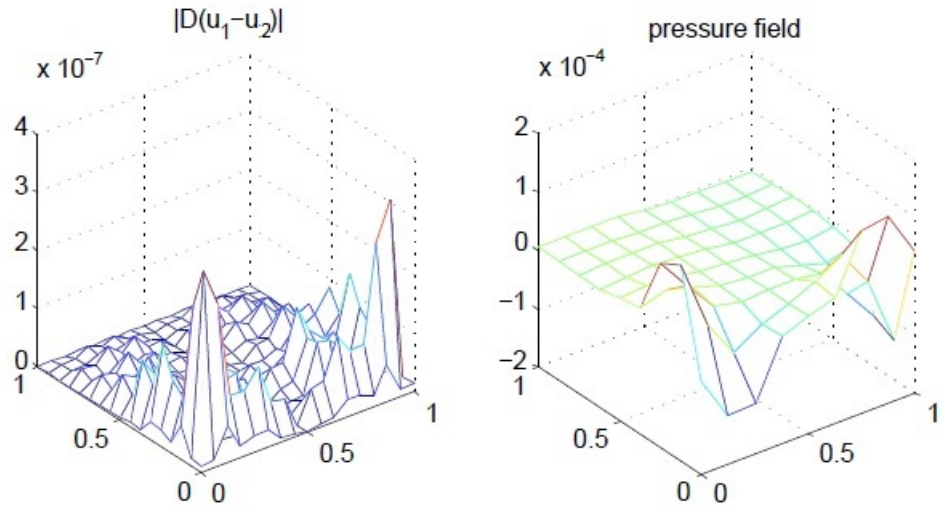

Figure 5.17: Tensor norm $|D(\mathbf{u}_1 - \mathbf{u}_2)|$. Pressure field for $p_1 - p_2$. $\epsilon = 10^{-2},\ m = 10^2$.

Mesh size was chosen to be $h = \frac{1}{32}$. Here and below

- $\mathbf{u}_1, p_1$ is the numerical solution with Papanastasiou regularization;
- $\mathbf{u}_2, p_2$ is the numerical solution with Bercovier-Engelman regularization;
- $\mathbf{u}_3, p_3$ is the numerical solution with Corrected regularization.

Figure 5.17 present the results for $\epsilon = 10^{-2},\ m = 10^2$, with the mesh size $h = \frac{1}{16}$ for the case shown at the table, and also pictures $|D(\mathbf{u}_1 - \mathbf{u}_2)|$, and the pressure field difference $p_1 - p_2$. The Figure 5.18 repeats the visualization of the results above to compare Bercovier-Engelman and Corrected regularization.

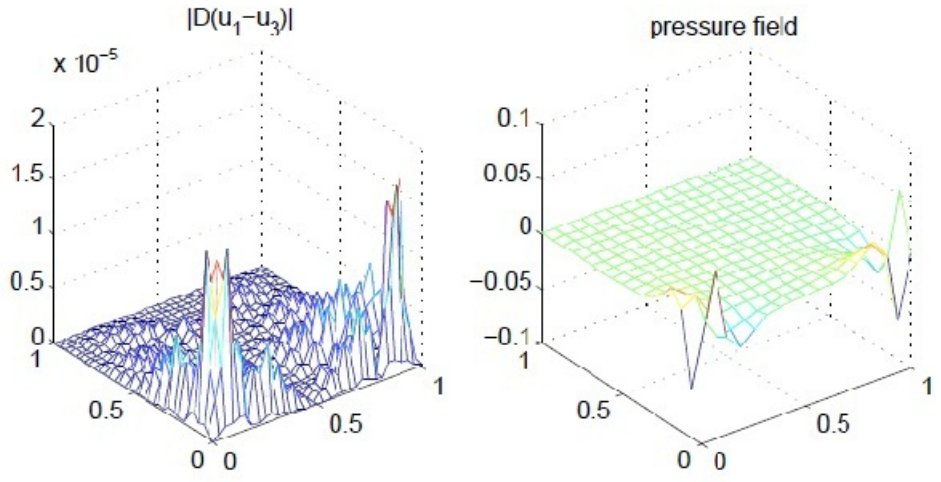

Figure 5.18: Tensor norm $|D(\mathbf{u}_1 - \mathbf{u}_3)|$. Pressure field for $p_1 - p_3$. $\epsilon = \delta = 10^{-3}$.

The dependence between the value of parameter $\epsilon = \frac{1}{m}$ and norms $\frac{||\mathbf{u}_1 - \mathbf{u}_2||_{L^2}}{||\mathbf{u}_1||_{L^2}}$, and $\frac{||p_1 - p_2||_{L^2}}{||p_1||_{L^2}}$ is illustrated on the Figures 5.19, 5.20.

Figures 5.21 and 5.22 demonstrate the dependence of the difference of $\mathbf{u}_1$ and $\mathbf{u}_3$, and p_1 and p_3 on the regularization parameter $\epsilon = \delta$.

The difference between solutions vanishes with $\epsilon \to 0$. Thus, all algorithms eventually arrive to the approximately the same solution. Also note that Bercovier-Engelman differs more from Corrected then from Papanastasiou's regularization results.

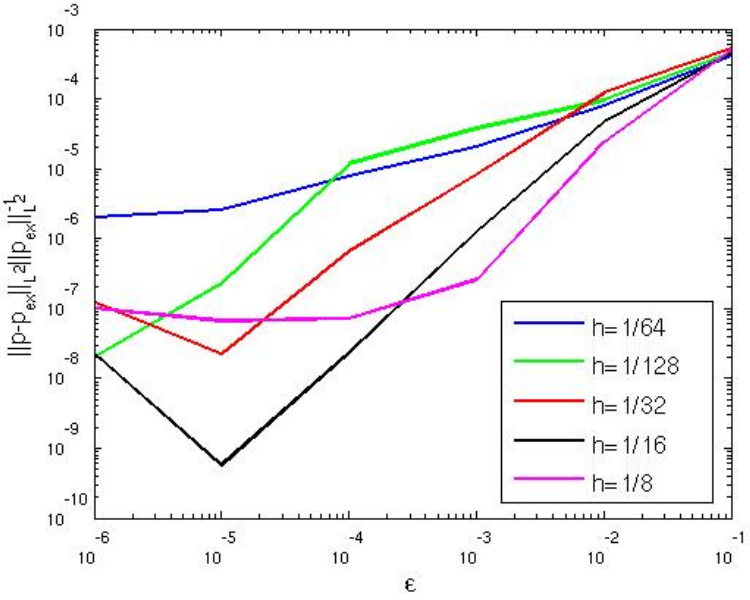

Figure 5.19: The dependence between $\epsilon = \frac{1}{m}$ and $\frac{||p_1 - p_2||_{L^2}}{||p_1||_{L^2}}$, res=$10^{-6}$.

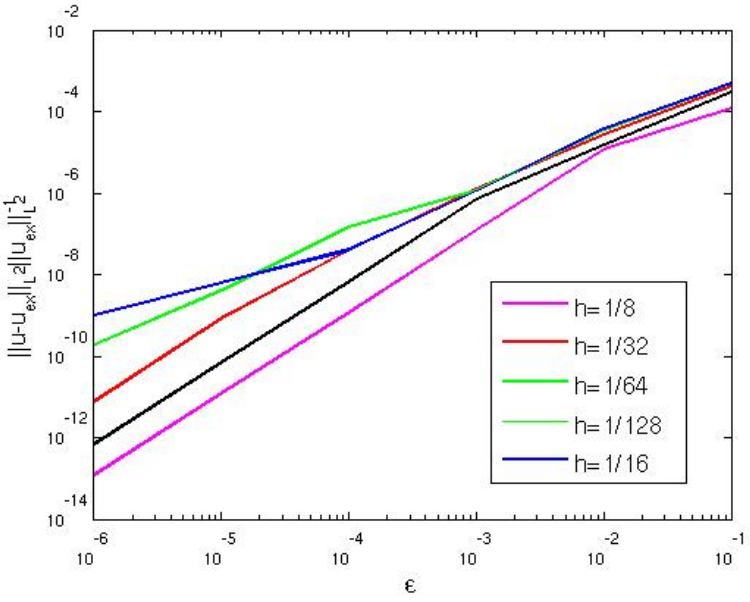

Figure 5.20: The dependence between $\epsilon = \frac{1}{m}$ and norms $\frac{||\mathbf{u}_1 - \mathbf{u}_2||_{L^2}}{||\mathbf{u}_1||_{L^2}}$, res=$10^{-6}$.

Table 5.10: **The number of iterations for lid-driven cavity ,** $res = 10^{-6}$**.**

	Bercovier-Egelman					**Papanastasiou**					**Corrected**				
$h \rightarrow$ $\downarrow \epsilon$	$\frac{1}{8}$	$\frac{1}{16}$	$\frac{1}{32}$	$\frac{1}{64}$	$\frac{1}{128}$	$\frac{1}{8}$	$\frac{1}{16}$	$\frac{1}{32}$	$\frac{1}{64}$	$\frac{1}{128}$	$\frac{1}{8}$	$\frac{1}{16}$	$\frac{1}{32}$	$\frac{1}{64}$	$\frac{1}{128}$
10^{-1}	8	8	7	6	6	8	8	7	6	6	8	8	8	7	6
10^{-2}	8	9	9	7	6	8	9	9	7	6	8	9	9	8	6
10^{-3}	9	9	9	8	7	9	9	9	8	7	9	9	9	8	7
10^{-4}	9	9	9	8	7	9	9	9	8	7	9	9	9	8	7
10^{-5}	9	9	9	8	7	9	9	9	8	7	9	9	9	8	7
10^{-6}	9	10	9	8	7	9	10	9	8	7	9	10	9	8	7

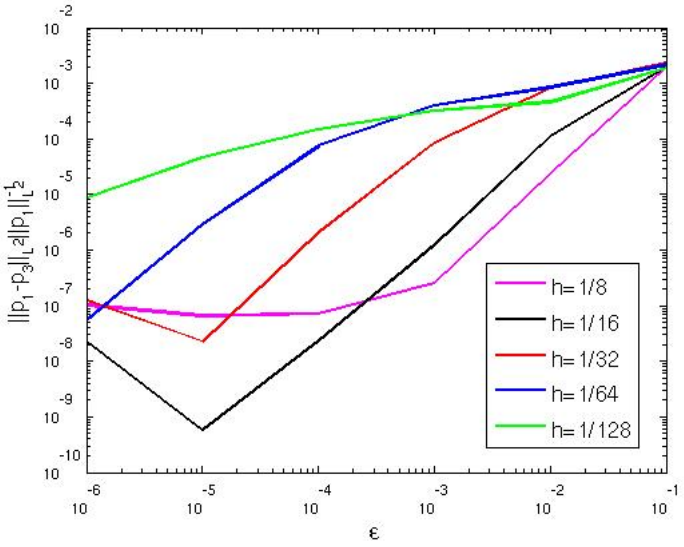

Figure 5.21: The dependence between $\epsilon = \delta$ and $\frac{||p_1 - p_3||_{L^2}}{||p_1||_{L^2}}$, res=$10^{-6}$.

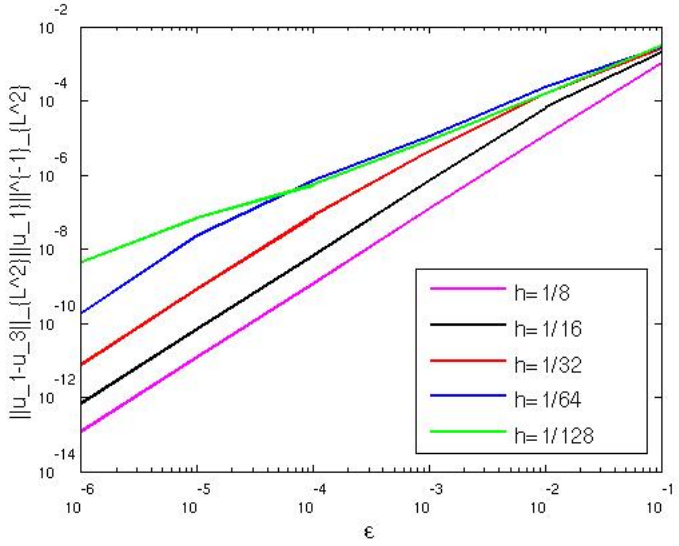

Figure 5.22: The dependence between $\epsilon = \delta$ and norms $\frac{||\mathbf{u}_1 - \mathbf{u}_3||_{L^2}}{||\mathbf{u}_1||_{L^2}}$, res=$10^{-6}$.

5.5 Inertia Flows

Here we consider the yield stress fluid flows through a sudden expansion. The model of the problem, and the considered region Ω are demonstrated on the Figure 5.23. We consider the important question of determination the extent and shape off plug and fluid regions in Ω for the range of Bingham numbers. Dimensionless yield stress, or Bimgham number is defined by

$$Bn = \frac{\tau_s H}{\mu u_0}, \tag{5.8}$$

where H is the channel width, u_0 is a characteristic speed taken as the average velocity of the inflow. The question of determining and conditions of changing of plug regions is quite interesting and was raised before many times, for example in [1, 2, 26, 27, 31, 46].

Abdali et al. [1] solved the benchmark entry flow problem of Bingham plastics through planar and axisymmetric 4:1 contractions, and the exit flow problem and determined the extrudate swell. That work showed the evolution of the phenomenon of viscoplasticity as a dimensionless yield stress or Bingham number increased from the Newtonian to the fully plastic limit.

In [26] Mitsoulis and Huilgol emphasize on determining plug and fluid regions along with the vortex shape, size and intensity for planar and axisymmetric expansion flows for Bingham numbers $0 < Bn < \infty$, and for Reynold numbers $0 \leq Re \leq 200$. The results show the progressive growth of plug region with increasing of Bn.

In [27] Soto, Martins-Costa, Fonseca, and Frey study the inertia flows with sudden planar expansion. They investigated yield stress effects on the fluid dinamics of viscoplastic materials via the ranging Bingham number

from 0.2 to 100. They also conclude that as Bn increases, plug regions monotonically increase too, or the higher the yield limit is, the easier for the condition $|\boldsymbol{\tau}| \leq \tau_s$ to occur.

To be consequent with the previous works described above, we apply to the solutions Papanastasiou's regularization. Application of this model to the problem of finding the yielded and unyielded regions is especially beneficial, since the regularization is valid in both (the yielded and unyielded) regions. Thus the usage of Papanastasiou's regularization eliminates the need for tracking the location of yield surfaces. Note that the same is true for Bercovier-Engelman and Corrected regularizations.

The difference of this experiment is that instead of the formulation in primitive variables, used before, we applied the mixed formulation for Bingham-Papanastasiou problem described here.

For implementations we use FreeFem++. FreeFem++ is a software developed to solve partial differential equations using finite element method, and is based on C++. It also has its own language. Starting with the zero vector as the initial guess, we perform Picard iterations until the initial residual r_0 drops by five orders of magnitude, i.e. $\frac{||r_k||_\infty}{||r_0||_\infty} \leq 10^{-5}$. Unless stated otherwise, we choose $\mu = 1$, $f = 0$, and Ω is the region described by Figure 5.23. The value τ_s varies depending on the choice of Bn.

We solve numerically the following problem

$$\begin{cases} \rho[\frac{\partial \mathbf{u}}{\partial t} + (\mathbf{u} \cdot \nabla)\mathbf{u}] - \nabla \cdot (2\mu D\mathbf{u} + \tau_s W) + \nabla p = \mathbf{f} \\ \nabla \cdot \mathbf{u} = 0 \\ |D\mathbf{u}|W = D\mathbf{u}(1 - \exp(-m|D\mathbf{u}|)) \\ \mathbf{u} = \mathbf{u}_g, \text{ on } \Gamma, \end{cases} \tag{5.9}$$

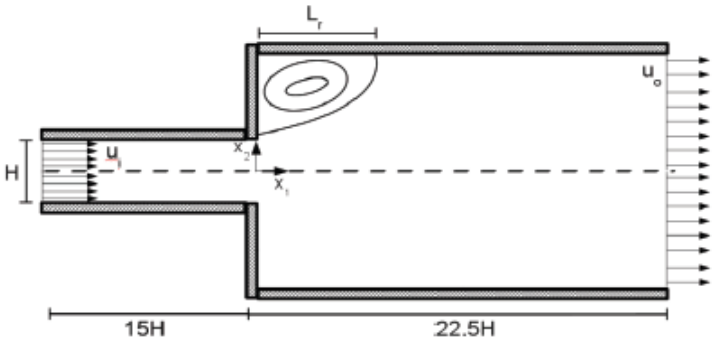

Figure 5.23: Flow through a sudden expansion. Image by Soto, H. P., Martins-Costa, M. L., Fonseca, C., Frey, S. [27].

where Γ is the boundary of the region Ω, $\mathbf{u}_g$ is boundary conditions. We run experiments assuming the parabolic conditions $\mathbf{u} = (\frac{H}{2} - y)(\frac{H}{2} + y)$ at the inlet, such that the mean velocity $\mathbf{u}_0 = 1m/s$, zero boundary conditions on the walls, and free traction at the flow outlet. We set $Bn = 1,\ 5,\ 10,\ 30,\ 50,\ 100$ and present found plug regions on the Figure 5.24. The velocity profile is shown on the Figure 5.25.

Clearly (see Figure 5.24), the plug region grows with increasing of the Bingham number Bn. Thus the results for the problem (5.9) are similar to the ones that have been shown in [1, 2, 26, 27, 31, 46]. Note that, due to different boundary conditions, notwithstanding that the shape of the plug regions is not exactly the same as in [26, 27] and others, the basic idea stays the same, and the fluid region shrinks with increasing of Bingham number.

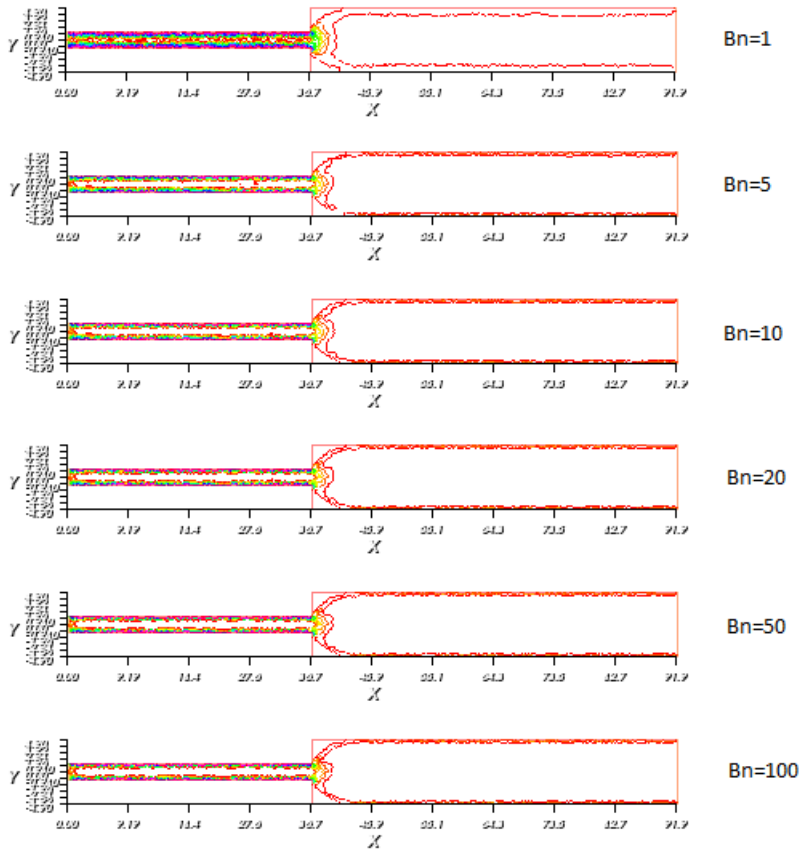

Figure 5.24: Progressive growth of plug regions. Colored - fluid region, white - plug region.

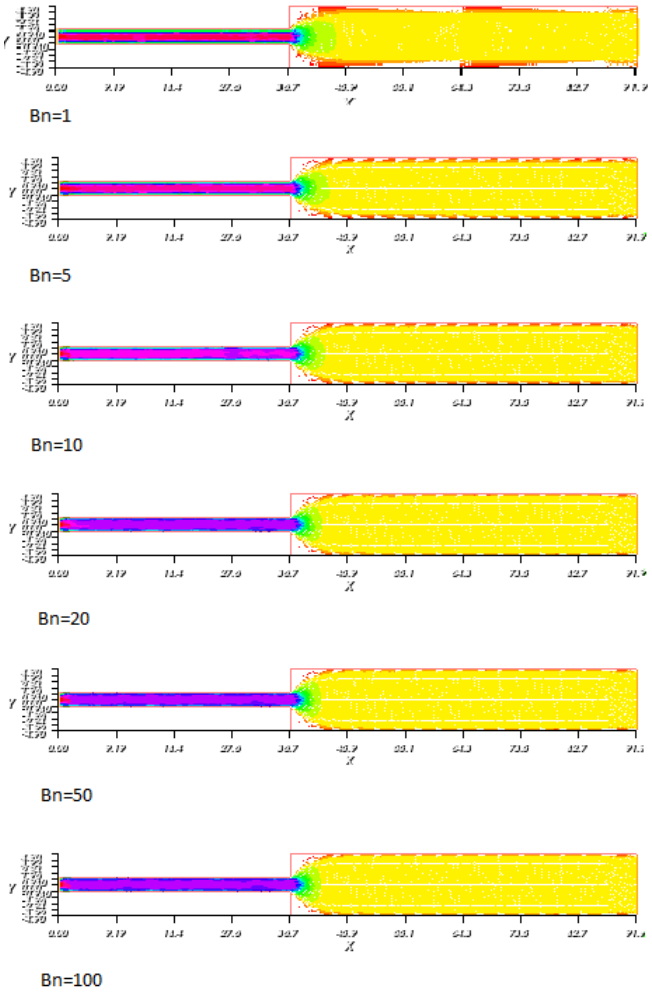

Figure 5.25: Velocity profile.

Chapter 6

Conclusion

In this thesis we have introduced the mixed formulation for the Bingham-Papanastasiou flow. The advantage of the mixed formulation compared to the formulation in primitive variables is that it is numerically more robust when the regularization parameter grows ($m \to \infty$).

We also introduced a new regularization (Corrected regularization), which is obtained by modifying the Bercovier-Engelman approach by an exponential term. The advantage of this regularization is that it provides more accurate results, compared to the classical Bercovier-Engelman and Papanastasiaou's regularizations. In addition, we introduced the formulation in primitive variables, and the mixed formulation for the new regularization.

We proved well-posedness results for the weak form of the problem and discussed algebraic properties of the discretized equations for both considered regularizations.

In Capter 5 we performed numerical experiments that support the conclusions of greater robustness of the mixed formulation for both consid-

ered cases: Papanastasiou's and Corrected regularization. The theoretical suggestion that the Corrected regularization provides more accurate result then other ones was approved by numerical results.

Summarizing the facts that the mixed formulation provides more robust convergence of the algorithms, and that the Corrected regularization helps to approximate the Bingham constitutive equations much closer then earlier known regularizations, we can conclude that the application of the mixed formulation to the Corrected regularization promises to be very beneficial.

Appendix

7.1 Notations

Throughout the manuscript we use the following notations:

$L^p(\Omega),\ H^k(\Omega)$	- standard Lebesgue and Sobolev spaces, $1 \leq p \leq \infty,\ k > 0$;
$L^2_0(\Omega)$	- the subspace of $L^2(\Omega)$ of functions with zero mean over Ω;
$H^1_0(\Omega)$	- the space of functions in $H^1(\Omega)$ with vanishing trace on $\partial\Omega$;
$\mathbf{L}^p(\Omega),\ \mathbf{H}^k(\Omega),$	
$\mathbf{L}^2_0(\Omega),\ \mathbf{H}^1_0(\Omega)$	- the corresponding spaces for vector functions;
$\mathbf{V}$	- the subspace of $\mathbf{H}^1_0(\Omega)$ of divergence free vector-functions;
$\mathcal{H}^k(\Omega)$	- tensors whose components are $H^k(\Omega)$ functions;
$\mathcal{L}^p_s,\ \mathcal{H}^k_s$	- symmetric tensors whose components are $\mathcal{L}^p$ functions, or correspondingly $H^k(\Omega)$ functions;
$\|\|\cdot\|\|$	- norm of L^2, or H^k;
$\|\|\cdot\|\|_k$	- norm of $H^k(\Omega)$;
$(\cdot,\cdot)$	- scalar product in L^2, or H^k;
$((\cdot,\cdot))$	- scalar product in H^1

Bibliography

[1] Abdali, S.S., Mitsoulis, E., Markatos, N.C., Entry and exit flows of Bingham fluids,. *Rheology*, Vol. 36, 1992, pp. 389-407.

[2] Alexandrou, A.N., Duc, E., Entov, V., Inertial, viscous and yield stress effects in Bingham fluid filling of a 2-D cavity,. *J. Non-Newtonian Fluid Mech.*, Vol. 96, 2001, pp. 383-403.

[3] Alexis Aposporidis, Numerical Analysis of Mixed Formulations for Bingham Fluids,. *Doctoral Dissertation*, Emory University, 2012.

[4] Alexis Aposporidis, Eldad Haber, Maxim A. Olshanski, Alessandro Veneziani, A mixed formulation of the Bingham fluid flow problem: Analysis and numerical solution,. *Comp.Meth.Appl.Mech.Eng*, V. 200 (2011), 2434-2446.

[5] M. Bercovier and M.Engelman, A finite element for the numerical solution of viscous incompressible flows,. *Journal of Computational Physics*, 30.2 (1979), 181-201.

[6] M. Bercovier and M.Engelman, A finite-element method for incompressible non-Newtonian flows,. *Journal of Computational Physics*, 36 (1980), pp.313-326.

[7] A. N. Beris, J. A. Tsamopoulos, R. C. Armstrong, and R. A. Brown, Creeping motion of a sphere through a Bingham plastic,. *Journal of Fluid Mechanics*, 158 (1985), pp. 219-244.

[8] E.C. Bingham, An Investigation of the Laws of Plastic Flow,. *U.S. Bureau of Standards Bulletin*, 13 (1916), 309-353.

[9] R. Byron-Bird, G. C. Dai, and B. J. Yarusso, The rheology and flow of viscoplastic materials,. *Reviews in Chemical Engineering*, 12 (1983), pp. 2-70.

[10] T. F. Chan, G. H. Golub, and P. Mulet, A nonlinear primal-dual method for total variation-based image restoration,. *SIAM Journal on Scientific Computing*, 20 (1999), pp. 1964-1977.

[11] E. J. Dean and R. Glowinski, Operator-splitting methods for the simulation of Bingham visco-plastic flow,. *Chinese Annals of Mathematics*, 23 (2002), pp. 187-204.

[12] E. J. Dean, R. Glowinski, and G. Guidoboni, On the numerical simulation of Bingham visco-plastic flow: Old and new results,. *Journal of Non-Newtonian Fluid Mechanics*, 142 (2007), pp. 36 - 62.

[13] G. Duvaut and J. L. Lions, Inequalities in Mechanics and Physics,. *Springer*, Berlin, 1976.

[14] H. Elman, D. Silvester, and A. Wathen, Finite Elements and Fast Iterative Solvers with Applications in Incompressible Fluid Dynamics,. *Oxford University Press*, Oxford, 2005.

[15] L.C.Evans, Partial Differential Equations (Graduate Studies in Mathematics, V.19,. *American Mathematical Society*, Providence, 1998.

[16] G. P. Galdi, A. M. Robertson, R. Rannacher, S. Turek, A. M. Robertson, A. Sequeira, and M. V. Kameneva, *Hemorheology*, vol. 37 of Oberwolfach Seminars, Birkh´auser, Basel, 2008

[17] V. Girault and P.Raviart, Finite element methods for navier-Stokes equations: theory and algorithms,. *Springer, Berlin*, 1986.

[18] Glowinski, R., Numerical methods for nonlinear variational problems,. *Springer-Verlag*, New York (1984).

[19] P. P. Grinevich and M. A. Olshanskii, An iterative method for the Stokes-type problem with variable viscosity,. *SIAM Journal on Scienti c Computing*, 31 (2009), pp. 3959-3978.

[20] T. Hayat, M. Farooq, Z. Iqbal, and A. Hendi, Stretched flow of Casson fluid with variable thermal conductivity,. *Walailak Journal of Science and Technology (WJST)*, 10 (2012).

[21] P. Hild, I. R. Ionescu, T. Lachand-Robert, and I. Rosca, The blocking of an inhomogeneous Bingham fluid. Applications to landslides,. *ESAIM: Mathematical Modelling and Numerical Analysis - Modelisation Mathematique et Analyse Numerique*, 36 (2002), pp. 1013-1026.

[22] T. Hayat, M. Farooq, Z. Iqbal, and A. Hendi, Stretched flow of Casson fluid with variable thermal conductivity,. *Walailak Journal of Science and Technology (WJST)*, 10 (2012).

[23] Hlaváček, I., J. Nečas, On inequalities of Korn's type,. *Arch. Rational Mech. Anal.*, Volume 36, Issue 4 , pp 312-334 (1970).

[24] J. Hron, A. Ouazzi, S. Turek, A Computational Comparison of two FEM Solvers For Nonlinear Incompressible Flow, Challenges in Scientific Computing,. *Springer*, 2004.

[25] Huilgol, R.R., Panizza, M.P., On the determination of the plug flow region in Bingham fluids through the application of variational inequalities,. *Non-Newtonian Fluid Mech.*, 58 (1995) 207-217.

[26] Mitsoulis, E., & Huilgol, R. R., Entry flows of Bingham plastics in expansions,. *Journal of non-newtonian fluid mechanics*, 122, no. 1 (2004): 45-54.

[27] Soto, H. P., Martins-Costa, M. L., Fonseca, C., & Frey, S., A numerical investigation of inertia flows of Bingham-Papanastasiou fluids by an extra stress-pressure-velocity galerkin least-squares method,. *Journal of the Brazilian Society of Mechanical Sciences and Engineering*, 32, no. SPE (2010): 450-460.

[28] Huilgol, R.R., Variational inequalities in the flows of yield stress fluids including inertia: theory and applications,. *Phys. Fluids*,14 (2002) 1269-1283.

[29] Huilgol, R.R., You, Z., Application of the augmented Lagrangian method to steady pipe flows of Bingham, Casson and Herschel-Bulkley fluids,. *Non-Newtonian Fluid Mech.*,128 (2005) 126-143.

[30] Khaldoun, A., E. Eiser, G. H. Wegdam, and Daniel Bonn, Liquefaction of quicksand under stress,. *Nature*,437, no. 7059 (2005): 635-635.

[31] Liu, B.T., Muller, S.J., Denn, M.M., Convergence of regularization method for creeping flow of a Bingham material about a rigid sphere,. *Non-Newtonian Fluid Mech.*, Vol. 102, 2002, pp. 179-191.

[32] E. Mitoulis, Flows of viscoplastic materials: models and computations,. *in Rheology Reviews, D. M. Binding, N. E. Hudson, and R. Keunings, eds.*, Glasgow, 2007, Universities Design & Print, pp. 135-178.

[33] E. A. Muravleva and M. A. Olshanskii, Two finite-difference schemes for the calculation of Bingham fluid flows in a cavity,. *Russian Journal of Numerical Analysis and Mathematical Modelling*, 23 (2008), pp. 615-634.

[34] T.C.Papanastasiou and A.G.Boudouvis, Flows of visciplastic materials: models and computations,. *Computers and Structures*, 64 (1997), pp.677-694.

[35] K. Raju, Fluid Mechanics, Heat Transfer, and Mass Transfer: Chemical Engineering Practice,. Wiley, Hoboken, 2011.

[36] Reddy, M.V. Subba; JayaramiReddy, B.; Reddy, M. Sudhakar; Nagendra, N., Long wavelength approximation to MHD peristaltic flow of a Bingham fluid through a porous medium in an inclined channel,. *International Journal of Dynamics of Fluids*, 2011.

[37] Roquet, N., Saramito, P., An adaptive finite element method for Bingham fluid flows around a cylinder,. *Comput. Methods Appl. Mech. Engrg.*, 192 (2003) 3317-3341.

[38] J. Steffe, Rheological Methods in Food Process Engineering,. *Freeman Press*, East Lansing, 1996.

[39] Song, Wenji; Xiao, Rui; Feng, Zi-ping, Experimental investigation on tetra-n-butyl-ammonium bromide clathrate hydrate slurry flows in a horizontal tube: flow behavior and its rheological model,. *HVAC & R Research*,2012.

[40] R. I. Tanner and J. F. Milthorpe, Numerical simulation of the flow of fluids with yield stress,. *Numerical Methods in Laminar and Turbulent Flow, C. Taylor, J. A. Johnson, and W. R. Smith, eds.*, Seattle, 1983, pp. 680-690.

[41] G. Vinay, A. Wachs, and J.-F. Agassant, Numerical simulation of weakly compressible Bingham flows: The restart of pipeline ows of waxy crude oils,. *Journal of Non-Newtonian Fluid Mechanics,* 136 (2006), pp. 93 -105.

[42] Vinay, G., Wachs, A., Agassant, J.-F., Numerical simulation of non-isothermal viscoplastic waxy crude oil flows,. *Non-Newtonian Fluid Mech.*, 128 (2005) 144-162.

[43] Vinay, G., Wachs, A., Agassant, J.-F., Numerical simulation of weakly compressible Bingham flows: application to the restart of waxy crude oils,. *Non-Newtonian Fluid Mech.*, 136 (2006) 93-105.

[44] G. Vinay, A. Wachs, and I. Frigaard, Start-up transients and eff-cient computation of isothermal waxy crude oil flows,. *Journal of Non-Newtonian Fluid Mechanics*, 143 (2007), pp. 141 - 156.

[45] W.R., Scott, and H. M. Jaeger, Impact-activated solidification of dense suspensions via dynamic jamming fronts,. *Nature*, 487, no. 7406 (2012): 205-209.

[46] Zinani, F., Frey, S., Galerkin Least-Squares Solutions for Purely Viscous Flows of Shear- Thinning Fluids and Regularized Yield Stress Fluids,. *J. of the Braz. Soc. Mech. Sci. & Eng.,*, Vol. 29/4, 2007, pp. 432-443.